Aus dem Institut für Immunologie
Geschäftsführender Direktor: Prof. Dr. Stefan Bauer
Des Fachbereichs Medizin der Philipps-Universität Marburg

In Zusammenarbeit mit CSL Behring Innovation GmbH

Titel der Dissertation:

Characterization of single point mutation in the gamma-carboxyglutamic acid domain of recombinant clotting Factor IX and its therapeutic potential

Inaugural-Dissertation zur Erlangung des Doktorgrades der Naturwissenschaften (Dr. rer. nat)

dem Fachbereich Medizin der Philipps-Universität Marburg

vorgelegt von

Steffi Knoll Machado

aus Caracas

Marburg, 2023

Angenommen vom Fachbereich Medizin der Philipps-Universität Marburg am:
27.04.2023

Gedruckt mit Genehmigung des Fachbereichs Medizin

Dekan: Prof. Dr. D. Hilfiker-Kleiner

Referent: Prof. Dr. Michael Bacher

1. Korreferent: Prof. Dr. Alexander Visekruna

In loving memory of my father

Content

1 ABBREVIATION, LIST OF FIGURES AND TABLES 4

1.1 ABBREVIATIONS 4

1.2 LIST OF FIGURES 7

1.3 LIST OF TABLES 9

2 INTRODUCTION 10

2.1 HEMOPHILIA B DISEASE 10

2.1.1 Hemostasis 11

2.2 CLOTTING FACTOR IX (FIX) 17

2.2.1 Molecular biology 17

2.2.2 Biological function 19

2.3 CLINICAL FEATURES 27

2.4 DIAGNOSIS AND TREATMENTS 27

2.4.1 History of the treatment in HB 29

2.4.2 Standard-of-care for HB 30

2.5 THE PHENOMENA OF EXTRAVASCULAR FIX RESERVOIR 31

2.6 AIM OF THE STUDY 34

2.6.1 Murine model of HB 34

3 MATERIALS AND METHODS 39

3.1 RECOMBINANT FIX (RFIX) CONSTRUCTS 39

3.1.1 Reference rFIX 39

3.1.2 Modified rFIX 39

3.2 LIST OF DEVICES, SOFTWARE AND REAGENTS 40

3.2.1 Devices and software 40

3.2.2 Disposables 42

3.2.3 Reagents and Kits 43

3.2.4 Buffers 46

3.3 MOLECULAR BIOLOGY 47

3.4 CELL CULTURE, TRANSFECTION AND PURIFICATION METHODS 48
3.5 DETERMINATION OF THE PROTEIN CONCENTRATION 50
3.5.1 UV- Spectrophotometrical measurement 50
3.5.2 One-stage clotting assay (OSCA) of purified rFIX 50
3.5.3 Enzyme-linked immunosorbent assay (ELISA) of purified rFIX 51
3.6 *IN VITRO* CHARACTERIZATION OF GENERATED RFIX VARIANTS 52
3.6.1 Activated partial thromboplastin time (aPTT) 52
3.6.2 Kinetics of activation of rFIX by rFXIa 53
3.6.3 FXa generation by activated rFIX 53
3.6.4 FIXa generation assay 54
3.6.5 Michaelis constant equations: 55
3.7 *IN VIVO* CHARACTERIZATION OF RFIX 55
3.7.1 Pharmacokinetics and liver sampling (PK) in HB mice 56
3.7.2 Tail clip bleeding model 56
3.7.3 Intravital microscopic mesentery arteriole thrombosis 57
3.7.4 Blood samples and plasma generation 58
3.7.5 Determination of FIX:Ag level in plasma 58
3.7.6 Determination of FIX:C level in plasma 58
3.7.7 Processing of tissue samples 58
3.7.8 Immunofluorescence staining 59
3.7.9 Fluorescent Image analysis 60

4 RESULTS 61

4.1 EXPRESSION AND PURIFICATION OF RFIX VARIANTS 61
4.2 *IN VITRO* CHARACTERIZATION OF THE K5 VARIANTS 63
4.2.1 The efficacy of rFIX proteins in FIX deficient human plasma 63
4.2.2 Activation of rFIX products 64
4.2.3 Generation of FXa by FIXa in a chromogenic assay 68
4.3 *IN VIVO* PK PROFILE AND TISSUE LEVELS OF RFIX IN HB MICE 71
4.3.1 PK behavior and tissue disposition of non-fused rFIX proteins 71
4.3.2 PK behavior and tissue disposition of albumin fused rFIX proteins 78

4.3.3 Colocalization of rFIX and Collagen IV *84*
4.3.4 Distribution of FIX and rFIX in human and murine liver *86*
4.4 *In vivo* efficacy of non-fused rFIX in HB mice 88
4.4.1 In vivo pharmacodynamic profile of non-fused rFIX proteins *88*
5 DISCUSSION 99
5.1 *In vitro* characterization of single point mutation at position 5 in albumin fused and non-fused rFIX 104
5.2 PK profile and tissue levels of fused and non-fused $rFIX_{K5A}$ and $rFIX_{K5R}$ in HB mice 106
5.2.1 PK of non-fused rFIX proteins *106*
5.2.2 PK of albumin fused rFIX proteins (rFIX-FP) *109*
5.2.3 Additional histological analysis of harvested liver tissues *111*
5.3 Efficacy of rFIX mutants in HB mice 113
5.3.1 Efficacy of intravenous rFIX replacement therapy *115*
5.3.2 Efficacy of subcutaneous rFIX replacement therapy *119*
5.4 Final conclusions and outlook 119
6 SUMMARY 122
7 ZUSAMMENFASSUNG 124
8 REFERENCES 126
9 APPENDIX I
9.1 Curriculum vitae I
9.2 Own contribution III
9.3 Publication list VI
9.4 Acknowledgement VII
9.5 Verzeichnis der akademischen Lehrer IX
9.6 Ehrenwörtliche Erklärung XI

1 Abbreviation, list of figures and tables

1.1 Abbreviations

% d.N.	Percent of the Normal Clotting Factor Level
a	Activated
A	Alanine
Ag	Antigen
APC	Activated protein C
aPTT	Activated Partial Thromboplastin Time
AT III	Antithrombin III
AUC	Area under the curve
BCS	Behring Coagulation System
BSA	Bovine Serum Albumin
BW	Body Weight
ca.	circa
Ca^{2+}	Calcium ion
$CaCl_2$	Calcium chloride
CHO	Chinese Hamster Ovary
CO_2	Carbon dioxide
DB	Dialyse Buffer
DNA	Deoxyribonucleic acid
e.g.	Exempli gratia
EDTA	Ethyl diamin tetra acid
EGF	Epithelial growth factor
ELISA	Enzyme-linked Immunosorbent Assay
ER	Endoplasmatic reticulum
et al.	Et alia
F	Clotting Factor
F9	FIX-Gene
FDA	The Food and Drug Administration
$FeCl_3$	Ferric chloride
FIX:Ag	FIX-Antigen level

FIX:C	FIX-Clotting activity level
FIX-ko	Factor IX-Knock-out
Gla	Gamma(γ) carboxylated glutamic acid
GV-Solas	Gesellschaft für Versuchstierkunde – Society of Laboratory Animal Science
HA	Hemophilia A
HB	Hemophilia B
hFIX	Human Wildtype FIX
HPLC	High performance liquid chromatography
HRP	horseradish peroxidase
HSA	Human Serum Albumin
i.e.	That is
i.v.	Intravenous
IU	International Units
K	Lysine
ko	Knockout
max.	Maximum
min.	Minimum
n=	Sample size
NCA	Non-Compartmental Analysis
OD	Optical Density
PBS	Phosphate Buffered Saline
PCR	Polymerase Chain Reaction
pd	Plasma-derived
pH	potential of Hydrogen
PK	Pharmacokinetic
PL	Phospholipid
PT	Prothombin Time
R	Arginine
rFIX	Recombinant Clotting Factor IX
rFIX-FP	Recombinant Clotting Factor IX-Fusion Protein
RP	Regeneration Buffer
rpm	Revolution Per Minute
RT	Room Temperature

s.c.	Subcutanous
SD	Standard Deviation
SDS-PAGE	Sodium Dodecyl Sulfate Polyacrylamide Gel Electrophoresis
SEM	Standard Error of the Mean
SHP	Standard Human Plasma
TBS	Tris Buffered Saline
TBST	Tris Buffered Saline with Tween
TF	Tissue Factor
TFPI	Tissue Factor Pathway Inhibitor
TMB	3,3′,5,5′-Tetramethylbenzidin
tPa	Tissue Plasminogen activator
vWF	Von Willebrand Factor
WB	Wash Buffer
WHO	World Health Organisation
WT	Wildtype
x g	Centrifugal force
°C	Degree Celsius
%	Percent
Da	Dalton
g	Gram
h	Hour
IU	International Units
L	Liter
m	Meter
M	Concentration [mol/l]
min	Minutes
s	Seconds
V	Volt

1.2 List of Figures

Figure 1. Primary hemostasis........ 13
Figure 2. Cascade model of coagulation. 15
Figure 3. Fibrinolytic system in hemostasis........ 16
Figure 4. Molecular structure of clotting factor IX (FIX) zymogen. 18
Figure 5. Calcium-dependent association of the glutamic acid (Gla) domain with the anionic phospholipid surface........ 19
Figure 6. Simulation of the intrinsic tenase complex........ 21
Figure 7. Regulation of blood coagulation by endothelial cells........ 24
Figure 8. Photograph of a tongue hematoma caused by trauma in a hemophilic patient........ 27
Figure 9. Schematic of tail clip bleeding assay in mice. 36
Figure 10. Setting-up of $FeCl_3$- induced mesenteric arterial thrombosis model...... 38
Figure 11. The plasmid DNA (pMARES) utilized for the generation of stable transfected Chinese Hamster Ovary (CHO) cells expressing rFIX constructs. 47
Figure 12. Image of the SDS-PAGE gel under non-reducing conditions. 61
Figure 13. Activated partial thromboplastin time (aPTT) correction after addition of rFIX proteins........ 64
Figure 14. Activation of $rFIX_{WT}$, $rFIX_{K5A}$ and $rFIX_{K5R}$ by rFXIa. 65
Figure 15. Activation of $rFIX_{WT}$-FP, $rFIX_{K5A}$-FP and $rFIX_{K5R}$-FP. 66
Figure 16. Kinetics of rFIXa activity using a proteolytic substrate........ 67
Figure 17. Kinetics of rFIXa activity using a proteolytic substrate........ 67
Figure 18. Formation of tenase complex. 68
Figure 19. Measurement of FXa generation in the Xase complex........ 69
Figure 20. Intravenous PK profile of non-fused rFIX proteins in HB mice........ 73
Figure 21. Subcutaneous PK profile of non-fused rFIX proteins in HB mice. 75
Figure 22. Immunohistochemistry staining of liver tissues (non-fused proteins). . 76
Figure 23. Representative image from liver section. 78
Figure 24. Intravenous PK profile for albumin fused rFIX in HB mice. 80

Figure 25. Subcutaneous PK profile of albumin fused rFIX in HB mice. 82

Figure 26. Immunohistochemistry staining of liver tissues (albumin fused proteins). 84

Figure 27. Colocalization of FIX and Collagen IV in murine liver tissues. 85

Figure 28. Endogenous FIX staining in human liver sections. 86

Figure 29. FIX staining in human and rFIX treated HB mouse liver tissues. 87

Figure 30. Tail clip bleeding model after intravenous administration. 90

Figure 31. Exposure of rFIX in plasma of HB mice after tail clip model (intravenous administration). 91

Figure 32. Tail clip bleeding model after subcutaneous administration. 93

Figure 33. Exposure of rFIX in plasma of HB mice after tail clip (subcutaneous administration). 94

Figure 34. Establishment of the $FeCl_3$-induced mouse mesenteric arteriole model in HB mice. 95

Figure 35. Representative images after $FeCl_3$ induced injury of mesenteric arteriole in HB mice. 96

Figure 36. Efficacy of rFIX proteins in the mesenteric artery thrombosis model. ... 97

Figure 37. Intravascular vs. intravascular rFIX depicted in a vessel. 102

1.3 List of Tables

Table 1. Classification and characteristics of HB 10

Table 2. Genotype-phenotype correlation in hemophilia 11

Table 3. rFIX one-stage clotting potency and specific activities 61

Table 4. N-glycan profile of generated rFIX 62

Table 5. The level of γ-carboxylation with ≥ 11 glutamate residues 63

Table 6. In vitro enzyme kinetics of FX activation in the tenase complex........... 70

Table 7. Non-compartment analysis (NCA) of the PK profile for intravenous administered rFIX (I).. 74

Table 8. Non-compartment analysis (NCA) of the PK profile for intravenous administered rFIX (II) 81

Table 9 Non-compartment analysis (NCA) of the PK profile for subcutaneous administered rFIX... 83

2 INTRODUCTION

2.1 Hemophilia B disease

Hemophilia B (HB) is an X-linked recessive bleeding disorder caused by deficiency of coagulation factor IX (FIX). Due to the sex-linkage of the disorder, the prominence amongst male is far greater than in females. It is clinically identical to Hemophilia A (HA), which occurs as a result of deficiency of FVIII. The prevalence of HB is ~1 in 30,000 males worldwide. HB is classified into three types: severe, moderate, and mild deficiency based on the plasma FIX activity levels as shown in Table 1. The severity of the disease is associated with pronounced increase in bleeding frequency per year (annual bleeding rate). Severe HB patients (< 1% of FIX activity) suffer from spontaneous bleeding, while moderate (< 6% of FIX activity) and mild (< 30 % of FIX activity) HB patients exhibit prolonged bleeding time after trauma events.

Table 1. Classification and characteristics of HB according to residual plasma FIX activity (Motlagh et al., 2018)

FIX activity (%)	Disease severity	Prevalence (%) among HB population	Clinical symptoms	Bleeding frequency	Mean age at diagnosis
<1	Severe	60	Spontaneous joint or deep muscle bleeding	Up to 2-5 per month	<2 years
1-5	Moderate	15	Seldom spontaneous bleeding, usually after minor trauma	Vary from 1 per month to 1 per year	2-5 years
>5-30	Mild	25	No spontaneous bleeding, usually bleeding after severe trauma, surgery and tooth extraction	Vary from 1 per year to 1 every 10 years	Often later in the life

Various FIX mutations, including several mutations in the promoter region (e.g., HB Leyden) are associated with a phenotype characterized by severe disease at birth (Reijnen et al., 1992). Frameshifts, nonsense mutations, large deletions, and splicing mutations are the most common genetic abnormalities that lead to severe HB. However, small deletions and missense mutations cause severe, moderate, or mild deficiency (Table 2). The majority of these mutations lead to an inactive or partially active form of FIX, and FIX antigen is detectable in those patients. These patients are classified as cross-reactive material positive (CRM +). In some cases, no FIX protein is expressed, and, in those cases, FIX antigen assays are negative. These patients are classified as cross-reactive material negative (CRM -). In both cases the normal hemostasis is compromised.

Table 2. Genotype-phenotype correlation in hemophilia (Motlagh et al., 2018).

Genetic abnormality	Severity of disease
Frameshifts	Severe (95%) *
Nonsense mutations	Severe (84%) *
Large deletions	Severe (100%) *
Splicing mutations	Severe (100%) *
Missense mutations	Severe, moderate, or mild deficiency, depending on the location of genetic abnormality

*The percentage refers to phenotype caused by the mentioned genetic abnormality.

2.1.1 Hemostasis

Hemostasis is a natural process that stop prevents bleeding after injury. This is a vital host defense mechanism that has evolved in vertebrates to maintain the integrity of a high-pressure closed circulatory system. Cellular and biochemical events must function collectively to keep blood in the liquid state within the veins and arteries and prevent blood loss following injury through the formation of a blood clot (Hoffbrand and Pettit, 1993). The proper functioning of this network requires a complex regulated system which is dependent on a delicate balance between the vascular system, coagulation system, fibrinolytic system, platelets, kinin system, serine protease inhibitors, and the complement system. When the endothelial lining of the blood vessel is disrupted by mechanical trauma, physical agents, or chemical trauma these systems work together to produce clots to stop bleeding. The clot is eventually dissolved through the fibrinolytic process, as a result of the tight regulation between growth and decay of the clot during hemostatic response (Versteeg et al., 2013).

2.1.1.1 Primary hemostasis

Primary hemostasis involves the response of the vascular system and platelets to vessel injury. The vascular system, which includes the blood vessels and the procoagulant, anticoagulant, and fibrinolytic proteins, plays a critical role in primary hemostasis. Under normal conditions, endothelial cells (EC) lining up the blood vessels, form an intact surface that promotes the fluid state of blood and prevents turbulence that may trigger activation of platelets and plasma proteins. In the sub-endothelium the ECs are surrounded by collagen-rich basement membrane and layers of connective tissues. A breakdown in the vascular system is rapidly repaired to maintain blood flow and the integrity of the vasculature by the formation of a platelet plug. Upon vascular injury, as shown in Figure 1, the affected vessels contract to seal off the wound (vasoconstriction) and platelets are mobilized to the site of injury, where they aggregate, and adhere to the exposed components of the subendothelial matrix. Platelet adhesion requires the presence of various factors such as von Willebrand factor (vWF) and platelet receptors. The activation of receptors on the surface of platelets trigger signaling by agonists such as collagen, thrombin, adenosindiphosphat (ADP), thromboxane-A2 (TxA2) and epinephrine. With the exception of collagen, each of these molecules works through one or more members of the G protein coupled receptor superfamily. Those soluble agonists, and in particular ADP released from granules of activated platelets, trigger a positive feedback cascade leading to rapid activation of large numbers of platelets. The final platelet plug is stabilized by interaction with fibrinogen (Broos et al., 2011).

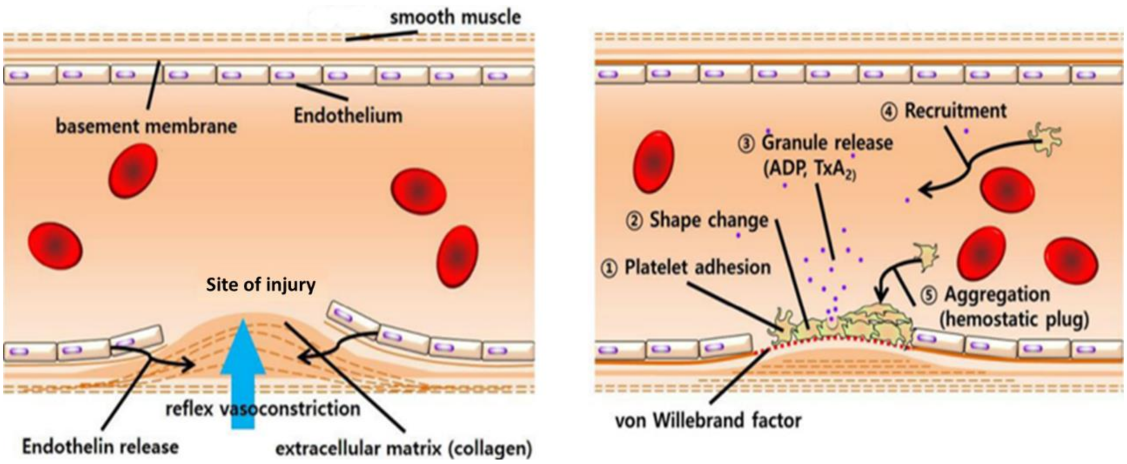

Figure 1. Primary hemostasis.
Vasoconstriction occurs immediately as a reflex mechanism of the nervous system right after vascular injury, which is enhanced by endothelin, a potent vasoconstrictor released from the endothelial cells constituting the vessel wall. Platelets bind to the von Willebrand factor (1) and attach to the extracellular matrix at the site ofinjury and change shape (2) and promote further recruitment (4) and aggregation of platelets (5) by releasing granules such as ADP and Tx A2 (3). Schematic representation showing the site of injury was taken from (Park and Koh, 2018).

2.1.1.2 Secondary hemostasis

Secondary hemostasis involves the response of the coagulation system to vessel injury as a continuation of the primary hemostatic mechanism. Multiple proteins of the coagulation system interact to form a fibrin clot by triggering the conversion of soluble fibrinogen to fibrin. The fibrin polymers are then cross-linked by activated clotting factor XIIIa (FXIIIa) to form a stable fibrin clot. The protein factors are designated by Roman numerals according to their sequence of discovery. Some of the coagulation factors such as fibrinogen and prothrombin are referred by their common names, whereas others such as factor VIII (FVIII) and XI are referred by their Roman numeral nomenclatures. The majority of coagulation factors, with exception of FVIII, are precursors of serine proteolytic enzymes known as zymogens that circulate in blood in an inactive form. Activation of each zymogen into serine proteases is indicated by the addition of a low case “a” next to the Roman numeral in the coagulation cascade such as VIIa, Xa, XIIa (Wright, 1962). The coagulation factors may be categorized into substrates, cofactors, and enzymes. Fibrinogen is the main substrate. The cofactors, tissue factor (TF) for the FVIIa enzyme; factor V (FV) for the FXa enzyme; factor VIII (FVIII) for the FIXa enzyme; and High-Molecular Weight Kininogen (HMWK) protein for the activation of Prekallikrein (PK), FXII, and FXI, accelerate the activities of the enzymes.

The coagulation model can be described in 3 pathways: the intrinsic pathway that starts with FXII, the extrinsic pathway that initiates with FVII, and the activation of X leading to the common pathway. *In vivo* the intrinsic and extrinsic systems cannot operate independently and are regulated by controlled mechanisms as shown in the schematic overview in Figure 2.

When vessels are damaged and blood leaks out, the anticoagulant environment that predominates normally in the vessels is shortly switched to a procoagulant environment within seconds. This acute response requires a refined and highly regulated system that can efficiently stop bleeding and return to the normal state without causing unintended damage like thrombosis in a pathological setting. This system is called coagulation cascade and is initiated by FVII that is present in plasma (extrinsic pathway). When the vessel wall is disrupted, FVII comes in contact with TF that is expressed in subendothelial layers. The FVIIa-TF complex can then activate FX (common pathway). At the same time, the platelets get activated in a procoagulant environment (biochemical pathways involving inhibition of anticoagulant molecules and activation of procoagulant molecules) and are recruited to the site of injury. At this point, the amplification phase is triggered by activation of FXII (intrinsic pathway) when it comes in contact with negatively charged phospholipids (PLPs) of activated platelets. FXIIa activates FXI, FXIa activates FIX, FIXa and its cofactor FVIIIa form a complex (called tenase complex), where FX is cleaved into activated FX (FXa). Finally, generation of FXa from this complex causes clot formation via the common pathway. In the common pathway, high amounts of FXa and its cofactor FVa (generated in the intrinsic and extrinsic pathway) cleave prothrombin to thrombin.

Thrombin can cleave the main substrate of the coagulation cascade, fibrinogen to fibrin. Fibrin stabilizes the clot and prevents two critical events: 1) leakage of blood and 2) formation of unstable clots that can break off, travel to another area and block blood flow (embolic events). In general, the outcome of primary hemostasis is the formation of the platelet plug, and the outcome of secondary hemostasis is the formation of a thrombus (Kenneth et al., 2016).

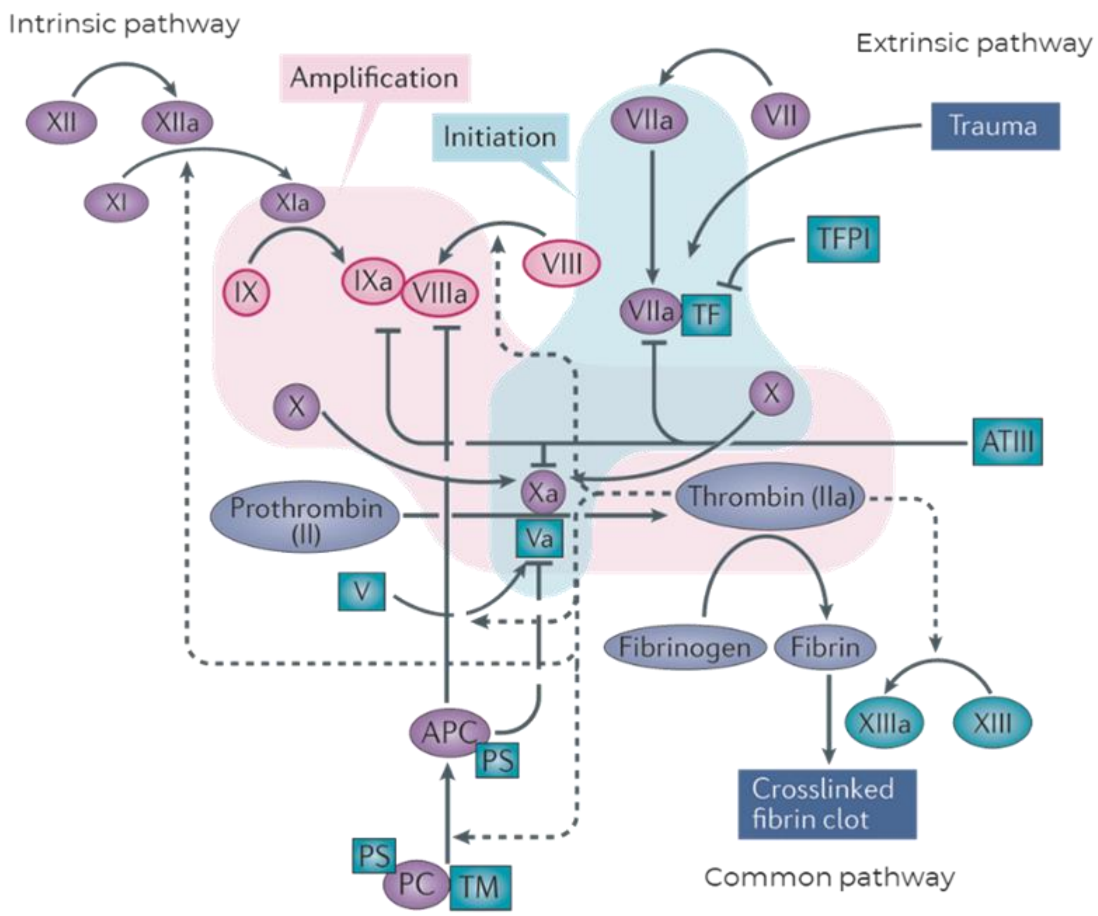

Figure 2. Cascade model of coagulation.
The figure shows successive activation of coagulation factors proceeding to thrombin generation and fibrin formation. The clot formation *in vivo* is best described by an initiation phase that is started in the vessel after an injury (shaded in blue). The amplification phase (shaded in pink) functions as positive feedback exponentially increasing the generation of thrombin and fibrin. The clotting factors are represented by the Roman numeral nomenclature and addition of a low case "a" indicates the

activated form. Proteins with procoagulant properties such as tissue factor (TF), activated protein C (PC) and anticoagulants such as protein S (PS), thrombomodulin (TM), and tissue factor pathway inhibitor (TFPI) are shown.

2.1.1.3 Fibrinolysis

Fibrinolysis is the physiological process that results in degradation of blood clots as shown in Figure 3. Fibrinolysis involves removal of insoluble fibrin clots through enzymatic digestion of the cross-linked fibrin polymers. Plasmin is responsible for the lysis of fibrin into fibrin degradation products.

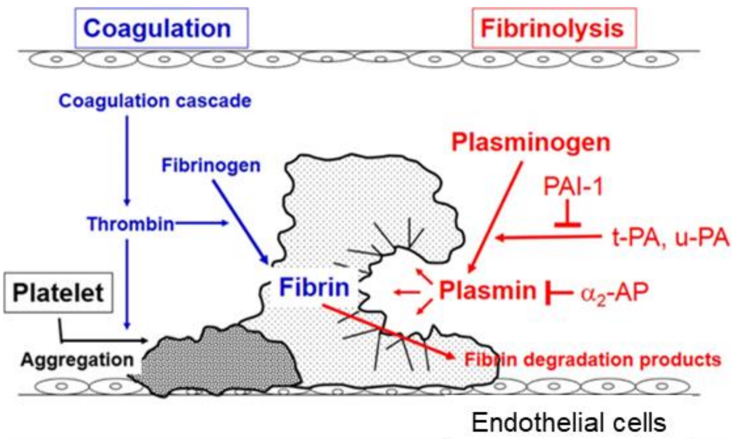

Figure 3. Fibrinolytic system in hemostasis.
Plasminogen is converted to enzymatically active plasmin by plasminogen activators (tissue-plasminogen activator, t-PA; urokinase-type plasminogen activator, u-PA). Plasmin degrades fibrin, the main component of a thrombus, to fibrin degradation products. Plasmin is inactivated by its specific inhibitor, α2-antiplasmin (α2-AP), while plasminogen activators are inactivated by plasminogen activator inhibitor 1 (PAI-1). Schematic representation taken from (Okada et al., 2020).

The fibrinolysis process occurs in parallel to healing of the injured tissue, and eventually cells of the mononuclear phagocytic system phagocytize the particulate products of the hydrolytic digestion. As mentioned above the proteolytic activity of this system is mediated by plasmin, which is generated from plasminogen. Although plasminogen cannot cleave fibrin, it has an affinity for fibrin, and is incorporated into the clot when it is formed. Plasminogen is activated by plasminogen activators like tissue-type plasminogen activator (tPA), urokinase (UK), streptokinase (SK), and acyl-plasminogen streptokinase activator complex that are present at various sites such as the vascular endothelium. Inhibitors of fibrinolysis include α2- plasmin inhibitor, tissue plasminogen activator inhibitor, and plasminogen activator inhibitor-1 (PAI-1) (Kenneth et al., 2016).

2.2 Clotting Factor IX (FIX)

2.2.1 Molecular biology

The FIX gene encoding for FIX is located on the long arm of the X chromosome (Xq27.1) and covers nearly 34 kb (Camerino et al., 1984). It is divided into eight exons that are transcribed into a 2802 bp mRNA that encodes a 28-residue signal pre-peptide followed by an 18-residue leader pro-peptide and a 415-residue mature protein (Anson et al., 1984). The signal peptide targets the protein for secretion from the hepatocyte to the circulation as a mature protein in its inactive form (zymogen). Before being released into the circulation, the signal sequence facilitates entry into the endoplasmic reticulum and the pro-peptide is necessary for posttranslational modification of 12 amino-terminal glutamic acid residues by a vitamin K-dependent gamma-glutamyl carboxylase (Furie and Furie, 2007). The amino terminus of FIX contains 12 gamma-carboxyglutamic acid (Gla) residues necessary for Ca^{2+}-dependent folding of the protein (Gillis et al., 1997). FIX undergoes further posttranslational modifications in the Golgi complex before being secreted into the circulation, including maturation of glycosylation, phosphorylation, hydroxylation, and sulfation. These posttranslational modifications are not only important for FIX structure and function but are also involved in the plasma clearance and distribution of FIX (Hansson and Stengflo, 2005). Finally, the mature FIX, a 55 kDa glycoprotein synthetized in hepatocytes, circulates in plasma at a concentration of 5 mg/mL (~90 nM). The molecular structure of the mature FIX protein consists of one gamma-carboxylglutamic acid (Gla) domain that contains 12 Gla residues, two epidermal growth factor (EGF) domains, a 35-residue activation peptide (AP), and the serine protease domain (Figure 4). The activated Factor XI (FXIa) or Tissue Factor-Factor VIIa (TF-FVIIa) complex cleave FIX at Arg145 and Arg180 to generate a two-chain serine protease that is composed of a light chain (Gla domain and EGF domains) and the catalytic heavy chain that is covalently linked by disulfide bonds to the Gla domain (Lenting et al., 1995; Lindquist et al., 1978; Zögg and Brandstetter, 2009).

The functionally active FIXa protease, after release of the active peptide (AP), can be also referred to as FIXαβ. If during FIX activation, the Arg145–Ala146 bond is cleaved first, it results in the formation of intermediate species, FIXα. In this case, the activation peptide (AP) is still attached to the heavy chain (serine protease). When Arg180 is cleaved first, the intermediate FIXaα is generated. In FIXaα, AP is temporarily still attached to the light chain (EGF2) (Smith and Gailani, 2014) .

The active form of FIX (FIXa) exhibits low catalytic efficiency. The interaction of FIX with its cofactor, activated Factor VIII (FVIIIa) enhances FIXa´s catalytic activation of FX more than 100,000-fold within the membrane-bound FIXa-FVIIIa complex (intrinsic tenase complex) assembly on activated platelet surface (Duffy et al., 1992; Gilbert and Arena, 1996).

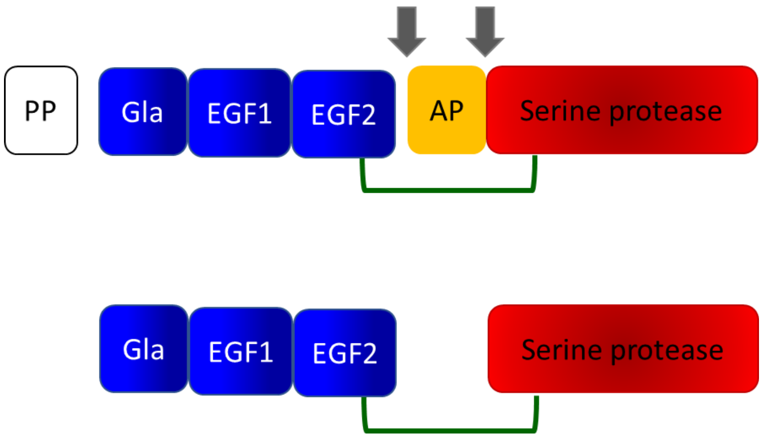

Figure 4. Molecular structure of clotting factor IX (FIX) zymogen.
The prepro (PP) leader sequence contains the signal peptide as well as the propeptide that directs gamma-carboxylation of glutamic acid (Gla) residues. Cleavage of the prepro-sequence from the mature protein is indicated by the separation between the two. The light chain (Gla, EGF 1, and EGF 2 domains) is shown in blue. The heavy chain (serine protease domain) shown in red. Cleavage sites to generate the active enzyme are indicated by the grey arrows. After cleavage of the activation peptide (AP), shown in yellow, the light chain remains covalently attached to the heavy chain by a disulfide bond, shown in green.

The Gla domain (Figure 5) is required for high affinity binding of calcium ions and for the formation of the tenase (Xase) complex on negatively charged lipid membranes during blood coagulation. Calcium ions induce conformational changes in the Gla domain and is necessary for the Gla domain to fold properly. A common

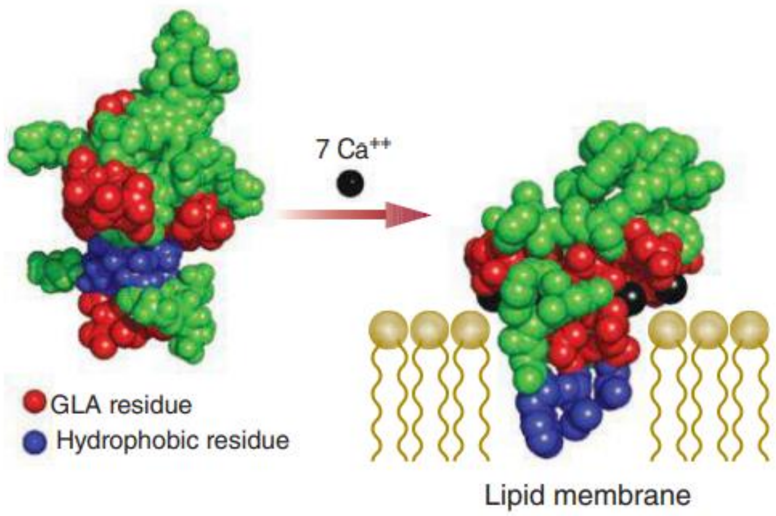

Figure 5. Calcium-dependent association of the glutamic acid (Gla) domain with the anionic phospholipid surface.
Circles represent amino acids, with the Gla domain residues indicated in dark red, hydrophobic residues in blue, and the calcium ions in black. Images taken from Williams Hematology Ninth Edition Copyright © 2016, by McGraw-Hill Education (K. et al., 2016).

structural feature of functional Gla domains is the clustering of N-terminal hydrophobic residues into a hydrophobic patch that mediates interaction with the cell surface membrane (Freedman et al., 1996). The residues involved in gamma carboxylation of the Gla domain of different human vitamin K-dependent proteins are highly conserved, which suggest the importance of this interactions.

2.2.2 Biological function

The main function of FIX, as a plasma protease is proteolytic conversion of FX to FXa resulting in the production of fibrin clot that seals the site of injury in the vessel. The damage of endothelial cells in the vessel triggers various changes in the vasculature: 1) vascular spasm 2) platelet plug formation, and finally 3) coagulation, in which FIX is involved. The first response of the body to damaged endothelial cells is the secretion of several chemicals and mediators locally creating a milieu that favors a hemostatic response (plug) and causes vascular contraction of the smooth muscles in the tunica media of the vessels to reduce leakage of blood.

Simultaneously, the exposed collagen and von Willebrand Factor (vWF) expressed on endothelial cells will interact with platelets and recruit the ones passing near the injured site.

The anticoagulant mediators, such as tissue factor pathway inhibitor (TFPI), thrombomodulin, endothelial protein C receptor (EPCR), and heparin-like proteoglycans, present in the healthy vessels (Yau et al., 2015), are inhibited by a prothrombotic milieu generated by the injured endothelial cells resulting in the binding of platelets at the site of injury. Activated platelets secrete transmitters e.g., adenosine diphosphate (ADP) that further mediates recruitment and aggregation of platelets forming an initial plug (primary hemostasis). Those platelets provide a negatively charged surface for the contact pathway and activation of FXII, FXI and cleavage of FIX by FXIa and subsequent assembly of the intrinsic Xase complex (FIXa-FVIIIa-FX) on activated platelets. Furthermore, damage in the tissue and exposure of tissue factor (TF) to the blood will activate the extrinsic pathway. TF is a transmembrane protein, that under physiologic conditions, is expressed around vessels and in the epithelium. Endothelial cells typically do not express TF constitutively but only after activation TF is upregulated (Collier et al., 2017).

The zymogen FVII is converted to activated FVII (FVIIa) by autoactivation or by activated FX (FXa) (Neuenschwander and Morrissey, 1992) and forms the TF-FVIIa complex, which catalyzes two reactions: the activation of FX to FXa and activation of FIX to FIXa. In summary, FIX can be activated by both the intrinsic and the extrinsic activators. In either case, FIXa undergoes a conformational change and then can bind with high affinity to FVIIIa. The precise nature of how FVIIIa binds to FIXa enzyme is unknown. In order to understand the structural details of the FVIIIa:FIXa complex, molecular dynamics simulation based on protein structure 3D models was conducted (Stoilova-McPhie et al., 2002).

The model showed that all four domains of FIXa wrap across FVIIIa that spans the co-factor binding surface of A2, A3 and C1 domains of FVIIIa (Figure 6). The region surrounding the 558-helix of the A2-domain of FVIIIa is predicted to be the key interaction site with the helical segments of Lys293-Lys301 and Asp332-Arg338 residues of the serine-protease domain of FIXa (Figure 6). The hydrophobic helical stack between the Gla and EGF1 domains of FIXa is predicted to be the primary interacting region with the C1-A3 domain interface of FVIIIa. The structural model of FIXa revealed that the Gla-EGF1-EGF2 domains are highly flexible. This is due to weak domain-domain interactions, while the interface between EGF2 and the serine protease (SP) is mostly rigid. The weak non-covalent domain-domain interactions explain the inherent instability of the proteins, and this translate to very short half-lives for both FIXa and FVIIIa (Venkateswarlu, 2014).

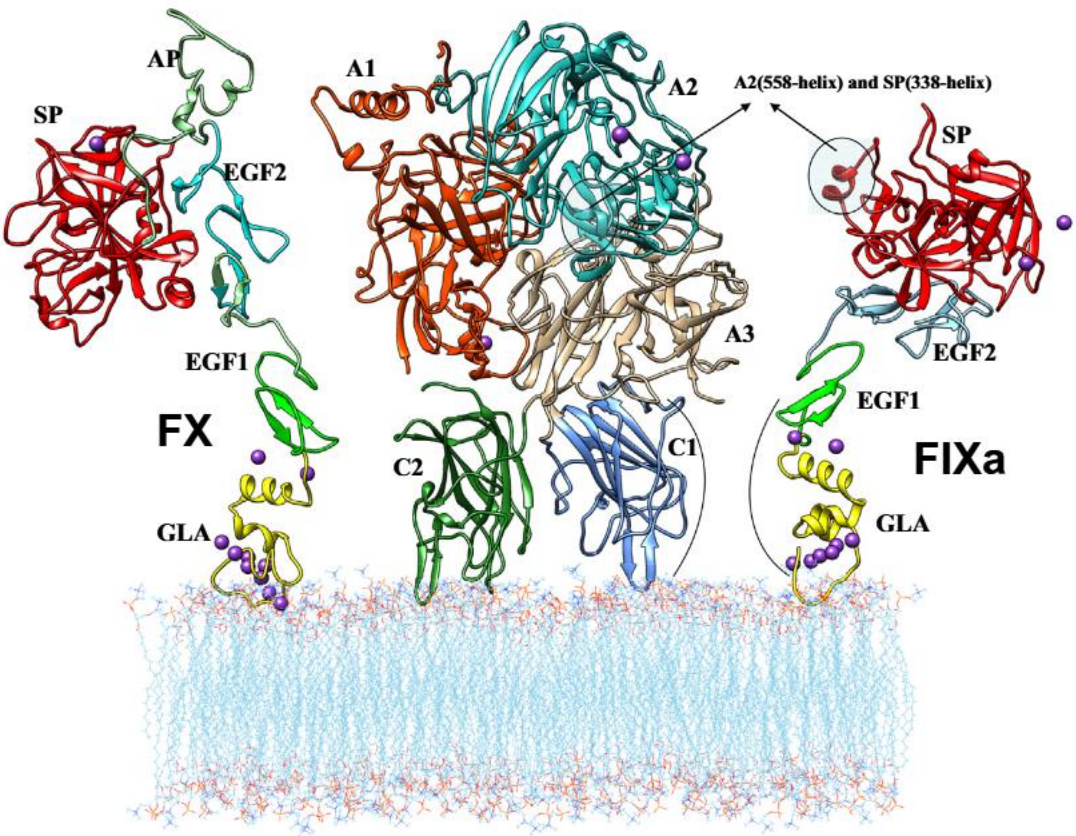

Figure 6. Simulation of the intrinsic tenase complex.
Models of FVIIIa cofactor (center), FIXa enzyme (right) and FX zymogen (left) on the hypothetical phospholipid membrane surface. The domain abbreviations for FX and FIXa: AP stays for activation peptide, SP for serine protease, EGF for epidermal growth factor, Gla for gamma-carboxyglutamic acid. FVIIIa consist of domains A1, A2, A3, C1, and C2. Image taken from (Venkateswarlu, 2014)

2.2.2.1 Cell-based model of coagulation

While the traditional coagulation cascade explains plasma-based *in vitro* coagulation, this model does not adequately explain the hemostatic process as it occurs *in vivo* (Becker, 2005; Furie and Furie, 2007; Hoffman, 2003; Roberts1 et al., 2006). Models beyond plasma-based assays that contemplate tissue-based proteins, and the vascular bed reflects better the physiological conditions. Similarly, while plasma-based in-vitro models divide the initiation of coagulation into two distinct parts, observations and experimental data suggest that extrinsic and intrinsic pathways operate dependently to generate FXa under physiological conditions.

Clinical manifestations due to the deficiency of individual coagulation factors, make it clear that intrinsic and extrinsic pathway operate in a dependent manner. Deficiencies in the initial components of the intrinsic pathway (FXII, High-Molecular-Weight Kininogen, or Prekallikrein) caused marked prolongation of the activated partial thromboplastin time (aPTT) that measures the time for the patient´s plasma to clot *in vitro*. However, *in vivo* deficiency of these proteins are not associated with a tendency for bleeding in mice or humans suggesting that they are not required for normal hemostasis (Gailani and Renné, 2007). In contrast, components of the intrinsic pathway like FXI deficiency in humans results in bleeding tendencies in some individuals and deficiencies of FIX and FVIII (intrinsic pathway proteins) are associated with mild to severe bleeding phenotypes even though those patients have an intact extrinsic pathway (Gailani and Renné, 2007).

Coagulation tests *in vitro* could erroneously give the impression that the intrinsic and extrinsic pathways operate independently. Experiments based on Tissue factor (TF)-activated whole blood and cell-based systems helped to better understand the complex coagulation processes occurring *in vivo* and is defined as the "cell-based model of coagulation". As mentioned earlier TF-FVIIa can generate thrombin on TF-bearing cells (epithelium, endothelium, monocytes and fibroblast) independent of the intrinsic coagulation factors. Subsequent propagation of thrombin generation is mediated by platelets that are localized in close proximity to TF-FVIIa complex during the primary hemostatic plug. FXa on the TF-bearing cells interact with FVa to form prothrombinase complexes that generate small amounts of thrombin that are sufficient to "prime" the clotting system for a subsequent propagation of thrombin generation. This model is supported by the observation that platelets can be activated by thrombin that is generated by direct TF–FVIIa activation of FX (Monroe et al., 2002, 1994). The small amounts of FVa required for prothrombinase assembly consisting of FVa, FXa, and thrombin (FVa-FXa-thrombin complex) are likely provided by activated platelets, by FXa activation, or potentially by noncoagulation proteases secreted by TF–bearing cells (Monroe et al., 1994; Schuijt et al., 2013; Wood et al., 2013).

The small amounts of thrombin generated are capable of accomplishing the following: (1) activation of platelets; (2) activation of FV; (3) activation of FVIII and dissociation of factor VIII from vWF; and (4) activation of FXI (Cawthern et al., 1998; Gailani and Jr., 1991; Monroe et al., 1994). The activity of the FXa formed by the TF–FVIIa complex will be mostly restricted to the TF–bearing surface because free FXa that diffuses off the cell surface is rapidly inhibited by tissue factor pathway inhibitor (TFPI), antithrombin (AT), and/or the protein Z-dependent protease inhibitor (ZPI) that inhibits both, FXa and FXIa. FIXa, on the other hand, will most likely act on activated platelets near the TF–bearing cell. This is because FIXa can diffuse to adjacent cell surfaces as it is not inhibited by TFPI and ZPI, while the rate of FIXa inhibition by AT is much lower than that of FXa (Olson et al., 2004). While more platelets adhere, a bigger negatively charged surface encounters components of the intrinsic pathway (FXII and FIX) leading to a marked amplification of thrombin generation and a sustained production of thrombin at the wound site.

2.2.2.1.1 Interaction with endothelial cells and platelets

Under physiological conditions endothelial cells (ECs) preferentially convert cyclic endoperoxides to prostacyclin, which is a potent inhibitor of platelet aggregation

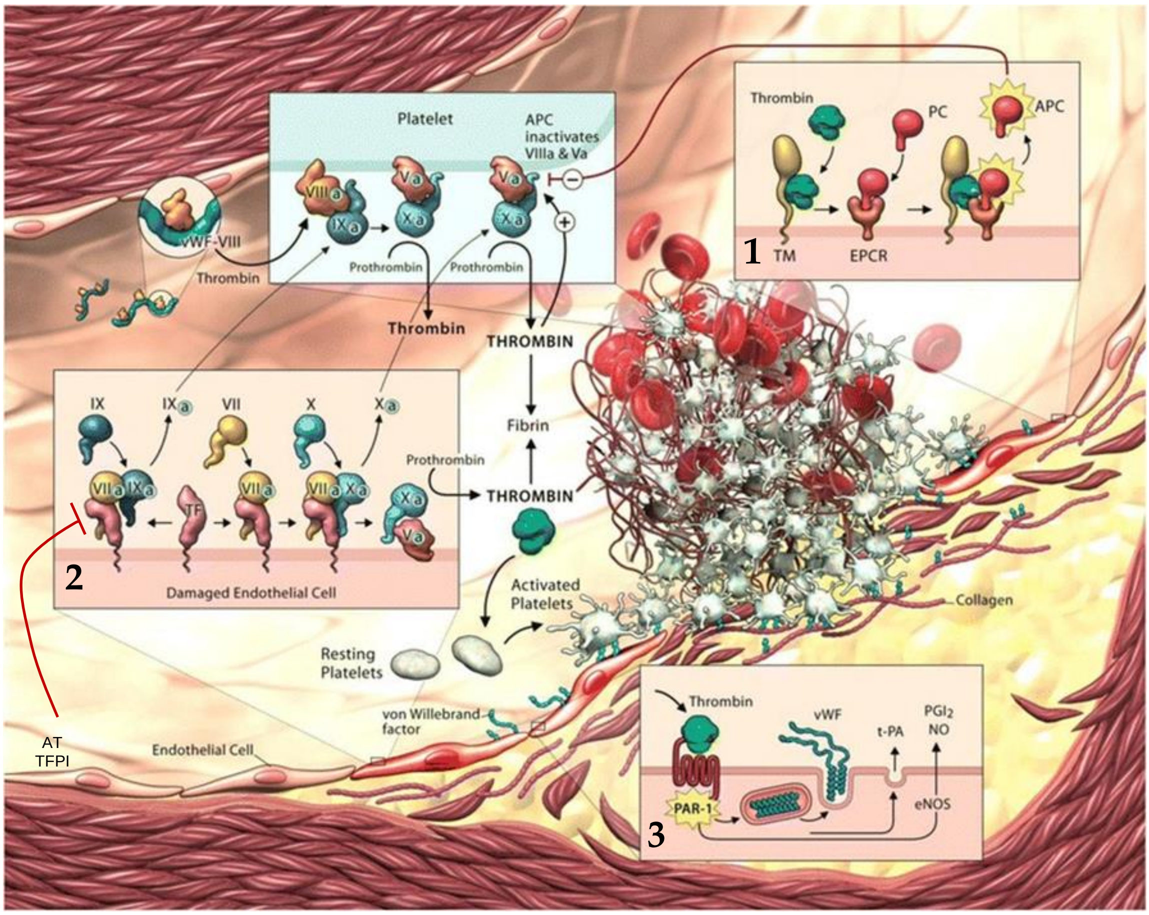

Figure 7. Regulation of blood coagulation by endothelial cells.
Activated protein C (APC), Protein C (PC), Thrombomodulin (TM); Endothelial Protein C Receptor (EPCR), von Willebrand Factor (vWF), Tissue Plasminogen Activator (t-PA), Prostaglandin I2 (PGI2), Nitric Oxide (NO), endothelial Nitric Oxide Synthetase (eNOS) (Yau et al., 2015b).

(Macintyre et al., 1978). Once a blood clot is formed to seal the injury, the clotting process must be terminated to avoid thrombotic occlusion in the adjacent, nonperturbed vascular bed. If the coagulation reactions are not controlled, clotting could occur throughout the entire vasculature, even after a modest procoagulant stimulus. Endothelial cells play a major role in confining the coagulation reactions to the site of injury and preventing clot extension to areas where the endothelium is intact. Endothelial cells have three major types of anticoagulant/antithrombotic activities (Figure 7). First (Figure 7;1), the anticoagulants protein C/protein S/thrombomodulin/ Endothelial cell protein C receptor (EPCR) are activated in response to thrombin generation. Thrombin present at sites other than that of vascular damage is able to generate activated protein C (APC), which subsequently inactivates the cofactors FVa and FVIIIa, thereby terminating or preventing downstream thrombin generation (Hanson et al., 1993). Second (Figure 7; 2), the protease inhibitors antithrombin (AT) and tissue factor pathway inhibitor (TFPI) are bound to heparan sulfates expressed on the undamaged endothelial surface, where they can inactivate proteases (Sandset, 1996), and third (Figure 7; 3), intact endothelial cells inhibit platelet activation by releasing the inhibitors prostacyclin (PGI2) and nitric oxide (NO), as well as degrading adenosine diphosphate (ADP) by their membrane ecto-ADPase (Marcus et al., 1997).

At sites of vascular injury, the endothelium shifts from an anticoagulant to a procoagulant/prothrombotic phenotype to prevent excessive blood loss. Beyond the initial responses like vasoconstriction (section 2.1.1.1), disruption of the endothelial continuity leads to exposure of collagen fibers and other subendothelial matrix proteins (Ruggeri, 2002). Circulating platelets rapidly adhere to these structures and start the hemostatic process. Platelets immediately aggregate to form thrombi. Platelets have a wide array of surface receptors and adhesion molecules and contain numerous granules which mediate platelet aggregation at the site of vascular injury (Saboor et al., 2013; Sharda and Flaumenhaft, 2018). The contribution of platelets to hemostasis and thrombosis is well defined. FIXa, viewed originally as a protein responsible exclusively for clot formation, also plays a primary role in platelet-mediated hemostasis. The binding of FIX and FIXa to thrombin-activated human platelets is well described, with 300–400 sites per platelet. Although hemostasis and thrombosis have different implications, a considerable overlap is noted in the molecular mechanisms involved in these interactions resulting from a coordinated series of events such as adhesion and promotion of coagulation. Platelets are anuclear fragments derived from the bone marrow megakaryocytes. The 2 major intracellular granules present in the platelets are the α-granules and the dense bodies. The α-granules contain platelet thrombospondin, fibrinogen, fibronectin, platelet factor 4, vWF, platelet derived growth factor, β-thromboglobulin, and coagulation factors V and VIII. The dense granules contain ADP, adenosine triphosphate (ATP), and serotonin. When stimulated, platelets release both the α-granules and the dense bodies through the open canalicular system (Fritsma, 2015; Jenne et al., 2013). When platelets aggregate, they lose their membrane integrity and form an unstructured mass called syncytium. In addition to the plug formation, platelet aggregates release micro-platelet membrane particles (micro-particles) rich in phospholipids and various coagulation proteins which provide localized environment that support plasma coagulation (White and Clawson, 2009). The procoagulant role of phospholipid-exposing platelets have been attributed to the high-affinity binding of Gla domain containing coagulation factors, i.e. (activated) Prothrombin, FVII, FIX, and FX (Monroe et al., 2002). Activated platelets regulate the coagulation system in various ways: 1) localization of coagulation reactions to the site of injury, as they adhere where TF is exposed to blood. In this process, the activation of platelets with exposure of negatively charged phospholipids facilitates the assembly of coagulation factors on the activated platelet membrane 2) expression of multiple proteins, within the platelets, involved in the regulation of coagulation cascade such as Fibrinogen, vWF, FVIII, and inhibitors of coagulation 3) acceleration of coagulation by sustaining thrombin generation. FXa generation is amplified on platelets and association with FVa lead to a burst of thrombin generation (Gomez and McVey, 2006) Subsequently, thrombin-activated factor VIII crosslinks fibrin and stabilizes the plug and thrombin also activates Thrombin Activatable Fibrinolysis Inhibitor (TAFI) that protects fibrin clot against lysis (Bajzar et al., 1995). The interaction of FIX with platelets is essential for the coagulation process because negatively charged phospholipids of platelets serve as the main and ideal surface for FIXa to undergo conformational change and form a complex with FVIIIa and FX.

2.3 Clinical Features

Figure 8. Photograph of a tongue hematoma caused by trauma in a hemophilic patient. Image was extracted from (Kenneth K. et al., 2016).

Bleeding episodes (Figure 8) in HB patients include joint hemorrhages (hemarthrosis), bleeding from the nose (epistaxis), hematoma of the tissue (ecchymosis), and post-dental extraction bleeding. The most common site of spontaneous bleeding is the joints, spontaneous bleeding in central nervous system (CNS) or umbilical cord are rather rare. The main long-term complications of recurrent joint bleeding and soft tissue hematomas are extensive arthropathy, and muscle contractures that result in disability and chronic pain (Qasim and Hassan, 2014). Restrictions on physical activities, concern about bleeding that might be life-threatening, the development of arthropathy, and the need for orthopedic procedures contribute to a lower health-related quality of life and greater pain severity in this population (Buckner et al., 2019).

2.4 Diagnosis and treatments

The diagnosis of HB is established by the clinical history and by measuring plasma FIX activity levels using one-stage clotting assay (OSCA) based on activated partial thromboplastin time (aPTT). aPTT is used for the measurement of FVIII, FIX, FXI and FXII (intrinsic pathway). Interestingly, other factors of the intrinsic pathway like FXII can also be assayed using this technique as can Prekallikrein (PRK) and High-Molecular-Weight Kininogen (HMWK) and although neither is associated with a bleeding tendency, they may result in significant prolongations of the aPTT as mentioned in the cell-based model, section 2.1.1.1. The Prothrombin time (PT) is used for assaying FX, FV and Prothrombin (FII). They are, therefore, called global assays. The assay of a specific clotting factor relies upon measuring the degree of correction of the aPTT when activator is added to a plasma sample specifically deficient in the factor to be measured. One-stage clotting assay (OSCA) is the most common assay to measure the FIX activity. It allows the measurement of the activity of FIX by measuring the rate of fibrin formation in plasma (clotting time) from patients (coagulometry) as in aPTT. Usually, the FIX clotting time is determined from the time of addition of an activator and Ca^{2+} ions to the plasma sample of the patient until the formation of a clot (turbidity). The difference to the global aPTT assay is that in FIX OSCA, FIX deficient plasma is mixed with the sample of the patient i.e., the ability to form a clot is limited by FIX contained in the sample. FIX deficient plasma contains normal levels of all the other factors. For OSCA, pooled normal plasma standards (standard human plasma, SHP) calibrated against the World Health Organization (WHO) plasma International Standard is used. The hemostatic potential of the standard human plasma is defined, for harmonization purposes, as 100% of the norm and corresponds to 1 IU/mL. The diagnosis is based on the hemostatic potential measured in the patient's samples. The category of severity is shown in Table 1. Activity levels below 30% are considered hemophilic individuals. Vitamin K deficiency should be excluded because deficiency of this vitamin results in lower activity levels of FIX and other vitamin-K-dependent proteins.

The treatment of HB patients consists of replacing the missing clotting factor, FIX. Therefore, FIX is administered intravenously, and repeated doses are needed. Another form of hemophilia is Hemophilia A (HA). The clinical features in these patients are similar to the HB patients, but in average A patients suffer a more severe bleeding condition requiring frequent administration of FVIII. Furthermore, inhibitory antibodies against FVIII in these patients present a major limitation for their treatment. HB is rarely complicated by the development of inhibitory antibodies. These antibodies occur in only approximately 3% of patients with severe HB and it is thought that some of the differences in the rate of antibody formation between HA and HB result because in HA patients, the lack of FVIII protein, is more common, while in HB patients the lack of FIX protein is rather seldom. This patient population carry nonfunctional proteins. (Puetz et al., 2014). Anaphylactic reactions to exogenous FIX is most common in patients with complete gene mutations or major derangements.

2.4.1 History of the treatment in HB

In the late 1950s and early 1960s, HB was treated using fresh frozen plasma or Prothrombin Complex Concentrates (PCCs). PCCs were prepared by absorbing the vitamin K-dependent proteins from plasma, and the final product contained not only FIX but also Prothrombin, FVII, and FX (Römisch and Pock, 2012). Due to the lack of purity, these products were associated with numerous complications including excessive activation of the coagulation pathway and requiring large therapeutic volumes (especially for fresh frozen plasma) to achieve desired FIX levels. By 1970, lyophilized powder concentrates of plasma-derived FIX became available, allowing for home storage and self-infusion. In the 1990s, plasma-derived FIX products with improved purity and safety entered the market.

Standard half-life (SHL) products. In 1997, the first recombinant FIX (a Pfizer product under the tradename BeneFIX®) was approved by the Food and Drug Administration (FDA. This SHL product is indicated for on-demand treatment, perioperative management of bleeding, and once weekly for routine prophylaxis (Packages insert - BeneFIX® - US). On-demand therapy involves treating severe bleeding episodes when they occur. This approach does not prevent intra-articular microbleeds, which eventually result in joint debilitation. Therefore, the World Federation of Hemophilia recommends the prophylactic administration (Srivastava et al., 2013).

Extended half-life (EHL) products. The goal of prophylaxis is to maintain trough level greater than 1-5% of the norm (Jiménez-Yuste et al., 2014). Prophylactic therapy is the administration of replacement therapy in the absence of bleeding as a protective measure to prevent future joint disease by early initiation of treatment (at 1–2 years of age). This medical need led to the production of recombinant FIX products with a longer half-life in the circulation that required less frequent infusions for prophylactic therapy. In 2014, the FDA approved a recombinant FIX product with an Fc fragment of IgG tagged to FIX (ALPROLIX®). In 2017, the FDA approved another EHL recombinant FIX product with albumin fusion protein (FIX-FP, IDELVION®) with a reduced dosing frequency to 14 days in HB patients (Packages insert - IDELVION® - US Food and Drug Administration). A GlycoPEGylated recombinant FIX, REBINYN® was also approved by FDA for routine prophylaxis and on-demand treatment of HB patients.

2.4.2 Standard-of-care for HB

Today's standard-of-care in HB patients is replacement therapy with EHL products. There are several EHL products on the market. They all achieve longer half-life but by using different strategies.

- IDELVION®, as mentioned previously, is tagged to albumin by a cleavable linker. In its inactive form, it circulates in plasma as a zymogen fused to albumin. Once activated, albumin is cleaved, and the active form is comparable to the normal plasma-derived FIX.
- ALPROLIX® contains the Fc region of human IgG1 fused to FIX at the C-terminus by a non-cleavable covalent linker. Therefore, the active form of FIX would retain the Fc fragment.

The long half-life of albumin and Fc portion of IgG is mediated by the neonatal Fc Receptor (FcRn) that functions as a recycling or transcytosis receptor, responsible for maintaining IgG and albumin in the circulation.

- Rebynin® is a PEGylated rFIX. PEGylation of proteins is a biochemical modification process of molecules with polyethylene glycol (PEG). The attachment of these PEG chains to proteins increases the size of the protein. Since kidneys filter substances based on size, PEGlylated molecules that have a higher molecular weight and larger hydrodynamic radius are cleared from the kidney at slower rates, resulting in increased *in vivo* half-life of pegylated molecules.

- BeneFIX® is a standard half-life product, as mentioned before. Interestingly, it has been approved for long term prophylaxis against bleeding.

Recently, the relevance of EHL FIX is being challenged by an emerging concept that in addition to circulating FIX, extravascular FIX that's not measurable in plasma, contributes to hemostasis. This suggests that the half-life of FIX and measurable levels in plasma may not be the only determining factor of hemostatic efficacy in the HB disease. In this work, the term extravascular space refers to non-circulating FIX that can bind outside the plasma, i.e., to the vascular endothelium or subendothelial extracellular matrix.

2.5 The phenomena of extravascular FIX reservoir

The notion of extravascular FIX was first reported in 1987, when Stern et al. injected increasing amounts of bovine FIX into baboons and measured the concentration of baboon FIX released into the circulation by using an antibody specific for baboon FIX: when high levels of bovine FIX were infused intravenously, the antigen levels of baboon FIX were found to rise to over twice normal levels (Stern et al., 1987a). Thus, there exists important evidence in a primate model that large amounts of FIX both exist and are displaceable from extravascular reservoirs. Their data showed a rapid, reversible equilibrium between blood and extravascular FIX (Stern et al., 1987b). Later studies demonstrated direct binding of FIX to culture endothelial cells. *In vitro* experiments show that the zymogen form of FIX binds reversibly to vascular endothelium (Chu et al., 1996; Stern et al., 1983; Wolberg et al., 1997a) and possibly to platelets (Ahmad et al., 1989).

Previous publications in mice and rats demonstrated that an albumin fused rFIX distributes into relevant target tissues and retains its clotting activity *in vitro*. Thus, extravascular rFIX can facilitate its therapeutic activity (Herrmann et al., 2020). More recently, experiments in HB mice have shown that rFIX can occupy endothelial and extravascular reservoirs and convey hemostatic protection for more than seven days while being undetected in plasma. This study also estimated in a mathematical model that there are several folds more FIX contained in these extravascular reservoirs than in circulation (Cooley et al., 2019). In an attempt to characterize the phenomenon of extravascular FIX reservoir, Cheng et al mutated the vitamin K-dependent γ-carboxyglutamic acid (Gla) domain of rFIX at residue 5 to a variant that strongly interacted with collagen IV. A single point mutation of Lysine to Alanine (FIX_{K5A}) or Arginine (FIX_{K5R}) at residue 5 of FIX molecule resulted in altered endothelial cell binding affinity in a radioactive competition binding assay (Cheung et al., 1992). The FIX_{K5R} variant was shown to have higher binding affinity to endothelial cells than wildtype FIX (FIX_{WT}) (Cheung et al., 1996a) and the FIX_{K5A} variant failed to bind bovine aortic endothelial cells but retained normal clotting activity (Cheung et al., 1992). Collagen IV was postulated as the candidate for FIX binding site on endothelial basement membrane (Stafford, 1992). In line with these findings, studies in HB mice exhibited prolonged efficacy in a saphenous vein bleeding model despite <1% of normal plasma FIX levels (Cooley et al., 2016). This finding argues that prolonged hemostatic efficacy is mediated not only by circulating FIX, but also by FIX sequestered in the extravascular space. In addition, treatment with exogenous rFIX yielded a better hemostatic efficacy in HB mice compared to transgenic mice expressing a dysfunctional human FIX, implying that saturation of extravascular FIX binding sites by dysfunctional FIX reduced hemostatic efficacy.

A knock-in mice model expressing FIX with low-binding affinity to components of the extracellular matrix (FIX_{K5A}) was developed (Gui et al., 2009a). Although the K5A knock in mice had 120% higher circulating FIX protein than wildtype, K5A knock in mice exhibited a mild bleeding tendency. A chromogenic assay based on FXa generation after activation by FXIa confirmed no detectable difference in FIX activity between K5A knock in mice and wildtype mice. Additionally, wildtype and K5A knock-in mice performed similar in a tissue factor-initiated thrombin generation assay. Despite similar FIX activity levels and tissue factor-initiated thrombin generation levels the K5A knock in mouse displayed a mildly hemophilic phenotype. The increased circulating level of FIX is potentially attributed to decreased binding of FIX_{K5A} to collagen IV in the extravascular space. The hemophilic phenotype was demonstrated using different methods including the demonstration of prolonged primary and secondary bleeding in the tail clip challenge, slow time to occlusive thrombus formation in the ferric chloride-treated mesenteric arterioles, all suggesting that there is likely a physiologic role for the binding of FIX to components of the extravascular space (Gui et al., 2009b).

The biological importance of extravascular FIX under physiological conditions is not yet clear and could explain in part some discrepancies in the outcome of patients suffering from HB. In patients who receive continuous infusion of FIX for surgery, the amount of FIX required to maintain a level of 100% decreases with time, although binding sites are being saturated. These data suggest the existence of a significant extravascular FIX compartment. Furthermore, FIX injected into patients with HB lacking antigen (CRM-) disappears more rapidly than FIX injected into patients with normal levels of inactive FIX (CRM+) (Feng et al., 2013; Uprichard et al., 2012). A possible explanation is that the inactive FIX in CRM+ patients occupy the extravascular space, but in CRM- patients, the injected FIX quickly disappears from plasma into the extravascular compartment.

Coagulation and hemostasis are long-standing research fields but despite great advances in therapeutic approaches for HB disease, the inaccessibility to samples beyond plasma makes investigations on extravascular FIX rather speculative. Elucidating the molecular and clinical impact of rFIX outside the plasma is challenging but is needed to understand these phenomena and its implication in hemostasis. It would not only give important insights on biological function of FIX but could help to optimize the treatment and therapeutic approaches. In addition, understanding extravascular FIX vs. circulating FIX in plasma opens new possibilities to identify novel strategies that can be incorporated in current HB therapies.

2.6 Aim of the study

The aim of this study is to investigate the biological importance of extravascular FIX using currently available SHL (BeneFIX®, $rFIX_{WT}$) and EHL (IDELVION®, $rFIX_{WT}$-FP) products. The single amino acid substitution, described by Darrel Stafford and colleagues, at position 5 from lysine to alanine (K5A) greatly decreased the binding to collagen IV, while a substitution from lysine to arginine (K5R) increased binding affinity (Stafford, 2016). Each of the rFIX variants were generated as SHL and EHL proteins, purified and characterized *in vitro* and *in vivo* in HB mice. The effect of substitutions at residue 5 of the FIX Gla domain on *in vivo* FIX function was investigated using a tail clip bleeding model and arterial thrombus model. The wildtype proteins BeneFIX® ($rFIX_{WT}$) or IDELVION® ($rFIX_{WT}$-FP) were used as reference for the SHL and EHL rFIX K5x variants, respectively. The disposition of $rFIX_{WT}$ and $rFIX_{WT}$-FP was characterized by pharmacokinetic studies, and direct measurements of rFIX distribution in the extravascular reservoirs was evaluated using immunohistochemistry. Finally, the efficacy studies in HB mice were restricted to SHL proteins ($rFIX_{WT}$, $rFIX_{K5A}$, and $rFIX_{K5R}$) to give insights on the role that rFIX likely plays while residing in the extravascular space and compare the results with available published data. Murine models of HB have played an essential role in the investigations in this field.

2.6.1 Murine model of HB

The strain used for this work was originally generated by the group of Darrel W. Stafford, who pursued a "plug-and-socket" strategy by deleting the promoter and the first three exons of the FIX gene by the insertion of a neo gene plus a partially deleted hypoxanthine phosphoribosyl transferase minigene. One advantage of the plug and socket design allows the subsequent insertion of other sequences into the same locus of correctly targeted embryonic stem cells. The generated FIX ko mouse (B6.129P2-F9<tm1Dws>) did not produce hepatic FIX mRNA and hence no detectable FIX protein was observed. These mice had a CRM- phenotype (no FIX antigen detectable) and exhibited excessive bleeding with hemostatic challenges such as tail clip. The FIX ko mice breed normally and only rare loss of homozygous females due to hemorrhage in the peripartum period was observed. Most pups survive normally to wean and into adulthood without bleeding. Aside from the FIX defect, the carrier female and hemizygous male mice had no liver pathology, were fertile and transmitted the FIX mutation in the expected Mendelian frequency. Spontaneous bleeding in the HB mice was rarely observed, although musculoskeletal bleeding was seen, in particular after fighting with cage mates (Lin et al., 1997).

Hemostatic correction in small animal model proved to be efficient in a preclinical setting and important insights in the FIX biology have been gained from *in vivo* experiments, amongst others: transcriptional regulation of FIX gene expression has been modeled extensively in engineered mouse models, mapping of transcription factor binding and regulation of the FIX promoter has been experimentally modeled in mice that recapitulate the hemophilia B Leyden phenotype, demonstrating age-dependent and sex-specific post-pubertal increases in FIX expression (Boland et al., 1995; Brady et al., 1998; Sweeney and Hoernig, 1993). Altogether, HB mice have been key for preclinical pharmacokinetic (PK) / pharmacodynamic (PD) evaluation and characterization of *in vivo* properties of therapeutic candidate molecules. Even though, it is clear that the mouse PK are not the same as in humans (Østergaard et al., 2011) for instance, the circulating half-life of FIX is shorter in mice than in humans. Nevertheless, there has been consistency in the relative kinetics that have been demonstrated in mice and those subsequently confirmed in humans (i.e., agreement that the novel therapeutic is biologically equivalent, inferior, or superior to approved rFIX in small and large species) (Østergaard et al., 2011). HB mice have been employed for preclinical testing of relative pharmacodynamic of therapeutic candidate FIX proteins in hemostatic challenges (Greene et al., 2010; Hoffman, 2008).

Altogether, HB mice have been proven as an effective model organism for pharmacokinetic and pharmacodynamic studies. For these reasons, the phenotype of HB mice was used to resemble the bleeding tendency in human disease. The efficacy of rFIX proteins was compared in well-known and established models of vascular challenge: Tail clip bleeding and mesenteric thrombosis models in HB mice.

2.6.1.1 Tail clip bleeding model

Bleeding assay is widely used as an *in vivo* assessment of hemostatic action of platelets in rodents. In brief, this assay involves a longitudinal incision or transverse

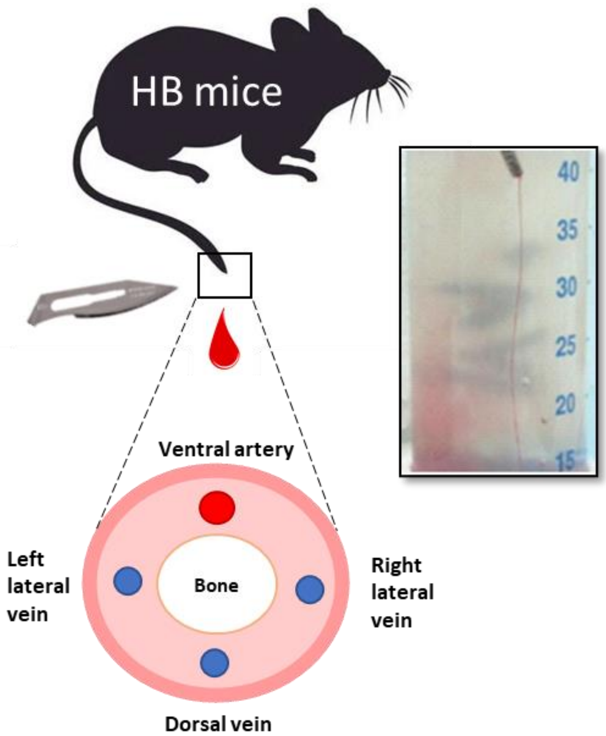

Figure 9. Schematic of tail clip bleeding assay in mice.
Bleeding assay was conducted by amputation of the tail tip which was immersed in saline (37°C). Blood is collected in a falcon tube (photo on the right) over a defined period.

amputation of the tip of the tail (Figure 9). Bleeding in then monitored over a defined period: Time to hemostasis is quantified as the time until bleeding stops. The volume of total blood loss is calculated by measuring the hemoglobin lost during the experiment. However, the protocol of the bleeding assay varies considerably among laboratories.

The collection of the blood is conducted in some labs with filter paper and in other labs dipping the tail into tubes with isotonic solution. Bleeding time (termed also as bleeding incidence) is usually defined as the time of the first cessation of bleeding although recurrence of bleeding is known to occur. Therefore, each lab defines their own criteria for the endpoints and the comparison of results between different labs is troublesome.

Though some of the available data in the literature is based on the survival after tail vein transection, many academic groups evaluate bleeding time as the final endpoint in fully anesthetized mice for ethical reasons. In this work, the latter model was conducted and the time to hemostasis was quantified as the time until bleeding stops for a minute.

2.6.1.2 Ferric chloride mesenteric thrombosis model

Bleeding time is largely determined by the interaction between platelets and damaged vessel wall leading to hemostatic thrombus formation. There is a wide spectrum of thrombosis models, with different triggers and techniques to induce thrombosis. Although, in the ferric chloride ($FeCl_3$) thrombosis model (Figure 10) the thrombus is induced by a chemical stimulus and does not mimic the pathophysiology of thrombosis in a clinical setting, it is a valuable tool to investigate platelet activation in the context of a closed vascular system. It is sensitive to both anticoagulant and anti-platelets drugs and is therefore, a very useful model to evaluate the importance of plasma proteins in thrombus growth.

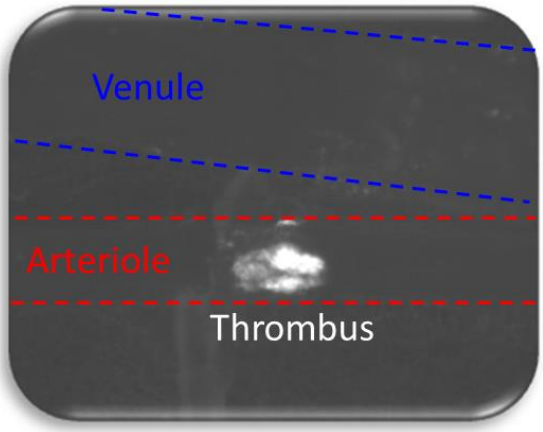

Figure 10. Setting-up of $FeCl_3$- induced mesenteric arterial thrombosis model.
After topical application, the thrombus formation is monitored by means of intravital microscopy.

The model has been successfully used to screen inhibitors of platelet activation and aggregation or antagonists of platelet receptors (Dogné et al., 2004; Hechler et al., 2011a; Saldanha et al., 2011). To mention a few, the role of platelet fibrinogen receptor, glycoprotein IIb/IIIa (Ni et al., 2000), the platelet ADP receptor, P2Y12 (André et al., 2003), platelet endothelial adhesion molecule-1 (Falati et al., 2006), inhibitor of FYa (Hechler et al., 2011b), cyclooxygenase 1/2 (Riehl et al., 2011), and microparticles (Thomas et al., 2009), have been elucidated using this mode. This vascular injury model has demonstrated the antithrombotic roles of clinically approved platelet aggregation inhibitors, including aspirin (Wang et al., 2006), clodiprogel (Wang and Xu, 2005), and ticagrelor (Patil et al., 2010). The model has been thoroughly characterized. Application of $FeCl_3$ at a defined concentration on the outer surface of artery results in a free radical-induced injury that disrupts the vascular endothelium but with limited collagen exposure in the subendothelial matrix. This vascular injury induced by $FeCl_3$ results in aggregation of platelets leading to thrombus formation and subsequent occlusion of the artery (Eckly et al., 2011).

3 MATERIALS AND METHODS

3.1 Recombinant FIX (rFIX) constructs

In this work, rFIX molecules modified at position 5 of Gla domain with ($rFIX_{K5A}$-FP and $rFIX_{K5R}$-FP) and without albumin fusion ($rFIX_{K5A}$ and $rFIX_{K5R}$) were investigated and compared with a marketed $rFIX_{WT}$ product (BeneFIX®) and $rFIX_{WT}$-FP (IDELVION®).

3.1.1 Reference rFIX

BeneFIX ® (Pfizer Limited, United Kingdom) is a recombinant FIX that is structurally equivalent to the wildtype FIX and was selected as a control for non-fused rFIX ($rFIX_{WT}$) variants. IDELVION® (CSL Behring, Germany) is a recombinant FIX fused to albumin that is described as rFIX fusion protein ($rFIX_{WT}$-FP) and is used as a control for albumin fused rFIX-FP variants.

3.1.2 Modified rFIX

The tested rFIX variants are distinguished by one substitution in the human amino acid sequence at position 5, which is expected to result in increased ($rFIX_{K5R}$) or decreased ($rFIX_{K5A}$) binding affinity to components of extracellular matrix. The single point substitution at position 5 from lysine to alanine (K5A) or arginine (K5R), was introduced in rFIX and rFIX-FP. The detailed methods on preparation, transfection, cultivation, and purification of rFIX and rFIX-FP variants are described in sections 3.3 and 3.4.

3.2 List of devices, software and reagents

3.2.1 Devices and software

Devices and Software	Company	Assay
Amaxa Nucleofactor™ II/2b	Lonza Group AG, Basel, Switzerland	1) Cell culture
AxioCam MR R3	Carl Zeiss Microscopy GmbH, Jena, Germany	1) Histology 2) Thrombosis model
Band-pass filters, beam splitters	Carl Zeiss Microscopy GmbH, Jena, Germany	1) Histology
BCS®XP	Siemens Healthcare Diagnostics Products GmbH, MBR, Germany	1) OSCA 2) aPTT
ChemiDoc™ MP Image System	Bio-Rad, Hercules, CA, USA	1) SDS-PAGE
ELISA Reader (ELx800)	BioTek Instruments GmbH, Winooski, Vermont, USA	1) ELISA
FIJI software	Image J, Public Domain	1) Histology
Gen 5 software ®	BioTek Instruments, Inc., Winooski, VT, USA	1) ELISA
GraphPad Prism 8.0 Software	GraphPad Softioare Inc., Winooski, VT, USA	
HXP 120 V lamp	Carl Zeiss Microscopy GmbH, Jena, Germany	1) Histology
Image Lab software	Bio-Rad, Hercules, CA, USA	1) SDS-PAGE
Leica EG1160 Tissue Embedding Station	Leica Microsystems AG, Wetzlar, Germany	1) Histology

Leica TP1020 Tissue Processor	Leica Microsystems AG, Wetzlar, Germany	1) Histology
Lunatic UV/Vis reader	Unchained Labs, Pleasanton, CA	1) Protein concentrations
Magellan™-Data Analysis Software	TECAN Group Ltd., Männedorf, Switzerland	1) ELISA 2) FXa generation
Manual rotatory microtome RM2255	Leica Microsystems AG, Wetzlar, Germany	1) Histology
Megafuge 1.0 R (75003060)	Thermo Electron LED GmbH, Osterode, Germany	1) Plasma samples
Microplate thermoshaker	Grant Instruments Ltd™, Shepreth, UK	1) FXa generation 2) FIXa generation
Microplate washer (ELx405)	BioTek Instruments GmbH, Winooski, Vermont, USA	1) ELISA
Milli-Q-Water purification system	Merck KGaA, Darmstadt, Germany	
Photometer (LED 96)	DEELUX Labortechnik GmbH, Gödenstorf, Germany	1) ELISA
Plan-Apochromat 20x/0.8 M27	Carl Zeiss Microscopy GmbH, Jena, Germany	1) Histology
ProtParam tool	Open access on ExPASy server	
Stretching Table OTS 40	Medite GmbH, Burgdorft, Germany	1) Histology
Thermo-Mixer®	Eppendorf AG, Hamburg, Germany	1) Activation of FIX

		2) FXa generation
Tissue floating bath Type 249000	Medax GmbH & Co, Rendsburg, Germany	1) Histology
Ventana Discovery XT	Roche Diagnostics GmbH, Mannheim, Germany	1) Histology
Vi-Cell™	Beckman Coulter Inc, CA, USA	1) Cell culture
Water bath, Typ P/3	Julabo Labortechnik, Seelheim, Germany	
Zeiss Axio Scan.Z1	Carl Zeiss Microscopy GmbH, Jena, Germany	1) Histology
ZEN 2.3 lite blue edition	Carl Zeiss Microscopy GmbH, Jena, Germany	1) Histology

3.2.2 Disposables

Material (catalog number)	Company
1 mL Solo Single-use Syringe OMNIFIX-F B (REF 9161502)	B. Braun AG, Melsungen, Germany
Clear Round-Bottom Immuno 2HB Nonsterile 96-Well Plates (3655)	Thermo Fisher Scientific, Waltham, MA, USA
Micropipette, Pipette tips & accessories	Eppendrof AG, Hamburg, Germany
Microtiter plate Nunc Immuno-Plate Maxisorp (449824)	Millipore Sigma, Burlington, MA, USA
Microtiter plate Nunc ™	Thermo Fisher Scientific, Waltham, MA, USA
Novex WedgeWell 8-16% Tris-Glycine Gel (10 Well)	Thermo Fisher Scientific, Waltham, MA, USA

Pasteur pipette, 2 mL (10001367)	PharmaServ, Marburg, Germany
Reaction vessels 1.5 mL (780500)	Brand GmbH & CO. KG, Wertheim, Germany
Scalpel Blades and Handles	Aesculap, Tuttlingen, Germany
Transparent 96-Well plate, Flat Bottom (781602)	Brand pureGrade ™, Brand GmbH, Wertheim, Germany

3.2.3 Reagents and Kits

Reagents and Kits (catalog number)	**Company**
1-Step™ TMB Buffer	Thermo Fisher Scientific, Waltham, MA, USA
AFSTYLA®	CSL Behring GmbH, Marburg, Germany
Aqua ad iniectabilia (WFI)	Braun Melsungen AG, Melsungen, Germany
BeneFIX®	Pfizer Inc, Philadelphia, PA, USA
BSA	Millipore Sigma, Burlington, MA, USA
$CaCl_2$ (ORHO 37)	Siemens Healthcare GmbH, Marburg, Germany
Carbonate-Bicarbonate Buffer (C-3041)	Millipore Sigma, Burlington, MA, USA
Cell conditioner (CC1) buffer	Roche Diagnostics GmbH, Mannheim, Germany
Chromogen TMB (OUVF)	Siemens Healthcare GmbH, Munich, Germany

Control plasma N (ORKE41)	Siemens Healthcare GmbH, Munich, Germany
Control plasma P (OUPZ 17)	Siemens Healthcare GmbH, Munich, Germany
FXa generation Assay (FIX chromogenic assay) Kit containing R1, R2, R3, and R4	CoaChrom Diagnostica, Vienna, Austria
FIX deficient plasma (OTXX17)	Siemens Healthcare GmbH, Marburg, Germany
FIXa substrate	Bachem GmbH, Bubendorf, Switzerland
FXIa substrate (233483)	Merck KGaA, Darmstadt, Germany
Hemoglobin Assay Kit (MAK115)	Sigma-Aldrich Co. LLC, St. Louis, MO, USA
Human plasma-derived FX	CoaChrom Diagnostica GmbH, Maria Enderdorf, Germany
IDELVION®	CSL Behring GmbH, Marburg, Germany
Imidazol Buffer (521536A)	Siemens Healthcare GmbH, Munich, Germany
Inhibitor CM	Roche Diagnostics GmbH, Mannheim, Germany
Ketamine 10% (1292)	CP-Pharma, Burgdorf, Germany
NaCl 0.9% (1.06400.1000)	B. Braun Melsungen AG, Melsungen, Germany
Narcoren®	Merial GmbH, Hallbergmoos, Germany

Novex Tris-Glycine SDS Running Buffer (LC2675)	Thermo Fisher Scientific, Waltham, MA, USA
Novex Tris-Glycine SDS Sample Buffer (LC2676)	Thermo Fisher Scientific, Waltham, MA, USA
OmniMap goat anti-rabbit HRP	Roche Diagnostics GmbH, Mannheim, Germany
Paired Antibody Test Kit (CL20041K)	Cedarlane Laboratories, Burlington, Ontario, CA
Pathromtin SL (OQGS35)	Siemens Healthcare GmbH, Marburg, Germany
PBS-Tween (Waschpuffer)	Millipore Sigma, Burlington, MA, USA
Quick Coomasie Stain (35081)	Serva Electrophoresis GmbH, Heidelberg, Germany
Rabbit anti-human FIX antibody	Abcam, Cambridge, UK
Rhodamine Kit	Roche Diagnostics GmbH, Mannheim, Germany
SeeBlue Plus 2 Pre-stained Standard (LC9525)	Thermo Fisher Scientific, Waltham, MA, USA
Standard Human Plasma (ORKL17)	Siemens Healthcare GmbH, Munich, Germany
Stop solution (OUVP25)	Siemens Healthcare GmbH, Munich, Germany
TBS with 1% BSA	Millipore Sigma, Burlington, MA, USA
TBS with Tween 20	Millipore Sigma, Burlington, MA, USA

Tranquisol 10 mg/mL *(Acepromazine)*	Ceva Tiergesundheit GmbH, Düsseldorf, Germany
Trisodium citrate 3,13% (F00054)	Eifelfango, Bad Neuenahr-Ahrweiler, Germany
Tween 20 (8.17072.1000)	Merck KGaA, Darmstadt, Germany
Xylazine 2% (1206)	CP-Pharma, Burgdorf, Germany

3.2.4 Buffers

Name	Recipe	Assay
Block buffer A	0.05 M Tris buffered saline (0.138 M NaCl; 0.002 KCl; bovine serum albumin - 1% (w/v), pH 8.0	ELISA
Block buffer B	5% (w/v) BSA-PBS	ELISA
Coating buffer	0.05 M Carbonate-Bicarbonate	ELISA
Dilution buffer A	50 mM Tris, 150 mM NaCl, 2 g/L Trehalose, pH 7.4	FIX activation
Dilution buffer B	50 mM Tris, 100 mM NaCl, 5 mM $CaCl_2$, 60% Ethylenglycol	FXa generation assay
Dilution buffer C	0.05 M Tris buffered saline (0,138 M NaCl; 0.003 KCl M); 0.05 % Tween 20, pH-Wert 8.0	ELISA
Dilution buffer D	10 mM L-Histidine, 260 mM Glycine, 1% Saccharose and 0.005% Tween 80, pH 6.8	FIXa generation assay
Equilibration buffer	20 mM HEPES, pH 6,2; 50 mM NaCl; 12 nM EDTA	Protein purification

Elution buffer	20 mM HEPES pH 6.2; 100 mM NaCl; 10 mM $CaCl_2$	Protein purification
Regeneration buffer	20 mM HEPES pH 6.2; 1000 mM NaCl	Protein purification
Wash buffer A	20 mM HEPES pH 6.2; 100 mM NaCl	Protein purification
Wash buffer B	0.05 M Tris buffered saline (0,138 M NaCl; 0.003 KCl M); 0.05 % Tween 20, pH-Wert 8.0	ELISA

3.3 Molecular biology

The proteins containing the single point mutation in the FIX proteins were generated by the Recombinant Technology department in CSL Behring Innovation GmbH.

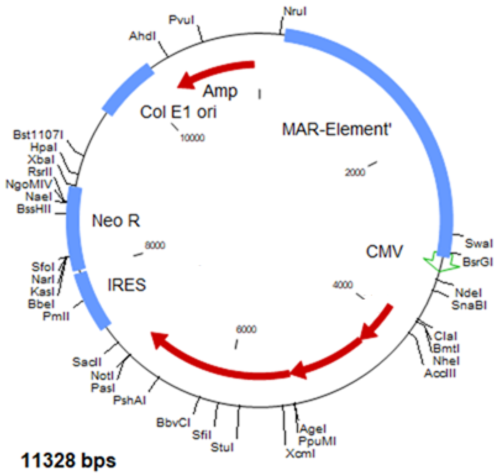

Figure 11. The plasmid DNA (pMARES) utilized for the generation of stable transfected Chinese Hamster Ovary (CHO) cells expressing rFIX constructs.

Single point mutation in the FIX gene was performed using site-directed mutagenesis techniques. The prepared FIX DNA was cloned into plasmid vector pMARES (Figure 11) by restriction digestion with the endonuclease *DpnI*, followed by fragment purification, fragment ligation, and transformation into an E. coli strain

(XL10-Gold Ultracompetent, Agilent Technologies) for plasmid amplification. The transformed colonies were selected by their resistance to Ampicillin due to the antibiotic-resistance gene in the plasmid. The colonies were picked cultivated, purified and digested with restriction enzymes, to confirm the successful cloning of the insert construct. The single point mutation was confirmed, by sequencing the mutation site.

3.4 Cell culture, transfection and purification methods

The proteins containing the single point mutation in the FIX proteins were purified and kindly provided by the Recombinant Technologies Department in CSL Behring Innovation GmbH. The mammalian Chinese hamster ovary (CHO) cell line was used for the expression of recombinant FIX variants. The combination of good genome stability and high rates of vector incorporation makes CHO cells an ideal tool for producing recombinant proteins. Furthermore, these mammalian cells tend to form the same post-translational modifications (PTMs) as human cells (Bryan et al., 2021). Cultivation in a chemically defined CHO medium Gibco® was performed in tissue culture flasks stored at 5-7.5% (+/- 1%) CO_2 and 37 °C (+/-1 °C) in a CO_2 incubator. The CHO cell culture grown in the exponential phase, with a cell density of $5x10^5$-$2x10^6$ and a vitality of ≥98% was prepared for transfection. A sample was taken to determine cell count and viability using the Vi-Cell™ cell counter device. A volume containing $1x10^6$ cells/ml was centrifuged at 300x g for 5 minutes at RT in the Heraeus Megafuge and the supernatant was removed. The pellets were then resuspended in 100 µL transfection buffer and 10 µL (4 µg) of DNA was added. After electroporation (electrical pulse) with the Amaxa Nucleofector™ (2b) device. The samples were then further cultured in 12 well plates with the addition of cell culture medium for 3 days in a CO_2 incubator. Transfected cells were then cultured in antibiotic-containing medium (Geneticin) as a selection pressure for clones transfected with the plasmid containing the neomycin resistance gene. To generate a homogeneous cell population (monoclonal cell line), the transfectant pool was diluted in a limiting dilution scheme into 96 well plates, for single clone selection. Selection parameters were high FIX antigen (FIX:Ag) and clotting activity (FIX:C) levels. The selected clones were frozen and stored at -150°C. The selected CHO single cell clones were cultivated in shaker flasks to build up a seed strain for protein production in a 5 L bioreactor, Biostat Digital Control Unit (DCUs) (Fa Sartorius, Germany). Biostat DCUs is a classical glass stirred tank reactor and allows good control and adjustment of optimal growth conditions for the cells to express the integrated protein, into the media. During fermentation, parameters such as temperature, pH, oxygen partial pressure and carbon dioxide content were continuously measured and controlled in situ. The cells were harvested after 5-7 days, when the cell culture reached the stationary growth phase. The cell suspension was harvested, and the supernatant was separated from the cells with a filter. The supernatant containing the target protein was stored at -20°.

The purification of proteins from the cell culture supernatant was performed with ÄKTA Avant chromatography system (GE Healthcare Life Sciences, USA) using anion exchange chromatography over a POROS™ 50 HQ column (Thermo Fisher Scientific, USA). Anion exchange chromatography is suitable for the purification of FIX due to isoelectric point of ~5.4. The further away the pH value is from the isoelectric point of the protein the stronger it binds. Therefore, the buffer used had a pH value of 6.2, which causes FIX to assume a net negative charge and bind to the anion exchange column medium. The column was first treated with equilibrium buffer (see section 3.2.4), which attaches free positive groups to the column. Negatively charged molecules bind as they pass through the positively charged column (30 mL/min). Positive and uncharged molecules are not retained and are easily remove with wash buffer A (see section 3.2.4). Column bound FIX protein is then eluted with a high salt concentration buffer containing calcium-chloride (elution buffer, see section 3.2.4). These ions have a high affinity for the charged groups of the column and displace bound protein. The eluate was further concentrated and purified via size exclusion chromatography on a S200 Resin

(Cytiva). Finally, the target protein was taken up from the gel filtration column in the regeneration buffer (RP; Section 3.2.4), thus the size exclusion chromatography (SEC) had two functions, the buffer exchange and purification of aggregates and proteins larger than ~200 kDa. The purified product was then subjected to protein analysis. The purity was determined by sodium dodecyl sulfate-polyacrylamide gel electrophoresis (SDS PAGE), the protein concentration was determined by measuring the UV absorption (see section 3.5.1) and by enzyme-linked immunosorbent assay (ELISA) (see section 3.5.3) and the activity was measured in a one-stage coagulation assay (see section 3.5.2). Finally, the product was aliquoted and stored at -20 °C until further use.

3.5 Determination of the protein concentration

3.5.1 UV- Spectrophotometrical measurement

The concentration of all recombinant rFIX proteins was determined by absorbance at 280 nm based on an extinction coefficient of 1.33 mg/mL/cm calculated by ProtParam for BeneFIX® and non-fused rFIX variants. IDELVION® and the albumin fused variants were measured based on an extinction coefficient of 0.9 mg/mL/cm. BeneFIX® ($rFIX_{WT}$) and IDELVION® ($rFIX_{WT}$-FP) were used as the wildtype reference proteins in all experiments.

3.5.2 One-stage clotting assay (OSCA) of purified rFIX

The potency assignment of rFIX substances was determined using OSCA (FIX:C) and is given in international units (IU) for its activity. The rFIX concentrates were determined with the silica surface activator Pathromtin® SL. The test was performed on a fully automated Behring Coagulation System (BCS) analyzer. FIX:C was estimated using a reference curve prepared from standard human plasma (SHP) which was calibrated by the manufacturer against the WHO international standard for FIX. Dilutions were performed in FIX deficient plasma. Each sample was manually prepared with measuring buffer with a minimum required dilution of 1:50. On the BCS device were then contained 20 µL of the prepared sample, 50 µL FIX deficient plasma, 75 µL aPTT and was incubated for 120 seconds before the addition of 75 µL $CaCl_2$ solution. If a higher dilution than 1:100 in FIX deficient plasma was required, the stock solution was pre-diluted in Imidazol buffer. Measurement of the stock solution was carried out using a validated and pre-defined program set-up in BCS. Prior to measuring the samples of interest, internal quality controls were tested. Two different quality control samples provided by the manufacturer of the BCS analyzer (normal range about 80-100% and pathological range about 30-40%) were measured at start of the run. The controls and samples were processed under identical conditions.

The specific activity was calculated as follows and stated in IU/mg:

FIX:C (IU/mL)/FIX protein amount (mg/mL).

The estimated potency was calculated as follows:

FIX:C (IU/L)/FIX molar concentration (nM), the molar concentration was calculated by dividing FIX protein amount by molar mass of FIX protein.

3.5.3 Enzyme-linked immunosorbent assay (ELISA) of purified rFIX

A paired antibody ELISA kit was used to estimate FIX concentrations. Stock solutions were thawed in a water bath at 37 °C and were diluted at least 1:100 with dilution buffer C (see section 3.2.4). SHP or $rFIX_{WT}$-FP were used as standards for the calibration curve. Concentration of FIX in the samples was measured on 96-well plates pre-coated overnight at RT with FIX capture antibodies that were diluted at 1:200 in coating buffer (see section 3.2.4). The plates were then washed 3 times with wash buffer B and blocked for 1.5 hours with block buffer A (see section 3.2.4) to prevent non-specific binding of detection antibodies to the plate. Block buffer was washed 3 times with wash buffer B (see section 3.2.4). The diluted stock solutions and plasma samples were incubated for 1.5 hours at RT. Following three wash steps, samples were incubated with peroxidase-conjugated secondary antibody (1:200

diluted) for 1.5 hours at RT. Finally, the Ultra tetramethylbenzidine (TMB)-Substrate, previously stored at RT in the dark, was added to the wells and incubated for ~30 minutes before stopping the reaction with stop solution (Cat. Nr OSFA from Siemens Healthcare Diagnostics Inc). Conversion of tetramethylbenzidine substrate was measured photometrically at 450 nm.

3.6 *In vitro* characterization of generated rFIX variants

The in-house generated rFIX proteins and reconstituted commercially available rFIX products were aliquoted and stored at -70 °C until further analysis. Reconstitution was performed as indicated in the manufacturer's instructions. Stock solutions were thawed in a water bath at 37 °C. For these experiments a maximum of 2 freeze-thaw cycles were allowed to keep experiments consistent and comparable.

3.6.1 Activated partial thromboplastin time (aPTT)

To assess the efficacy *in vitro*, clotting time was determined on the BCS XP with Pathromtin® SL as activator and SHP as reference curve. The stock solutions of rFIX were prediluted in NaCl to 0.5 µM concentration and the final dilution was performed in FIX deficient plasma to achieve a final matrix ratio of 20% NaCl and 80% of FIX deficient plasma (0.1 µM). At the end, each sample contained 50 µL of FIX spiked in deficient plasma (diluted 20/80), 75 µL of the activator and 75 µL $CaCl_2$ solution. Measurement of the stock solution was carried on using a validated and pre-defined program set-up in BCS. Prior to measuring the samples of interest, internal quality controls were tested. Two different control samples provided by the manufacturer of BCS analyzer (normal range about 80-100% and pathological range about 30-40%) were measured at the start of the run. The controls and samples were processed under identical conditions.

3.6.2 Kinetics of activation of rFIX by rFXIa

To quantify the enzyme kinetics of FIX activation by FXIa, the cleavage of rFIX was monitored over time in 8-16% Tris-glycine SDS-PAGE. For activation of rFIX, final concentrations of 2 µM rFIX and 5 µM Ca^{2+} in dilution buffer A (see section 3.2.4) were mixed with 0.002 µM FXIa diluted in Imidazol buffer. Reaction mixture (1 mL) was incubated for 360 minutes in an Eppendorf Thermo-Mixer® at 37°C and aliquots of the reaction mixture were stopped with SDS loading buffer at various timepoints (0 min, 3 min, 5 min, 10 min, 30 min, 60 min, 90 min, 120 min, 240 min, and 360 min). The "0 min" sample was taken prior to the addition of rFXIa. The samples were treated for 5 minutes at 95 °C and were stored at -70 °C until loading on an SDS gel. The band intensities were detected by ChemiDoc™ MP Image System and quantification was performed using Image Lab software. A reaction mixture where rFIX was replaced by dilution buffer A was included in these experiments and served as negative control.

3.6.3 FXa generation by activated rFIX

The rate of FXa generation was determined using a reconstituted intrinsic factor Xase assay commercially available as FIX activity Biophen Kit. This chromogenic assay is described for FIX activity measurement in solution. In brief, the principle of the chromogenic FIX assay consists of a first step where the inactive tenase components FVIII and FX (R1) are mixed with FIX contained in the sample, then, the activation of FX is initiated by adding phospholipids, calcium, FXIa and FIIa (R2). Finally, the amount of activated FX is measured in a chromogenic reaction using FXa specific substrate (R3). The amount of tenase complex generated is in molar ratio to the amount of FX. This assay provides a linear correlation of FXa to FIX concentrations. In this study, the modification of the assay was required to study enzymatic kinetic of the individual components of the tenase complex (FX, FVIII, or FIX). The enzymatic kinetic measurements of the non-fused or albumin fused rFIX K5 variants were compared to their respective wildtype molecules, BeneFIX® or IDELVION®. Dilution series of either rFIX proteins, rFVIII or FX were prepared in Tris-BSA buffer (R4). The assay was carried out according to the manufacturer's instructions at 37 °C in a microplate thermoshaker, with the following modifications: R1 (FVIII and FX) reagent was prepared freshly before each experiment in serial dilutions of either rFIX (10-0.02 nM), FVIII (6-0.01 nM) or FX (200 -0.4 nM) and the other components were kept at constant concentrations: 3 nM for rFVIII (AFSTYLA®), 50 nM FX or 1.25 nM rFIX. The optimal concentrations were investigated in previous experiments using all the components contained in the kit as suggested by the manufacturer. The activation of rFIX was initiated after adding pre-warmed R2 (phospholipids, calcium, FXIa and FIIa) reagent. A standard curve of known FX concentrations and FXa activity was used to determine the concentration of FXa generated after addition of a FXa specific substrate, SXa-11, provided in the kit as R3 (FXa specific substrate). The measured OD was plotted as a function of time, and a linear fit in Microsoft Excel was used to calculate the initial rate of FXa generation (nM/min). The rate constants were estimated by fitting Michaelis-Menten kinetics model to individual experiment from three independent experiments. $rFIX_{WT}$, $rFIX_{K5A}$ and $rFIX_{K5R}$ proteins were tested under identical conditions and in the same plate. Similarly, albumin fused $rFIX\text{-}FP_{WT}$, $rFIX\text{-}FP_{K5A}$ and $rFIX\text{-}FP_{K5R}$ were tested together.

3.6.4 FIXa generation assay

FIXa activity was determined by a FIXa specific chromogenic substrate. A 2-fold serial dilution of the purified rFIX proteins with starting concentration of 2 µM to 0.16 µM was performed in a Tween-containing buffer (Dilution buffer D, section 3.2.4). The FXIa solution was diluted in Imidazol buffer to 0.001 µM or 0.002 µM for reaction mixtures containing non-fused rFIX and albumin fused proteins, respectively. The reaction mixture contained 5 mM $CaCl_2$ solution to initiate FIXa generation over 60 minutes at 37 °C in a microplate thermoshaker with 200 rpm. Finally, the amount of FIXa generated was determined using a FIXa specific chromogenic substrate at a concentration of 2.93 mM in ethylenglycol buffer (Dilution buffer B, section 3.2.4), according to manufacturer's instructions. After FIX activation was completed, the amount of FIXa was determined by measuring the rate of increase in absorbance at 405 nm every minute over 60 minutes at 37 °C. This absorbance was plotted as a function of time, and a linear fit in Prism Software was used to calculate the Michaelis-Menten constant (Km). The Km of the wildtype protein (rFIX$_{WT}$ or rFIX$_{WT}$-FP) were set as 100% and the Km of the K5 variants were compared to its respective wildtype protein. Each dataset (WT, K5A, and K5R) was generated simultaneously under identical conditions and in the same plate.

3.6.5 Michaelis constant equations:

Vmax refers to maximum velocity, km refers to Michaelis constant and h refers to hill constant. The Hill coefficient describes the steepness of the binding curve saturation and can provide the measure of cooperativity of ligand binding.

1) FXa generation calculated in Matlab R2019b using Hill-equation:

$$FXa = \frac{Vmax * x^h}{km + x^h}$$

x = Substrate concentration

2) FIXa generation calculated in Prism using Michaelis-Menten equation

$$FIXa = \frac{Vmax * x}{km + x}$$

x = Substrate concentration

3.7 *In vivo* characterization of rFIX

All animals were managed in accordance with animal care protection laws. All experiments were carried out with the approval of the Regional Council of Giessen Society of Laboratory Animal Science Associations (FELASA). HB mice (B6.129P2-F9tm1Dws/J) were obtained from Charles Rivers Breeding Laboratories (Germany).

3.7.1 Pharmacokinetics and liver sampling (PK) in HB mice

If not stated otherwise, rFIX proteins were administered intravenously at doses of 25 nmol/kg based on protein amount to HB mice (n=3-5) and blood samples were collected at several timepoints: 5 minutes, 2, 6, 24, 48, 72, 120, and 144 (6 days), 168 (7 days), 240 (10 days), and 336 hours (14 days). Blood samples to generate plasma were taken retro-orbitally at all timepoints as described in section 3.7.4, and additionally terminally by puncturing of the vena cava under deep anaesthesia (Ketamin 65 mg/kg, Xylazin 13 mg/kg, and Acepromazin 2 mg/kg, mixed in the same syringe and given i.p.). Plasma samples were stored at approximately -70°C until further analysis of rFIX antigen and activity. After terminal bleeding, 3 animals per group were perfused with PBS and the liver was harvested for further analysis using immunohistochemistry. These animals received buprenorphine (0.3 mg/kg) s.c. 30-60 minutes prior to organ sampling. A non-compartmental approach was chosen to analyze the FIX antigen levels and was performed by Dr. Marcel Mischnik. The area under the curve from zero to the last measurable timepoint was calculated by the trapezoidal rule. The terminal elimination rate constant λ was estimated by fitting a linear regression line to the last 3, 4 and 5 natural logarithm transformed plasma levels by ordinary least squares. The model with the largest adjusted R^2 value was used for estimating the terminal elimination rate λ, the corresponding intercept b and the modeled plasma level at the last measured timepoint.

3.7.2 Tail clip bleeding model

Efficacy of rFIX molecules was studied in the tail clip bleeding model following 15 min, 24 hours, 72 hours, 168 hours or 336 hours post single intravenous or subcutaneous administration of FIX:C 50 IU/kg in 10±2 weeks old HB mice. $rFIX_{WT}$ concentrate was reconstituted and diluted to the proper dose based on the potency claimed in the label and the potency of the K5 variants was determined by OSCA. Animals were anaesthetized with pentobarbital (Narcoren®), 74.5 mg/kg intraperitoneal followed by amputation of the tails 3 mm from the tip. The shed blood was collected into 15 mL conical tube containing warm saline (37°C) for 30 minutes, with the tubes being changed every 10 minutes. Bleeding was followed visually over 30 minutes and time of cessation of blood flow was recorded and reported as bleeding incidence. A quantitative estimate of blood loss was determined by measuring the hemoglobin content of blood collected in saline. Erythrocytes within the tubes were lysed by a freeze-thaw cycle, and the absorbance of the sample was measured at a wavelength of 400 nm with a Hemoglobin Assay Kit according to the manufacturer's instructions. The animals were sacrificed, and terminal samples were collected from vena cava to determine plasma antigen and activity levels of injected FIX proteins.

3.7.3 Intravital microscopic mesentery arteriole thrombosis

Three-week-old male mice were injected with the labeled anti-platelets antibody (1 µg per gram body weight) via the lateral tail vein. The mesentery was exteriorized gently through a midline abdominal incision. Arterioles (35- to 65-µm diameter) were visualized with a Zeiss Axiovert.Z1 inverted microscope equipped with a MRm monochrome camera (Carl Zeiss Microscopy GmbH, Jena, Germany). The resting blood vessel was recorded for a few seconds, and 18% ferric chloride ($FeCl_3$; Sigma-Aldrich Chemie GmH, Taufkirchen, Germany) was topically applied on mesenteric arterioles with a piece of Whatman paper. Images were acquired every second and the thrombus formation of fluorescently labeled platelets was monitored for 40 minutes or until complete occlusion of the vessel. Time to complete occlusion of the arteriole, the size of thrombus normalized to the vessel area at complete occlusion, and the time of first thrombus formation was recorded. One blood vessel was recorded per animal. The experiments were performed in a randomized and blinded, only after analysis the results were unblinded.

3.7.4 Blood samples and plasma generation

If not stated otherwise, 10% citrate blood from vena cava or retroorbital plexus was collected using a syringe containing 1/10 of volume trisodium citrate (0.106 mol/L) at the end of *in vivo* studies to determine plasma exposure of rFIX proteins. Plasma was separated by centrifugation at RT for 10 minutes at 1800 x g and stored at -70 °C.

3.7.5 Determination of FIX:Ag level in plasma

The protocol described in section 3.5.3 was used to determine FIX protein concentration in plasma from HB mice. The FIX protein used in respective *in vivo* studies (injection solution) was used as standard. Additional experiments investigated the lower limit of quantification (LLOQ), linearity, recovery, and matrix effects in citrated mouse plasma of HB mice.

3.7.6 Determination of FIX:C level in plasma

The protocol described in section 3.5.2 was used to determined FIX:C activity levels in plasma from HB mice treated with human rFIX. This protocol uses SHP as the standard as mentioned above. If not stated otherwise, murine plasma samples were diluted at least 1:1.5 in human FIX deficient plasma. The lower limit of quantification (LLOQ), linearity, and recovery was tested for each rFIX solution separately.

3.7.7 Processing of tissue samples

Tissue samples from mice were harvested at various timepoints. Tissue samples (median lobe of the liver) were placed into 10% buffered formalin for fixation for ~48-72 hours in a formalin: tissue ratio of 10:1 (e.g., 5 mL of formalin per 0.5 cm^3 of tissue). After fixation, specimens were trimmed using a scalpel to enable them to fit into a tissue cassette and were then processed. The tissue processing consisted of dehydration, clearing with Xylene, and embedding the samples to enable their sectioning. Dehydration was performed to remove the water and the formalin from the tissue. This is achieved by immersing the specimen in increasing concentrations of alcohol (30% -90%). First, samples were watered for 1 hour to remove the formalin, the dehydration was performed manually in a graded ethanol series (30%, 50%, 70% ethanol, 1 hour each) and further incubation steps were performed in an automated tissue processor (Leica TP1020) using a pre-defined program (70, 80, 90, 2 x 96, 3 x 100% ethanol, 2 x Xylene, 2 x Paraffin, 1.5 hours each). The organic solvent Xylene was used to remove the alcohol from the sample and enable infiltration with Paraffin wax. Finally, specimens are embedded in paraffin wax in the embedding station (Leica EG1160). Once the block solidified, it was cut into thin 5 µm sections. The sectioning was performed in a rotatory microtome (Leica RM2255) and the thin slices were carefully transferred to a warm tissue floating bath (Medax GmbH, Neumünster, Germany) at 38-42 °C to allow the sample to stretch and remove wrinkles and folds for a better tissue adhesion to the glass of the slide. The slides were dried overnight in a stretching heating plate (MEDITE Medical GmbH, Burgdorf, Germany) at 37 °C prior to staining applications.

3.7.8 Immunofluorescence staining

Tyramide signal amplification (TSA) staining was performed on 5 µM thick sections from formalin-fixed-paraffin tissue using an automated staining system (Ventana Roche Diagnostics GmbH, Mannheim, Germany). Briefly, following heat-mediated deparaffinization and antigen retrieval in Tris-EDTA buffer, the endogenous peroxidase in the tissue was inhibited with Inhibitor CM. Slides were incubated with rabbit anti-human FIX antibody at 1µg/mL at RT for 1 hour followed by incubation with OmniMap goat anti-rabbit HRP. Sections were subsequently incubated with Rhodamine and H_2O_2 and mounted with DAPI mounting medium for further imaging analysis. Whole section images were acquired using identical acquisition settings in the Zeiss Axio Scan.Z1 with the Plan-Apochromat 20x/0.8 M27 objective and a monochromatic camera (AxioCam MR R3). The scanner was equipped with a HXP 120 V lamp, 395/570 beam splitter and a 335–383 band-pass emission filter for the red channel and a 538–562 band-pass emission filter for the blue channel.

3.7.9 Fluorescent Image analysis

Image analysis was performed either using ZEN 2.3 lite or FIJI image-processing package. All samples within an individual study were imaged with identical microscope settings. Fluorescence intensities in the liver samples were determined using a semi-quantitative method to determine the relative FIX protein abundance retained in the tissue at the timepoints of sampling.

ZEN 2.3: For analysis of immunostaining intensity, the grey values from at least 20 selected areas (FIX positive regions) for each liver cross-section were measured. The fluorescence immunostaining is reported as the mean fluorescence intensity (MFI) after correction for background fluorescence of the negative control treated with identical immunohistochemical procedure. Livers harvested from HB mice injected with saline buffer served as the negative control.

FIJI: For analysis of immunostaining intensity, the mean grey values (average of intensity) from 20 selected areas (FIX positive regions) for each liver cross-section were measured. Selections were created by drawing a rectangular region of interest (ROI) and the mean grey value corresponding to the fluorescence channel of interest was obtained. The fluorescence immunostaining is reported as the mean fluorescence intensity (MFI) after correction for background fluorescence (mean grey values from 20 selected areas) of the negative control (as mentioned above) treated with identical immunohistochemical procedure.

4 RESULTS

4.1 Expression and purification of rFIX variants

The amino acid substitution at position 5, K5A or K5R was introduced in the human wildtype rFIX and rFIX-FP through site-directed mutagenesis. Identical chromatography procedures were used to purify the proteins from supernatants of stable CHO clones.

Table 3. rFIX one-stage clotting potency and specific activities

Protein	Molar weight (kDa)	FIX:C Activity (IU/mL)	Protein content $OD_{280-320}$ (mg/mL)	Calculated specific activity (IU/mg)	Estimated potency (IU/nmol)
$rFIX_{WT}$	55	86	0.4	208 ± 25§	11.5 ± 1.4
$rIFX_{K5A}$	55	590	6.1	178 ± 26§	9.8 ± 1.5
$rFIX_{K5R}$	55	405	6.7	238 ± 37§	13.1 ± 2.0
$rFIX_{WT}$-FP	123	83	1.4	61 ± 4§	7.5 ± 0.5
$rIFX_{K5A}$-FP	123	1077	9.0	66 ± 6§	8.1 ± 0.5
$rFIX_{K5R}$-FP	123	1588	6.7	60 ± 2§	7.4 ± 0.3

§neither of the non- fused and albumin fused K5 variant´s specific activity differed significantly from their respective wildtype ($rFIX_{WT}$ or $rFIX_{WT}$-FP) in an unpaired student's t-test.

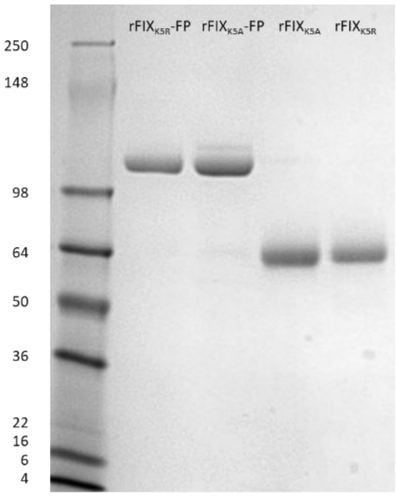

Figure 12. Image of the SDS-PAGE gel under non-reducing conditions.

The purity and size of the generated proteins loaded was verified by SDS-PAGE. The loaded proteins on the gel are outlined in Figure 12, where single bands with ~115 kDa and ~64 kDa molecular mass were revealed by Coomassie staining. The ~115 kDa bands correspond to the albumin fused rFIX proteins and the ~64 kDa bands correspond to the non-fused rFIX proteins. The specific activities are summarized in Table 3 (the mean and SD of 3 independent experiments).

N-glycan assay was carried out by the Recombinant Product Development team at CSL Behring Innovation GmbH. The N-glycan profile was studied by enzymatical digestion of rFIX proteins by N-glycosidase F (PNGase F). The released N-glycans were purified and labeled with a fluorophore, 2-anthranilic acid. The labeled glycans were separated by HPLC and detected by fluorescence. Results from rFIX proteins were compared to a reference standard as relative area percent per sialylation group (Table 4).

Table 4. N-glycan profile of generated rFIX

N-glycan	$rFIX_{K5A}$	$rFIX_{K5R}$	$rFIX_{K5A}$-FP*	$rFIX_{K5R}$-FP*	$rFIX_{K5A}$-fp*	$rFIX_{K5R}$-fp*
Asialo	2.8 %	2.7 %	3.2 %	6.7 %	4.4%	7.1%
Monosialo	5.4 %	4.4 %	2.6 %	7.8 %	5.3%	10%
Disialo	28.4 %	24.1 %	13.7 %	22.5 %	29.9%	37.3%
Trisialo	42.4 %	43.1 %	41.5 %	42.7 %	37.9%	29.9%
Tetrasialo	18.8 %	22.7 %	31.4 %	17.9 %	19.7%	13.9%
> Tetrasialo	2.3 %	3.0 %	7.6 %	2.4 %	2.8%	1.9%

*$rFIX_{K5X}$-FP and $rFIX_{K5X}$-fp are from the same clone/transfection but different batches. $rFIX_{K5X}$-FP were used for the pharmacokinetic study in mice.

The N-glycans existed predominantly in di-, tri- and tetrasialic forms, while neutral and asialic- /mono-sialic glycol-forms never exceeded 17.5 % of total sialylation.

The γ-carboxylation status was tested by Sabine Schweisgut, a PhD Student at CSL Behring Innovation GmbH, who kindly provided the following results. Anion-exchange chromatography (AEXC) with UV detection was used for separation of different γ-carboxylated forms in rFIX molecules.

The signal for specific gamma-carboxylated glutamic acid residues (Gla)-containing peptides corresponding to 12, 11, 10 or 9 carboxyl groups is expressed as a distribution profile of the relative abundance of each of the peptides. In Table 5 results are reported as the percentage of rFIX protein containing ≥ 11 Gla residues within the Gla domain.

Table 5. The level of γ-carboxylation with ≥ 11 glutamate residues

Gla-content	$rFIX_{K5A}$ (%)	$rFIX_{K5R}$ (%)	$rFIX_{K5A}$-FP* (%)	$rFIX_{K5R}$-FP* (%)	$rFIX_{K5A}$-fp* (%)	$rFIX_{K5A}$-fp* (%)
R.A.	75	78	76	92	87	94
11 + 12 Gla	(29+64)	(44+34)	(46+30)	(30+62)	(45 + 42)	(26 + 67)

R.A = relative area of the 11 Gla + 12 Gla from the total 9 Gla, 10 Gla, 11 Gla, and 12 Gla (100% of the area). *$rFIX_{K5X}$-FP and $rFIX_{K5X}$-fp are from the same clone/transfection but different batches. $rFIX_{K5X}$-FP were used for the pharmacokinetic study in mice.

All molecules showed a similar γ-carboxylation pattern with a content of at least 75% of peptides with ≥11 carboxylates, while the portion of 9 Gla species was neglectable.

4.2 *In vitro* characterization of the K5 variants

4.2.1 The efficacy of rFIX proteins in FIX deficient human plasma

The efficacy of rFIX proteins was confirmed *in vitro* by the ability of each protein to restore fibrin clot formation in FIX deficient plasma (aPTT). The rFIX proteins were spiked at equimolar concentrations in human FIX deficient plasma and all rFIX proteins decreased the time for clot formation substantially from 76 to 37 ± 1 sec (Figure 13A-B).

The aPTT is a global test used to detect deficiencies in the intrinsic clotting pathway, where FXIa activates FIX as part of the contact factor (intrinsic) pathway. If a clotting factor (e.g., FIX) is missing, the aPTT will be prolonged and after addition of the missing factor, in this case FIX, the aPTT is reduced. These results clearly show that all tested rFIX proteins were functionally active and effectively reduced fibrin clotting time in human FIX deficient plasma.

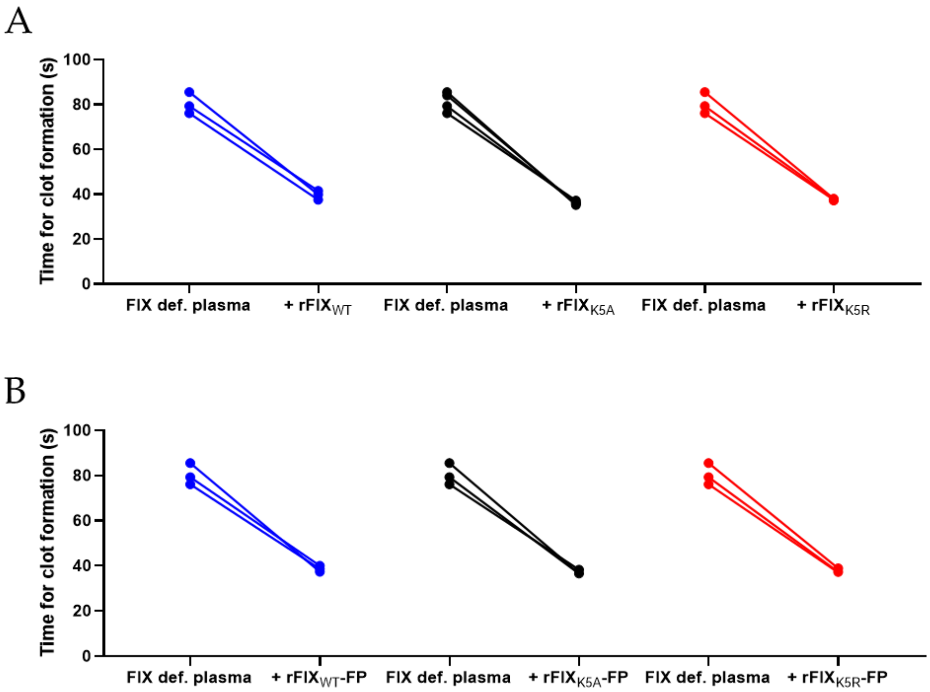

Figure 13. Activated partial thromboplastin time (aPTT) correction after addition of rFIX proteins. WT is depicted in blue, K5A is depicted in black and K5R is depicted in red in both, non-fused and albumin fused rFIX proteins. (**A**) The non-fused rFIX$_{WT}$, rFIX$_{K5A}$, and rFIX$_{K5R}$ proteins were spiked at equimolar concentration in human FIX deficient plasma and tested simultaneously. (**B**) The albumin fused rFIX$_{WT}$-FP, rFIX$_{K5A}$-FP, and rFIX$_{K5R}$-FP proteins were spiked at equimolar concentration in human FIX deficient plasma and tested simultaneously. Each line represents an individual experiment within each group and at least three independent experiments were performed.

4.2.2 Activation of rFIX products

4.2.2.1 Visualization of rFIX activation in SDS-PAGE

The activation of rFIX molecules by FXIa was investigated in more detail. As shown in Figure 14 and Figure 15, the rate of conversion of inactive form of rFIX/rFIX-FP proteins to active form were analyzed. The size observed for the inactive (~64 kDa) and active (~54 kDa) forms of non-fused rFIX protein were consistent with the cleavage of the activation peptide (AP) (Figure 14B).

Similarly, activation of the albumin fused rFIX proteins (~120 kDa) resulted in the active (~54 kDa) form following the cleavage of an activation peptide (~11 kDa), and the cleaved albumin portion and the cleaved albumin portion (~64 kDa) (Figure 15B).

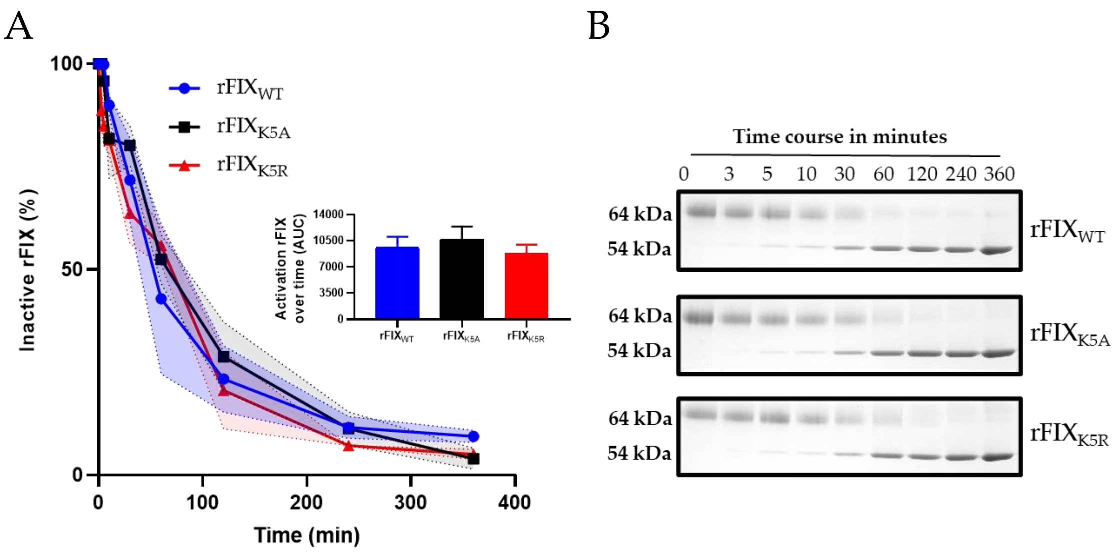

Figure 14. Activation of rFIX$_{WT}$, rFIX$_{K5A}$ and rFIX$_{K5R}$ by rFXIa.
The rate of activation of rFIX was determined by SDS PAGE under SDS-reducing conditions and the percentage of non-cleaved, inactive rFIX was determined over time in relation to the baseline value (100%) at timepoint 0. (**A**) Each data point represents the mean value of 3 independent experiments, and the error bands (shaded area) show ± SEM. The area under the curve was plotted in the insert as a bar graph (mean ± SEM) and (**B**) a representative image of an SDS-PAGE gel depicts the cleavage of zymogen rFIX (ca.64 kDa) into activated rFIX with light and heavy chain held together by disulfide bond (ca. 54 kDa). Each timepoint (0; 3; 5; 10; 30;60; 90; 120; 180; 360 minutes) was loaded in lanes 1-10.

The kinetic of activation was compared between proteins by semi-quantification of the relative amount of inactive rFIX over time (100% of the proteins are inactive at the start of the assay and as they get activated, the relative amount of inactive rFIX decreases over time. The area under the curve (AUC) was calculated for the activation profile of each protein Figure 14A and Figure 15A).

These data indicate that the substitution at position 5 from lysine to arginine or from lysine to alanine does not lead to major differences in the activation of rFIX by FXIa. Activated rFIX protein (ca. 54 kDa) and the cleaved albumin band (ca. 60 kDa) was observed in the albumin fused rFIX proteins. In general, no major differences were observed between the K5 variants in non-fused, albumin fused rFIX forms, and their respective WT proteins.

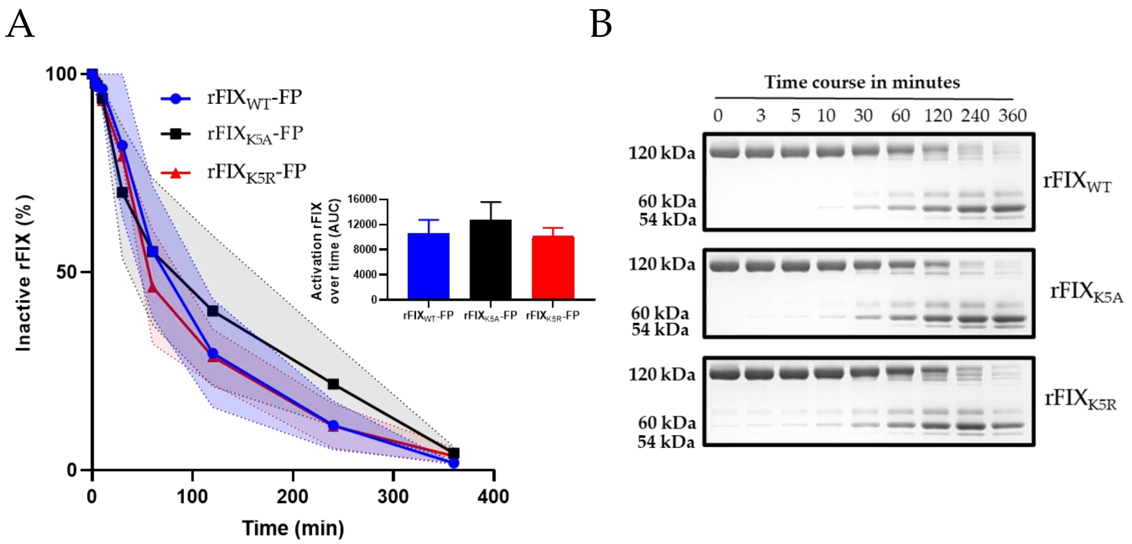

Figure 15. Activation of rFIX$_{WT}$-FP, rFIX$_{K5A}$-FP and rFIX$_{K5R}$-FP.
The rate of activation of rFIX was determined by SDS PAGE under SDS-reducing conditions and the percentage of non-cleaved, inactive rFIX was determined over time in relation to the baseline value (100%) at timepoint 0. (**A**) Each data point represents the mean value of 3 independent experiments, and the error bands (shaded area) show ± SEM. The area under the curve was plotted in the insert as a bar graph (mean ± SEM) and (**B**) a representative image of an SDS-PAGE gel depicts the cleavage of albumin fused rFIX zymogen (ca.120 kDa) over time. The activated rFIX with light and heavy chain held together by disulfide bond (ca. 54 kDa) right below the cleaved albumin (ca. 60 kDa) are shown. Each timepoint (0; 3; 5; 10; 30;60; 90; 120; 180; 360 minutes) was loaded in lanes 1-10.

4.2.2.2 Detection of FIXa in a chromogenic assay

The structural integrity and the activation of the generated rFIX proteins was confirmed in a chromogenic assay (section 3.6.4) using a peptidyl substrate, which is specific for rFIXa, and the Km was determined for all proteins (Figure 16 and Figure 17). The proteins were measured at several timepoints at different concentrations (2-0.03 µM). Each set of proteins (wildtype and variants) was tested at least 3 times. The Km was calculated for each protein and compared to the wildtype protein. Therefore, the wildtype protein was set as 100%. While no differences were observed between the non-fused or the albumin fused variants, the Km of the rFIX variants was lower compared to the corresponding wildtype protein.

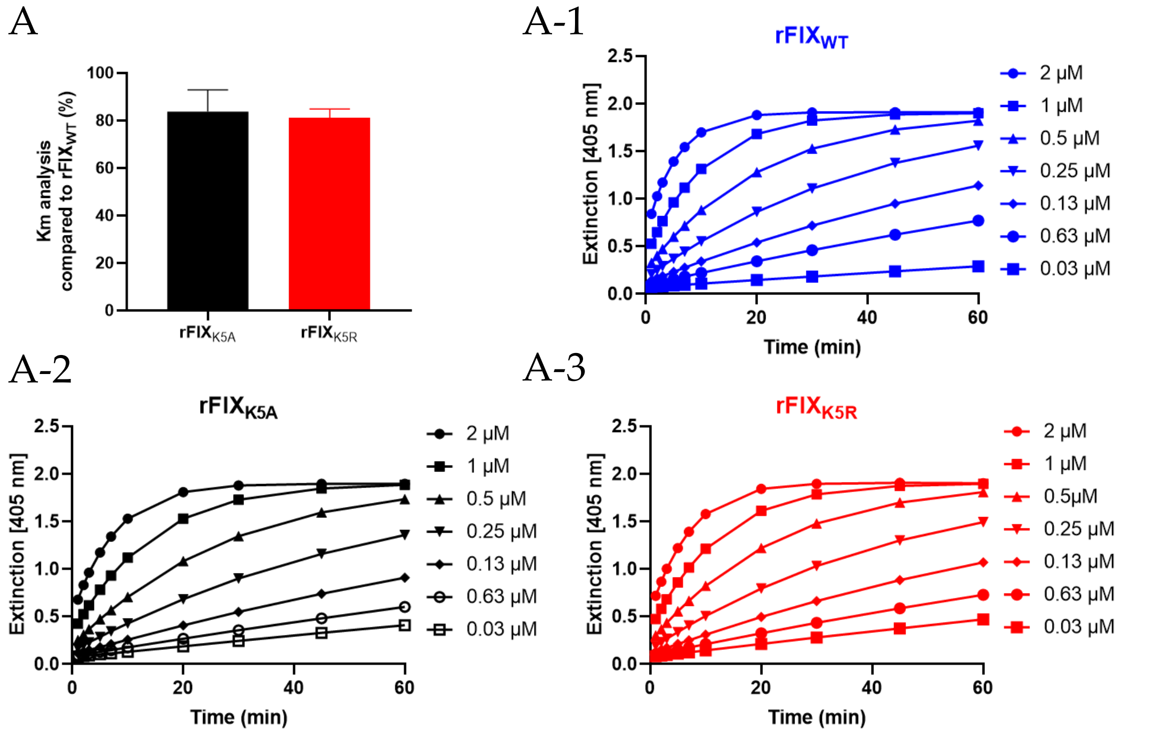

Figure 16. Kinetics of rFIXa activity using a proteolytic substrate.
A set of non-fused rFIX molecules ($rFIX_{WT}$, $rFIX_{K5A}$ and $rFIX_{K5R}$) were tested simultaneously under identical conditions. (**A**) The Km of 3 independent experiments were calculated and $rFIX_{WT}$ was set as 100% enzymatic activity. Representative data from one experiment shows the reaction over 60 minutes at several concentrations ranging from 0.031 µM to 2 µM for $rFIX_{WT}$ (**A-1**), for $rFIX_{K5A}$ (**A-2**) and $rFIX_{K5R}$ (**A-3**) molecules.

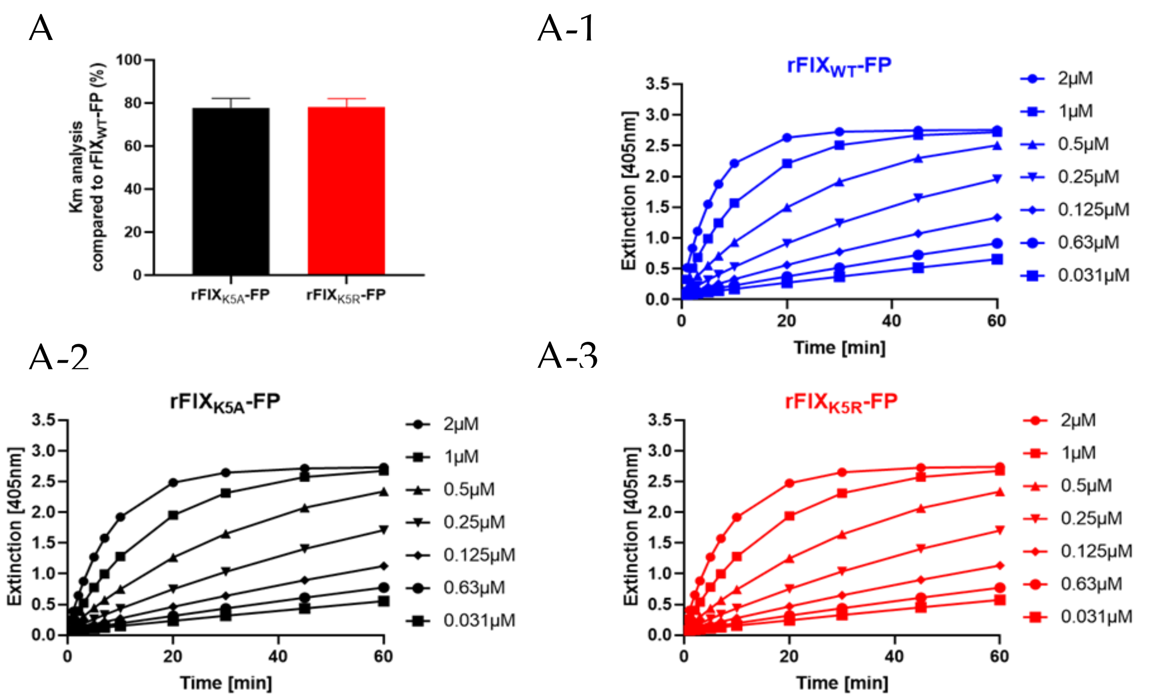

Figure 17. Kinetics of rFIXa activity using a proteolytic substrate.
A set of albumin fused rFIX molecules ($rFIX_{WT}$-FP $rFIX_{K5A}$-FP and $rFIX_{K5R}$-FP) were tested simultaneously under identical conditions. (**A**) The Km of 3 independent experiments were

calculated and rFIX$_{WT}$-FP was set as 100% enzymatic activity. Representative data from one experiment shows the reaction over 60 minutes at several concentrations ranging from 0.031 µM to 2 µM for rFIX$_{WT}$-FP (**A-1**), for rFIX$_{K5A}$-FP (**A-2**) and rFIX$_{K5}$R-FP (**A-3**) molecules.

This effect is mainly due to the fact that the inter-experiment variability was not taken into account for the wildtype proteins (as they were set as 100%). The results show the outcome of three independent experiments and its variability.

4.2.3 Generation of FXa by FIXa in a chromogenic assay

The functional (proteolytic) activity of non-fused and albumin fused activated rFIX$_{K5x}$ variants and rFIX$_{WT}$ to its physiological substrate, FX were compared in a coagulation assay.

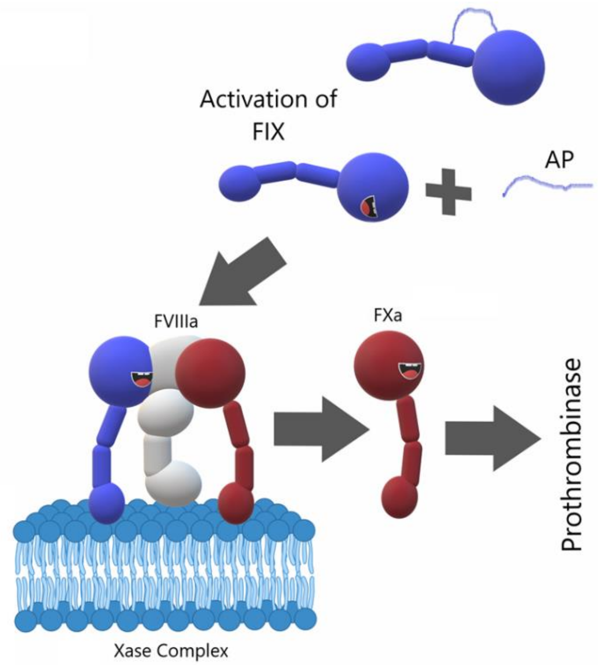

Figure 18. Formation of tenase complex.
FIX is activated and forms a complex with FVIIIa and FX on activated platelets surface.

The rate of FXa generation was determined using a reconstituted intrinsic factor Xase assay as described in section 3.6.3. This assay was designed to mimic the biological events of FIX activation by FXIa and the formation of the intrinsic tenase complex (Figure 18). The enzyme kinetics for FX activation in the presence of constant amounts (3nM) of FVIII was investigated at increasing concentrations of albumin fused and non-fused rFIX ranging from 0 to 10 nM (Figure 19A and Figure 19B). In general, the curve progression related to generation of active FX was similar between the groups when FIX was the limiting factor (Figure 19A and Figure 19B). However, when FVIII was the limiting factor in the reaction, even low amounts of FVIII in the reaction containing rFIX$_{K5R}$ led to a high level of FXa generation (Figure 19A-1).

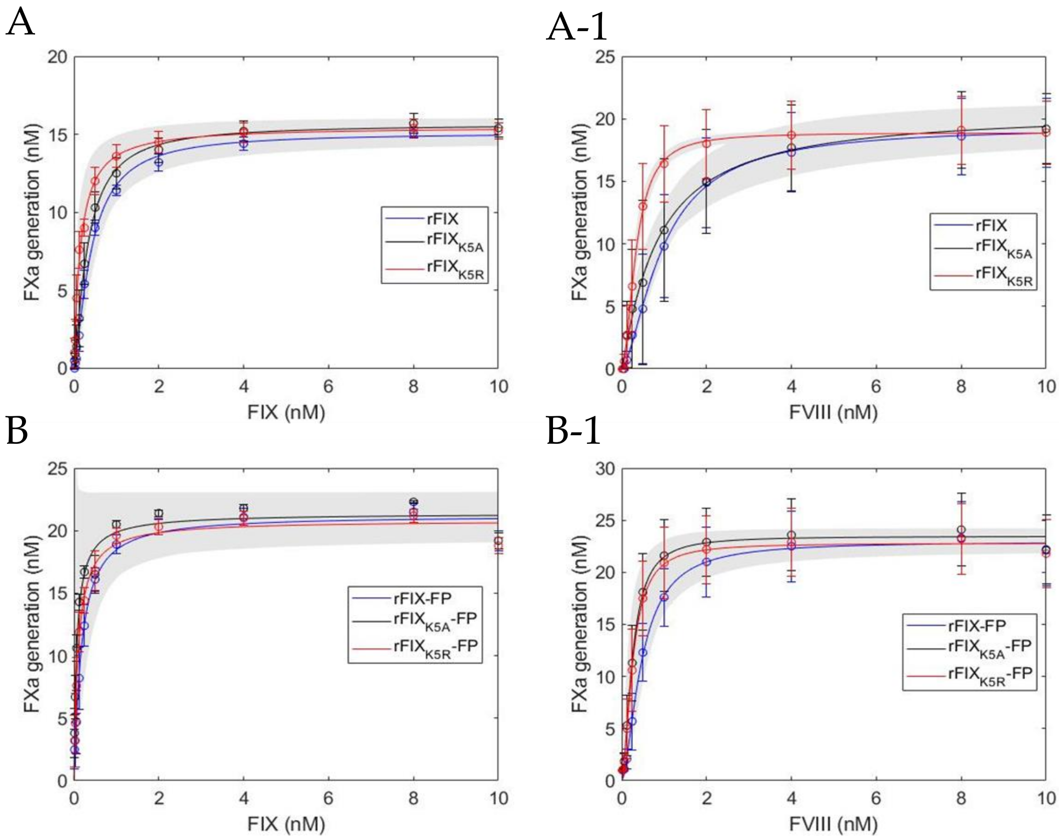

Figure 19. Measurement of FXa generation in the Xase complex.
The Xase complex was simulated using a modified FXa generation assay kit. The fitted curves of FXa generation at (**A**) increasing concentration of non- fused rFIX proteins or (**A-1**) at increasing rFVIII concentrations, while maintaining rFIX at constant concentration and at (**B**) increasing concentration of albumin fused rFIX proteins or at (**B-1**) increasing rFVIII concentrations, while maintaining rFIX-FP at constant concentration. The data was fit to the Michaelis-Menten model using Matlab software. Each data point represents the mean value of 3 independent experiments, error bands in grey show confidence intervals for fitted curves, and the error bars show ± SEM.

In contrast, no major difference was observed when FVIII was the limiting factor in the reaction containing albumin fused rFIX proteins (Figure 19B-1). These results suggest that rFIX$_{K5R}$ is more efficient in activating FX via formation of the tenase complex and potentially the steric hinderance of albumin fusion in $rFIX_{K5R}$-FP negates this effect. The enzyme kinetics for FX activation when rFIXa is the limiting factor in the reaction showed that the velocity of the rFIXa-FVIIIa-FX reaction increases and reaches saturation at ~15 nM (Table 6) and in the presence of increasing concentrations of cofactor rFVIII (Table 6), the saturation is reached at ~19 nM with all rFIX proteins. Under the mentioned conditions, $rFIX_{K5R}$ is slightly more efficient (Km) in activating FX at lower concentrations and displayed a 2-fold lower Km compared to $rFIX_{WT}$ but the Km of $rFIX_{WT}$ and $rFIX_{K5A}$ proteins was similar as shown in the Table 6. Similar results were observed by increasing rFVIII concentrations. Here, $rFIX_{K5R}$ was more efficient at lower concentrations (Km) compared to $rFIX_{WT}$ and Km between $rFIX_{K5A}$ and $rFIX_{WT}$ were similar (Table 6). The maximal velocity (Vmax) was similar between the tested set of proteins corroborating the ability of the enzymes involved in the tenase complex (Figure 18; FIX, FVIII, and FX) to form a complex and speed up the FXa generation rate. Here, no differences were observed between the K5 variants and the wildtype protein.

Table 6. *In vitro* enzyme kinetics of FX activation in the tenase complex depicted in Figure 19.

	Set-up A and B in Figure 19 (FIX titration)			**Set-up A-1 and B-1 in Figure 19 (FVIII titration)**		
Enzyme	**Vmax (min^{-1})**	**Km (nM)**	**Hill coefficient**	**Vmax (min^{-1})**	**Km (nM)**	**Hill coefficient**
$rFIX_{WT}$	15.2 ± 0.51	0.30 ± 0.02	1.35 ± 0.16	18.7 ± 2.93	1.51 ± 0.62	2.13 ± 0.28
$rFIX_{K5A}$	15.9 ± 0.82	0.26 ± 0.06	1.22 ± 0.16	19.2 ± 2.89	1.70 ± 0.92	2.10 ± 0.15
$rFIX_{K5R}$	15.6 ± 0.76	0.15 ± 0.02	1.05 ± 0.13	18.7 ± 2.60	0.13 ± 0.06	2.23 ± 0.23
$rFIX_{WT}$-FP	21.0 ± 0.65	0.12 ± 0.01	1.27 ± 0.26	22.8 ± 3.55	0.27 ± 0.02	0.26 ± 0.17
$rFIX_{K5A}$-FP	21.4 ± 0.21	0.08 ± 0.01	0.96 ± 0.07	23.4 ± 3.36	0.09 ± 0.01	0.07 ± 0.10
$rFIX_{K5R}$-FP	20.9 ± 0.54	0.10 ± 0.04	1.09 ± 0.20	22.7 ± 3.30	0.08 ± 0.01	0.20 ± 0.14

Data is presented as the mean value and standard error of the mean (SEM) of 3 independent experiments.

The albumin fused rFIX-FP proteins had similar Km when rFVIII was kept at constant concentrations (Table 6) but when increasing rFVIII are tested and rFIX-FP were kept constant, the km of $rFIX_{WT}$ was ca. 3-fold higher compared to the K5 variants (Table 6). The hill coefficients ranged between 0.07 – 0.26 and 2.1 – 2.3 for albumin fused and non-fused rFIX proteins, respectively (Table 6). Low values describe a smaller slope and non-sigmoidal activation curve observed in Figure 19, where the y-axis displays the proportion of generated rFXa and the x-axis is the concentration of FVIII or FIX. As Hill coefficient is increased, the saturation curve becomes steeper (small slope).

4.3 *In vivo* PK profile and tissue levels of rFIX in HB mice

4.3.1 PK behavior and tissue disposition of non-fused rFIX proteins

Pharmacokinetics (PK) is described as what the body does to the drug and refers to the movement of the drug into, though, and out of the body, as well as all metabolic processes in which the drug is involved. A PK profile describes the time course of the drug's absorption, distribution, metabolism and excretion. The PK profile is impacted by numerous factors, including target-binding specificity and affinity, molecular size, and physiochemical property among others. The interaction of rFIX proteins with other molecules would therefore be reflected in the progression of the plasma-concentration-time curve.

4.3.1.1 In vivo PK profile

HB mice were intravenously injected with a dose of 25 nmol/kg $rFIX_{WT}$, $rFIX_{K5A}$ and $rFIX_{K5R}$ via the lateral tail vein (Figure 20) or subcutaneously in the neck (Figure 21). As shown in Figure 20 in general the plasma exposure of rFIX was comparable for all proteins ($rFIX_{WT}$, $rFIX_{K5A}$ and $rFIX_{K5R}$). However, when focusing on the early timepoints (insert in Figure 20) it is evident that the clearance of $rFIX_{K5A}$ was monophasic (linear profile in a semi-logarithmic plot) compared to $rFIX_{WT}$ and $rFIX_{K5R}$. $rFIX_{WT}$ and $rFIX_{K5R}$ demonstrated a biphasic profile, potentially suggesting a faster distribution to the extravascular compartment during the initial phase (insert Figure 20).

Plasma levels of FIX antigen after intravenous administration were used for non-compartmental PK analysis as summarized in Table 7. The total exposure after intravenous injection was evidently higher for $rFIX_{K5A}$ which exhibited an area under the curve (AUC), from the time 0 to the last measurable concentration ($AUC\_{}_{0\text{-last}}$), of ~1560 h*pmol/mL, followed by lower AUC levels of $rFIX_{WT}$ (~981 h*pmol/mL) and $rFIX_{K5R}$ (~955 h*pmol/mL) Figure 20 and Table 7). The predicted maximum concentration (C_{max}_pred) of rFIX was measured to be highest for the $rFIX_{K5A}$ (~268 pmol/mL) group, succeeded by $rFIX_{WT}$ (~233 pmol/mL) and $rFIX_{K5R}$ (~203 pmol/mL).

In general, $rFIX_{K5A}$ reached ca. 32% higher C_{max}_pred compared to $rFIX_{K5R}$ and the total exposure over time was ca. 63% and 65% higher for $rFIX_{K5A}$ compared to $rFIX_{K5R}$ ($AUC\_{}_{0\text{-last}}$ and AUC_0-inf; Table 7). $rFIX_{K5A}$ exhibited the shortest terminal half-life (~ 4 hours), the lowest systemic clearance (~16 mL/h/mg), and the lowest mean retention time (MRT) (~4.68 hours) compared to $rFIX_{WT}$ and $rFIX_{K5R}$ (Table 7). However, $rFIX_{K5A}$ had the highest *in vivo* recovery (~42.9%), while $rFIX_{WT}$ (37.2%) and $rFIX_{K5A}$ (32.4%) exhibited a slightly lower *in vivo* recovery (IVR) as shown in Table 7.

The apparent volume of distribution in the central compartment (Vc), at steady state (Vss), and during the terminal elimination phase (Vz) were lowest for $rFIX_{K5A}$ which suggests low tissue distribution of $rFIX_{K5A}$. The fraction of dose absorbed by the extravascular compartment can only be estimated (indirectly) based on the plasma levels measurements. In general, the characterization of PK parameters can be performed by non-compartmental or compartmental methods.

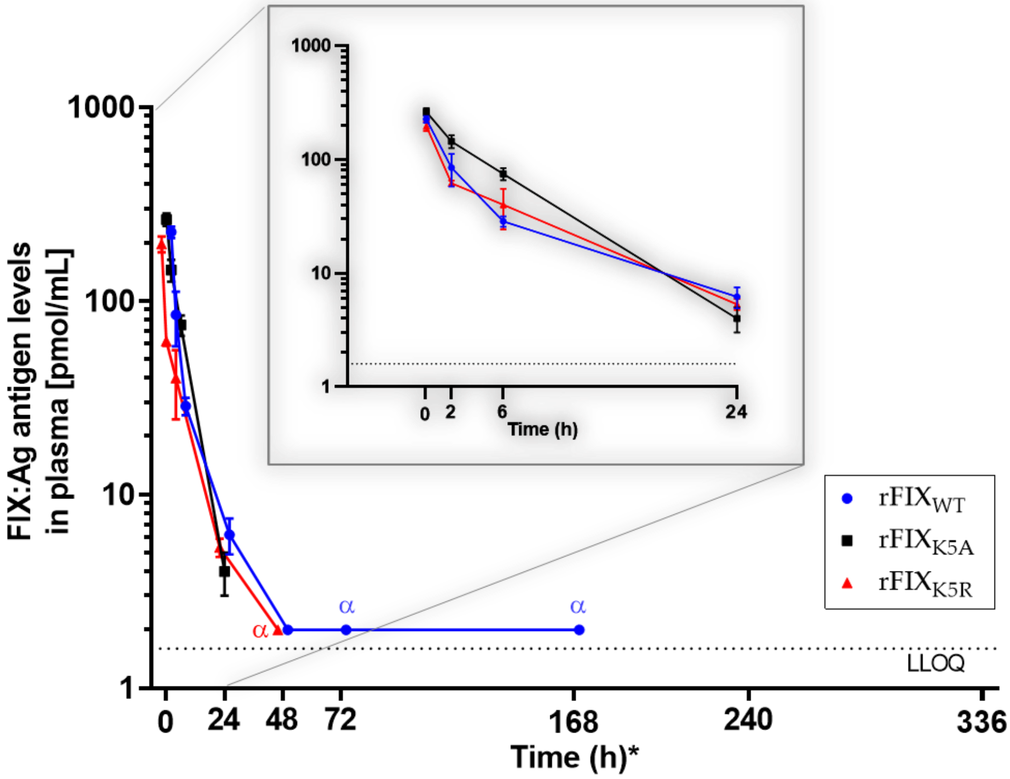

Figure 20. Intravenous PK profile of non-fused rFIX proteins in HB mice.
HB mice were injected with equimolar doses (25nmol/kg) of $rFIX_{WT}$, $rFIX_{K5A}$ and $rFIX_{K5R}$ via the lateral tail vein. Pharmacokinetic profiles of $rFIX_{WT}$ in blue (n=5), $rFIX_{K5A}$ in black (n=3), and $rFIX_{K5R}$ in red (n=3) were determined by measuring rFIX antigen levels at various timepoints. Each point represents the mean ± SD of n=3-5 mice and α indicates n=1 measureable value. LLOQ (1.6 pmol/mL) refers to the lowest concentration of rFIX antigen that can be reliably detected based on ELISA. Values ≤ LLOQ were not plotted (excluded). Timepoints plotted in the intravenous group: 0.083, 2, 6, 24, 48, 72, 120, 144, 168, 240 and 336 hours. Only 1 out of 3 animals (α) had detectable levels in the $rFIX_{K5R}$ group at 48 hours and only 1 out of 5 animals (α) had detectable levels at 72 and 168 hours in the $rFIX_{WT}$ group. *Graph except the insert: All points within a data set (group) were nudged on the x-axis to improve visualization. Wildtype in blue (-2), K5A variant in black (0), and K5R variant in red (2).

The non-compartmental analysis (NCA) does not rely on assumptions about body compartment (assumption that clearance occurs only from the central "blood" compartment), but it is a standard and widely utilized PK analysis because it is a simple method for evaluating the exposure of a drug.

Based on these results, it can be speculated that the relative contribution in terms of binding to the peripheral compartment is not preponderant for $rFIX_{K5A}$, as it is for $rFIX_{WT}$ and $rFIX_{K5R}$.

Table 7. Non-compartmental analysis (NCA) of the PK profile for intravenous administered rFIX (Figure 20)

PK parameter	Unit	$rFIX_{WT}$	$rFIX_{K5A}$	$rFIX_{K5R}$
$AUC\_{0\text{-}last}$	h*pmol/mL	981±112	1560±100	955±21
AUC_{inf}	h*pmol/mL	995±111	1590±103	966±22
extrap	%	1.4±2	1.6±0.3	1.2±0.8
C_{max}_pred	pmol/mL	233±51	268±17	203±16
Clearance	mL/h/kg	25.1±3.0	15.8±1.0	25.9±0.8
$t_{1/2}$_term	h	13.8±8	4.24±0.2	8.02±0.3
MRT	h	9.55±4	4.68±0.2	7.34±0.4
IVR	%	37.2±8	42.9±3	32.4±3
Vc	mL/kg	107±63	93.6±6	123±9
Vss	mL/kg	240±110	73.9±4	190±13
Vz	mL/kg	499±285	96.8±7	299±15

$AUC\_{0\text{-}last}$, area under the curve to the last value above the limit of detection; AUC_{inf}, AUC to infinite time; extrap, extrapolated portion of AUC; C_{max}_pred, predicted C_{max}; $t_{1/2}$_term, terminal half-life; MRT, mean residence time; IVR, in-vivo recovery; Vc, volume of distribution in central compartment, Vss, volume of distribution at steady-state; Vz, volume of distribution during the terminal phase. Parameters were estimated in Matlab R2019b. Data is given as mean ± SD for n=3-5.

Interestingly, the K5A mutation had a positive effect on plasma exposure after subcutaneous dosing compared to $rFIX_{WT}$ and $rFIX_{K5R}$ (Figure 21). The data generated in the subcutaneous arm is limited to few data points >LLOQ and was therefore, not appropriate for reliable PK analysis other than C_{max}, t_{max} and $AUC_{0\text{-}last}$.

Even though bioavailability cannot be calculated reliably from this data set, the area under the plasma drug concentration-time curve that reflects the actual plasma exposure of the drug is clearly smaller by $rFIX_{K5R}$ (Figure 21). While $rFIX_{K5A}$ reaches the highest concentration in plasma after subcutaneous or intravenous administration. All together, these results suggest that after subcutaneous administration, $rFIX_{K5A}$ enters the circulation easier and the release of $rFIX_{K5R}$ to the circulation from site of injection seems to be slower and/or less efficient, especially since $rFIX_{WT}$ is the first drug to get higher values.

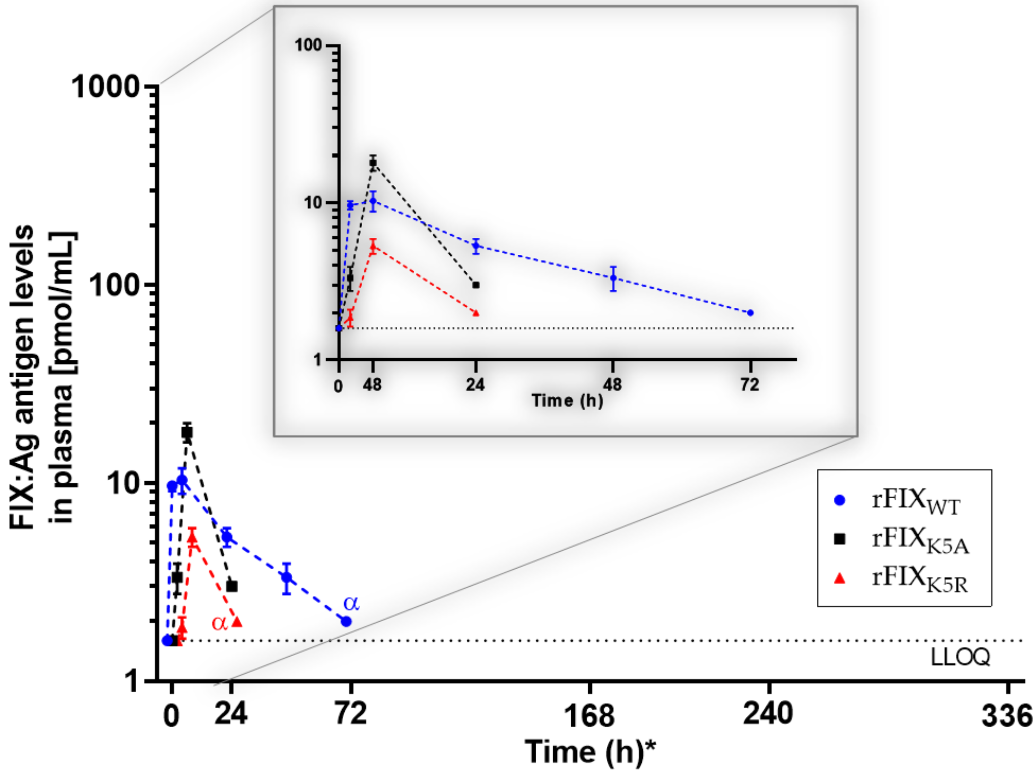

Figure 21. Subcutaneous PK profile of non-fused rFIX proteins in HB mice.
HB mice were injected with equimolar doses (25nmol/kg) of $rFIX_{WT}$, $rFIX_{K5A}$ and $rFIX_{K5R}$ in the neck. Pharmacokinetic profiles of $rFIX_{WT}$ in blue (n=3), $rFIX_{K5A}$ in black (n=3), and $rFIX_{K5R}$ in red (n=3) were determined by measuring rFIX antigen levels at various timepoints. Each data point represents the mean ± SD of n=3-5 mice and α indicates n=1. LLOQ (< 1.6 pmol/mL) refers to the lowest concentration of rFIX antigen that can be reliably detected based on ELISA. Values ≤ LLOQ were not plotted (excluded). Timepoints plotted: 0 (timepoint of the injection), 2, 6, 24, 48, 72, 120, 144, 168, 240 and 336 hours. Only 1 out of 3 animals (α) had detectable levels in the $rFIX_{K5R}$ group at 24 hours and in the $rFIX_{WT}$ group at 72 hours. * Graphs except the insert: All data points within a data set (group) were nudged on the x-axis to improve visualization. Wildtype in blue (-2), K5A variant in black (0), and K5R variant in red (2).

4.3.1.2 Tissue absorption of rFIX

Beyond the assessment of plasma, the sampled livers from the intravenous treated group were processed and quantification of FIX immunostaining in at least 6 independent sections is shown in Figure 22A. Representative images are shown in Figure 22B. In the subcutaneous group the low signal-to-noise ratio made the quantification unreliable (data not shown). The specificity of the signal in the immunohistochemistry staining was confirmed by staining tissue sections from untreated FIX ko mice (HB mice). A section of a HB mouse treated previously with rFIX was stained under identical conditions in presence and absence of the primary antibody (rabbit anti-hFIX).

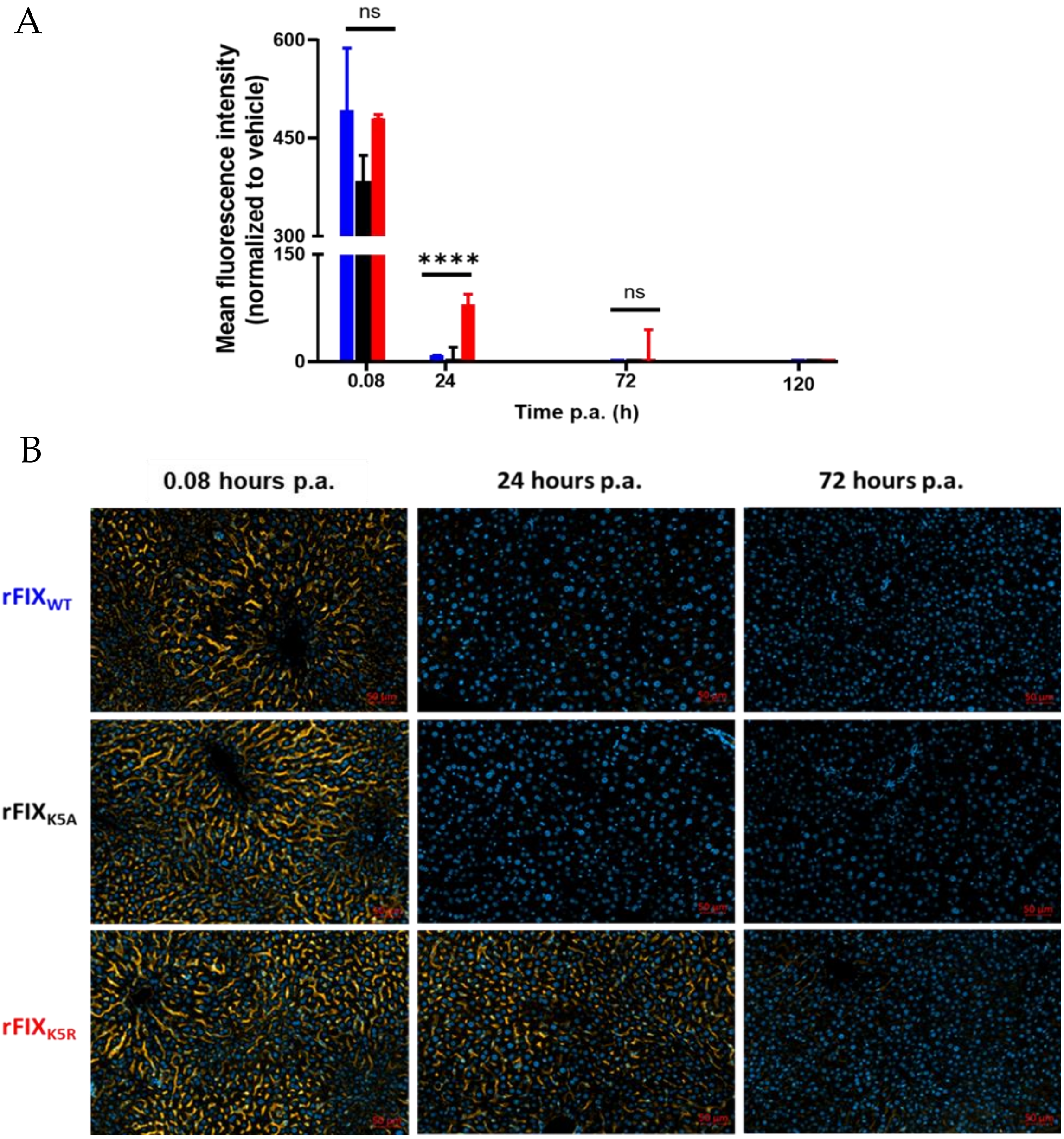

Figure 22. Immunohistochemistry staining of liver tissues (non-fused proteins).
Livers from HB mice (n=3) following intravenous administration of rFIX (25 nmol/kg). (**A**) Quantitative analysis (samples from each group were prepared and imaged in parallel under identical conditions) of FIX positive liver sections collected at 5 min, 24, 72, and 120 hours after treatment with rFIX proteins was performed in ZEN Software. Each bar represents the median ± 95% CI of 2-3 sampled livers. The blue, black and red bars represent $rFIX_{WT}$, $rFIX_{K5A}$, $rFIX_{K5R}$, respectively. The groups were compared at each timepoint using 1-way ANOVA test to determine the p-value. ns, not significant and ****$p < 0.0001$. (**B**) Representative images from liver section stained for nuclei using DAPI (blue) and for FIX using Rhodamine (yellow).

Results confirmed that the second antibody did not bind unspecific to the specimen and that the signal observed in the section incubated with the first antibody came from the first antibody.

In the intravenous group, 15 minutes following injection, all three rFIX proteins were detected in the liver with similar mean fluorescence intensities (MFI). However, at 24 hours following intravenous injection, only rFIXK5R was detected in the liver sections with a strong and robust signal, while faint signals were detected under identical conditions in the rFIXK5A and rFIXWT treated groups (Figure 22B).

The specificity of the FIX staining was confirmed in liver sections from HB mice that received previously saline buffer (human FIX negative samples). Those sections served as negative control and were stained under identical conditions (including primary and secondary antibodies) as liver samples of mice treated previously with rFIX.

Only samples from animals treated previously with human rFIX displayed a signal (Figure 23). The representative image in Figure 23 shows the distribution of FIX in the liver, and it can be observed that FIX is localized in the extracellular space, as expected in the liver of a HB mice that received exogenous human rFIX. We observed that rFIX did not distribute uniformly in the murine liver. A strong FIX signal was observed in the region surrounding the peri-central zone whereas the portal triad (circumscribed in Figure 23) region had no FIX signal.

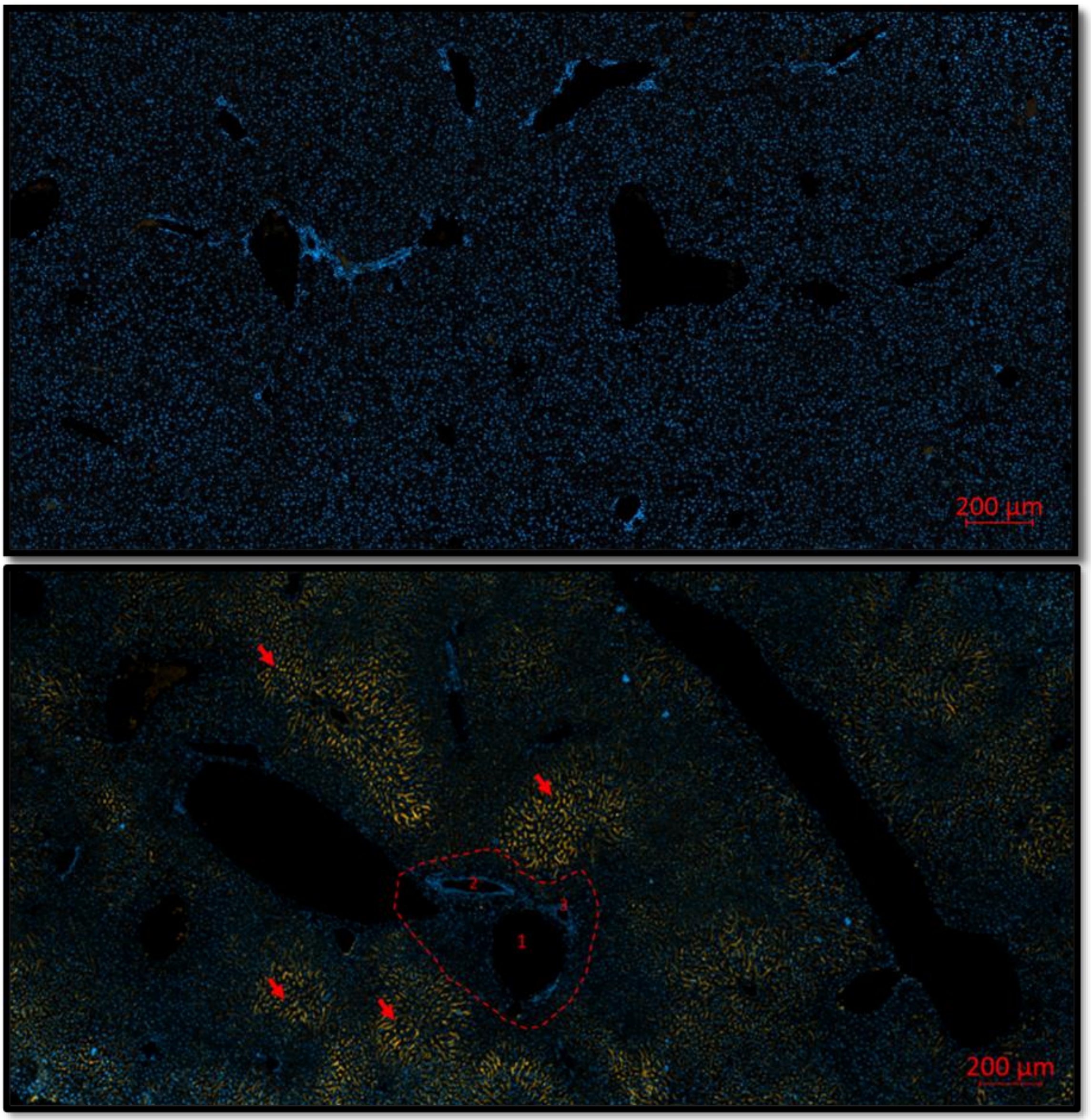

Figure 23. Representative image from liver section.
Upper image: Liver of HB mice treated with saline buffer as control for the specificity of the FIX staining. A higher magnification of the same section is inserted in the upper left corner. Lower image: Liver section from the 5 minutes timepoint and rFIXK5A treated group. Liver was stained for FIX (yellow). The portal triad is circumscribed by a dotted line: 1-branch of hepatic portal vein, 2-branch of hepatic artery, and branch of bile duct. FIX positive regions are indicated by red arrows.

4.3.2 PK behavior and tissue disposition of albumin fused rFIX proteins

4.3.2.1 Kinetics in sampled plasma

Mice were injected with a dose of 200 IU/kg (21 nmol/kg for rFIX$_{WT}$-FP, 15 nmol/kg for rFIX$_{K5A}$-FP, and 19 nmol/kg for rFIX$_{K5R}$-FP) based on antigen concentration. The antigen concentration (FIX:Ag) of each protein was previously determined using ELISA against $rFIX_{WT}$-FP with a known concentration (one stage clotting potency, FIX:C). The measured concentrations (FIX:Ag) of $rFIX_{K5A}$-FP (840 IU/mL), $rFIX_{K5R}$-FP (722 IU/mL), and $rFIX_{WT}$-FP (229 IU/mL) were diluted as needed and administered intravenously via the lateral vein (Figure 24) or subcutaneously in the neck (Figure 25). Blood samples were collected from the saphenous vein at several timepoints: 5 min, 2, 8, 16, 24, 32, 72, 96, 120 (5 days), 144 (6 days), and 168 hours (7 days). Samples taken from saphenous vein were collected in EDTA tubes (Sarstedt Microvette CB 300 DI-Kalium-EDTA). Plasma level of rFIX (FIX:Ag) after intravenous and subcutaneous administration was used for non-compartmental model as summarized in Table 8 for intravenous administration and Table 9 for subcutaneous administration.

It is important to mention that the albumin fused proteins (K5A and K5R variants) used in this part of the work were different from the batch used in the *in vitro* part (section 4.2). Both batches were generated from the same clone. As described in the material section 3.4., all proteins mentioned here were purified through anion exchange chromatography (AEC). The main difference of the proteins use in this part of the work was that in addition to AEC, the rFIX-FP were isolated using an affinity resin for capturing human albumin. The endotoxin concentrations were within acceptable ranges (≤ 5 IU/kg).

The acceptance limits in glycoform profile were met (low content of neutral glycans, consisting of ≤ 10 % of total area for this structure, confirming that N-glycans on the generated rFIX-FP proteins were of the complex type (mono-, di-, tri-, tetra-sialic, and > tetra-sialic). Therefore, these batches were used for PK profile and detailed data can be found in section 4.1.

The graph in Figure 24 shows the intravenous profile of the proteins. The rapid elimination from the plasma in the initial phase observed in the non-fused rFIX protein carrying the K5R mutation was also observed in the albumin fused $rFIX_{WT}$-

FP, even though in a less pronounced manner – potentially overlayed by half-life prolongation from albumin fusion. The mutant rFIX$_{K5A}$-FP exhibits a slower and more linear initial distribution phase.

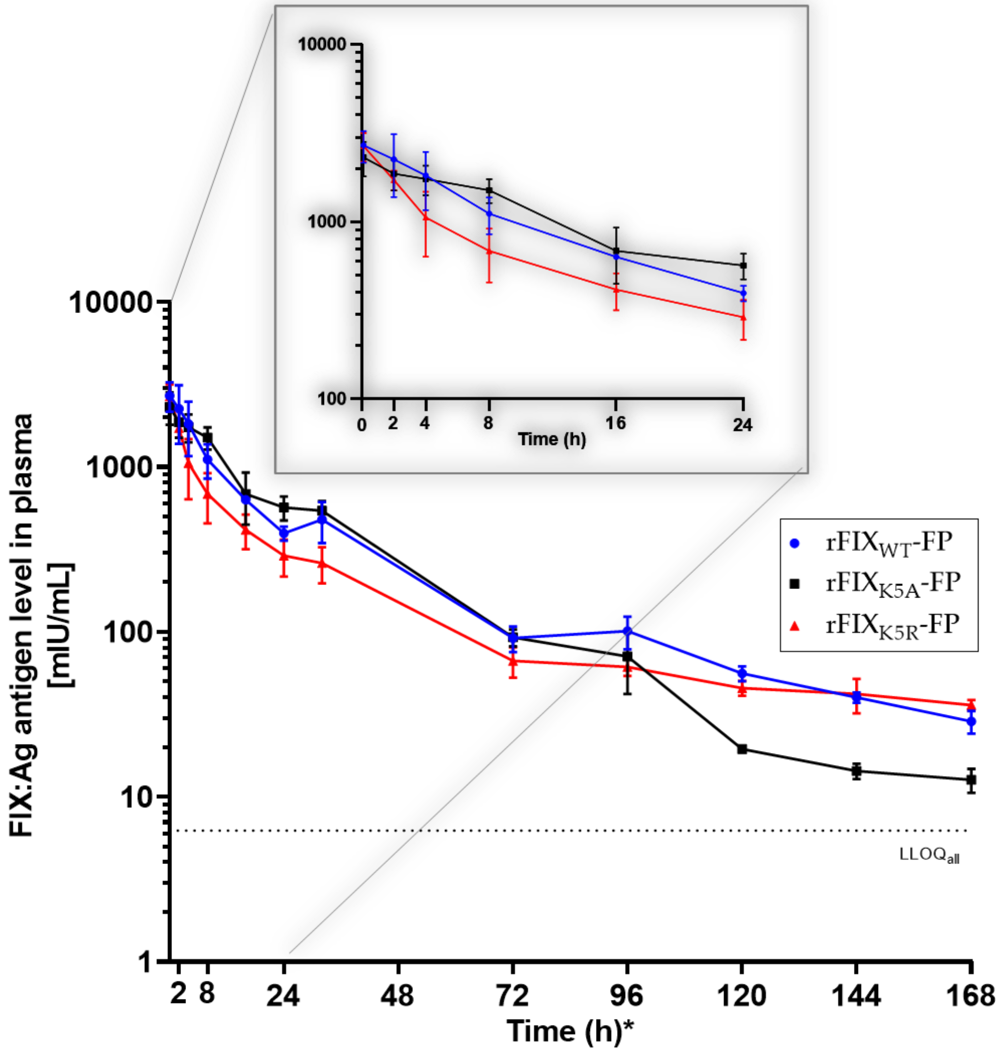

Figure 24. Intravenous PK profile for albumin fused rFIX in HB mice.
HB mice (n=3) were injected with rFIX antigen dose of 200 IU/kg of rFIX$_{WT}$-FP (blue), rFIX$_{K5A}$-FP (black) and rFIX$_{K5R}$-FP (red) via the lateral tail vein. The timepoints (0.08, 2, 6, 24, 48, 72, 120, 144, 168, 240 and 336 hours) of blood sampling are plotted in the X axis. Intravenous pharmacokinetic profiles of rFIX$_{WT}$-FP, rFIX$_{K5A}$-FP, and rFIX$_{K5R}$-FP were determined by measuring rFIX antigen levels (FIX:Ag) at various timepoints. LLOQ refer to the lowest concentration of FIX:Ag that can be reliably detected based on ELISA. Each point represents the mean ± SD of n=1-3 mice.

The systemic elimination (clearance) and the mean residence time (MRT) were higher for rFIX$_{K5R}$-FP (~5 mL/h/kg and ~80 h) but comparable between rFIX$_{K5A}$-FP (~4 mL/h/kg and ~35 h) and rFIX$_{WT}$-FP (~4 mL/h/kg and ~38 h). rFIX$_{K5A}$-FP in-vivo recovery was decreased (~47%), while $rFIX_{WT}$-FP (54%) and $rFIX_{K5A}$-FP (54%) exhibited a slightly higher in-vivo recovery (IVR) as shown in Table 8.

Table 8. Non-compartmental analysis of the PK profile for intravenous injected rFIX (Figure 24)

PK Parameter	Unit	$rFIX_{WT}$-FP	$rFIX_{K5A}$-FP	$rFIX_{K5R}$-FP
$AUC\_{0\text{-}last}$	h*IU/mL	47.6±8.0	49.2±6.2	31.5±4.3
AUC _inf	h*IU/mL	49.3±8.1	50.6±5.1	37.4±4.0
extrap	%	3.5±0.2	3.0±3.1	15.9±2.6
C_{max}_pred	IU/mL	2.77±0.55	2.33±0.52	2.72±0.51
Clearance	mL/h/kg	4.1±0.7	4.0±0.4	5.4±0.6
$t_{1/2}$_term	h	42.7±3.9	74.1±59.6	114.9±14.5
MRT	h	37.6±3.3	34.5±11.4	80.2±11.8
IVR	%	54.4±10.9	46.7±10.4	54.4±10.2
Vc	mL/kg	75.7±16.8	88.6±19.5	75.2±13.9
Vss	mL/kg	156.4±34.5	139.6±57.4	436.4±107.1
Vz	mL/kg	254.1±44.0	444.4±382.6	896.5±176.1

AUC_last, area under the curve to the last value above the limit of detection; AUC_inf, AUC to infinite time; extrap, extrapolated portion of AUC; C_{max}_pred, predicted C_{max}; $t_{1/2}$_term, elimination half-life; MRT, mean residence time; IVR, in-vivo recovery; Vc, volume of distribution in central compartment, Vss, volume of distribution at steady-state; Vz, volume of distribution during the terminal phase. Parameters were measured in Matlab R2019b.

In Table 8, the total exposure after intravenous injection was comparable between $rFIX_{K5A}$-FP and $rFIX_{WT}$-FP and exhibited $AUC\_{0\text{-}last}$ of ~48 h*IU/mL and ~49 h*IU/mL, followed the lower concentration of $rFIX_{K5R}$-FP (~32 h*IU/mL) (Figure 24 and Table 8). The maximum concentration (C_{max}) of rFIX was predicted to be similar for $rFIX_{K5R}$-FP (~2.7 IU/mL), $rFIX_{WT}$-FP (~2.8 IU/mL), and $rFIX_{K5A}$ (~2.3 IU/mL). $rFIX_{K5R}$-FP exhibited the longest half-life (~115 h) succeeded by $rFIXK_{5A}$-FP (~74 h) and $rFIX_{WT}$-FP (~43 h).

The results on the half-life of the protein were rather unexpected as it was increased by both proteins $rFIX_{K5A}$-FP and $rFIX_{K5R}$-FP compared to wildtype. At $rFIX_{K5A}$-FP, however, the terminal half-life exhibited a very high standard deviation. $rFIX_{K5R}$-FP exposure in the extravascular space (EVS) was expected to be higher than $rFIX_{K5A}$-FP. This is in line with volumes of distribution (Vss and Vz) which were highest for $rFIX_{K5R}$-FP and the AUC which was lowest for $rFIX_{K5R}$-FP.

Overall, the progression of the curves is very similar for rFIX$_{K5R}$-FP and rFIX$_{WT}$-FP, while rFIX$_{K5A}$-FP exhibits a linear clearance from blood at initial timepoints and at later timepoints (> 96 hours) the plasma concentration drops faster compared to the other two proteins.

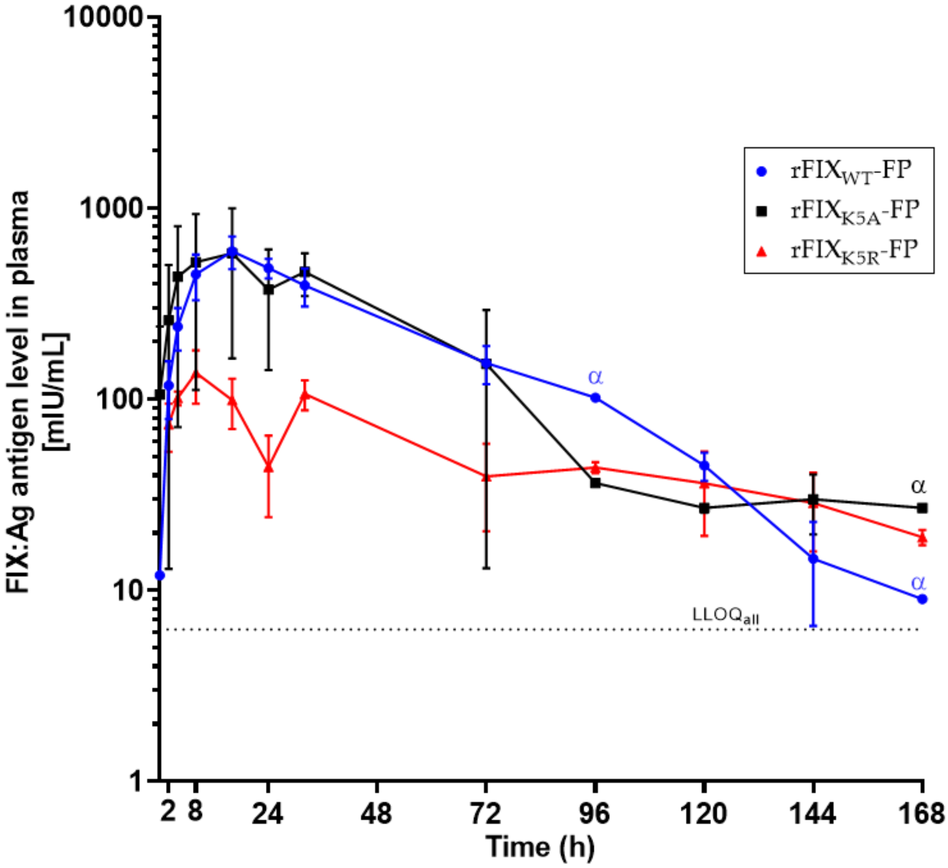

Figure 25. Subcutaneous PK profile of albumin fused rFIX in HB mice.
HB mice (n=3) were injected with rFIX antigen dose of 200 IU/kg of rFIXWT-FP (blue), rFIX$_{K5A}$-FP (black) and rFIX$_{K5R}$-FP (red) in the neck. The timepoints (0.08, 2, 6, 24, 48, 72, 120, 144, 168, 240 and 336 hours) of blood sampling are plotted in the X axis. Subcutaneous pharmacokinetic profiles of rFIX$_{WT}$-FP, rFIX$_{K5A}$-FP, and rFIX$_{K5R}$-FP were determined by measuring rFIX antigen levels (FIX:Ag) at various timepoints. LLOQ refer to the lowest concentration of FIX:Ag that can be reliably detected based on ELISA. Each data point represents the mean ± SD of n=1-3 mice. Only 1 out of 3 animals (α) had detectable levels in the rFIX$_{WT}$ and rFIX$_{K5A}$ group at 168 hours.

In the subcutaneous arm, rFIX$_{K5R}$-FP exhibit the lowest maximal concentration (C_{max}) and the lowest area under the curve (AUC). Therefore, the bioavailability was calculated to be the lowest for this protein (Figure 25). These results are consistent with the observations made for the non-fused equivalent, rFIX$_{K5R}$ protein (Figure

20). The investigation of the subcutaneous profile revealed a lower $AUC\_{0\text{-}last}$ (~9 h*IU/mL), AUC_{inf} (~12 h*IU/mL) and C_{max} (~0.1 IU/mL for $rFIX_{K5R}$-FP compared to $rFIX_{WT}$-FP (~31 h*IU/mL; ~31 h*IU/mL; ~0.6 IU/mL) and $rFIX_{K5A}$-FP (~32 h*IU/mL; ~34 h*IU/mL; ~0.8 IU/mL).

Table 9 Non-compartment analysis of the PK profile for subcutaneous administered rFIX (Figure 25)

PK parameter	Unit	$rFIX_{WT}$-FP	$rFIX_{K5A}$-FP	$rFIX_{K5R}$-FP
$AUC\_{0\text{-}last}$	h*IU/mL	30.7±1.4	32.0±7.8	8.9±1.0
AUC_{inf}	h*IU/mL	31.0±1.4	33.6±8.3	11.5±1.1
extrap	%	0.9±0.1	4.7±2.7	22.1±15.8
C_{max}	IU/mL	0.60±0.12	0.77±0.25	0.14±0.33
Clearance	mL/h/kg	6.5±0.3	6.2±1.8	17.5±1.6
$t_{1/2}$_term	h	18.0±3.5	46.6±26.6	144.3±164.1
MRT	h	42.5±3.0	47.0±6.0	153.2±113.3
BA	%	62.9±6.6	66.4±11.5	30.8±3.1

$AUC\_{0\text{-}last}$, area under the curve to the last value above the limit of detection; AUC_{inf}, AUC to infinite time; extrap, extrapolated portion of AUC; C_{max}, maximum concentration observed; $t_{1/2}$_term, elimination half-life; MRT, mean residence time; and BA, bioavailability. Parameters were measured in Matlab R2019b.

The bioavailability of the $rFIX_{K5R}$-FP was lower (~31%) compared to $rFIX_{K5A}$-FP (66%) and $rFIX_{WT}$-FP (~63%) (Table 9). These results suggests that $rFIX_{K5R}$-FP (stronger binding in the extravascular space) potentially adheres longer at the site of injection resulting in lower plasma levels and bioavailability.

In general, the area under the curve (AUC) of the albumin fused proteins were higher compared to the non-fused proteins, as expected. Albumin fusion prolongs the time rFIX can circulate in the body before being degraded.

4.3.2.2 Kinetics in sampled tissue

At 72, 144, and 168 hours post administration (terminal timepoints), livers were harvested for immunohistochemical analysis. The mean fluorescence intensity (MFI) and the rFIX concentration in plasma is correlated in Figure 26.

At 72 hours, the mean fluorescence of the stained livers showed comparable fluorescence intensities between $rFIX_{WT}$-FP and $rFIX_{K5R}$-FP groups but a lower signal for $rFIX_{K5A}$-FP. However, at 144 hours post administration of rFIX, only considerableamount of $rFIX_{K5R}$-FP and relative low amounts of $rFIX_{WT}$-FP were detected in the liver tissues and at 168 hours no signal was detectable in any of the groups. These results of prolonged tissue absorption of $rFIX_{K5R}$-FP were similar to the observations in the immunohistochemical analysis of non-fused rFIX proteins (Figure 22).

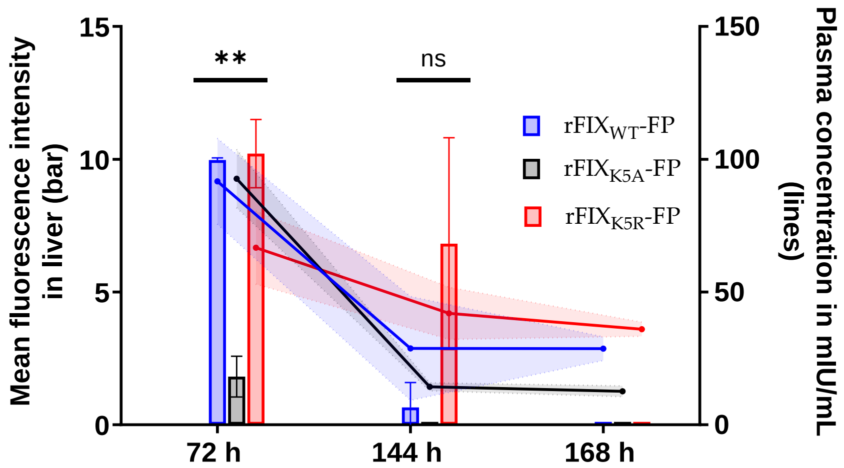

Figure 26. Immunohistochemistry staining of liver tissues (albumin fused proteins).
Livers from HB mice n=3) following intravenous administration of rFIX-FP (200IU/kg). Quantitative analysis of FIX positive liver sections collected at 72 h, 144 h, and 168 hours after treatment with rFIX proteins was performed in ZEN Software. Each bar and symbol (circle) represent the median ± 95% CI of at least 6 sections from sampled livers. The blue, black and red bars represent $rFIX_{WT}$-FP, $rFIX_{K5A}$-FP, $rFIX_{K5R}$-FP, respectively. The dotted lines represent the error bands (95% CI) for the plasma concentrations (FIX:Ag). The groups were compared separately at each timepoint using 1-way ANOVA test to determine the p-value and was reported as not significant (ns) or $p < 0.01$ (**).

4.3.3 Colocalization of rFIX and Collagen IV

Immunohistochemistry colocalization staining of rFIX and collagen IV in the liver of HB mice treated with rFIX exhibited a high degree of spatial overlap. Because of similar distribution of FIX and collagen IV, a ubiquitously expressed extracellular matrix protein. Interestingly, some areas surrounding hepatic vascular structures were restricted to collagen IV but no FIX signal was detected at these sites, as highlighted by the white arrow in Figure 27A. The respective controls (secondary antibodies in the absence of primary antibodies) confirmed that the signal was specific to the primary antibody FIX and Collagen IV.

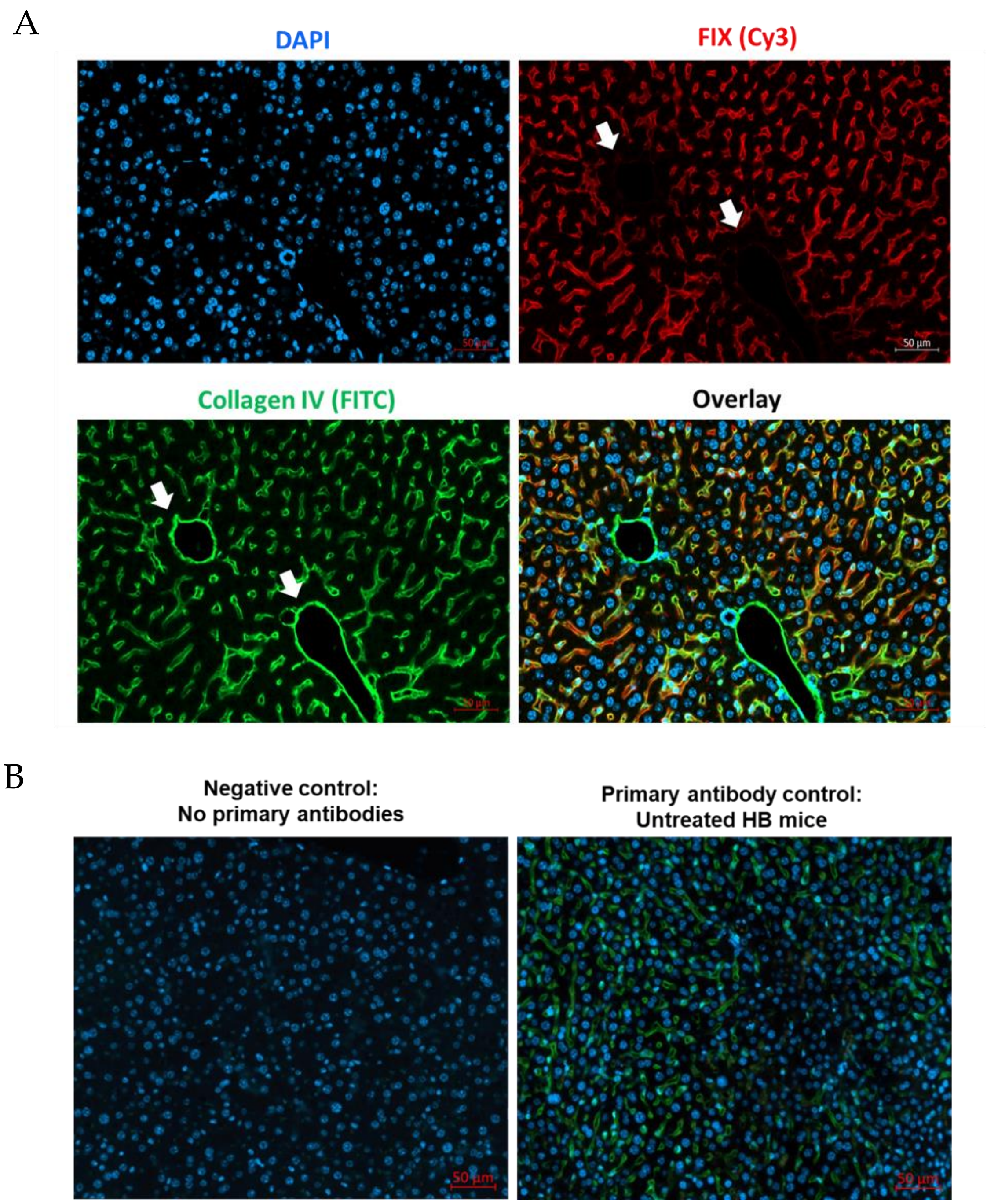

Figure 27. Colocalization of FIX and Collagen IV in murine liver tissues.
(**A**) Livers from rFIX-FP treated hemophilia B mouse was co-stained for FIX (red, Cy3), and Collagen IV (green, FITC). Merged image of DAPI, Cy3, and FITC channels show the overlap between FIX and Collagen IV. White arrows indicate blood vessels in the liver. (**B**) On the left, the negative control refers to the FIX staining conducted under the same conditions as Figure 27A but omitting the primary antibodies. On the right, the primary antibody control refers to the FIX staining under the same conditions as described previously of liver sections derived from untreated HB mice.

Unspecific binding to the tissue or cross-reactions between the secondary antibodies was discarded as the controls were negative (no signal) as shown in Figure 27B.

When the FIX/Collagen IV co-staining is performed in sections of untreated HB mice (no FIX available), only Collagen type IV but no FIX signal is detected and when sections containing FIX are stained in absence of the primary antibody (anti-human FIX) no signal is observed, as expected.

4.3.4 Distribution of FIX and rFIX in human and murine liver

Further, an immunohistochemical (IHC) staining of endogenous FIX was performed in pathologically normal human liver tissue samples from non-hemophilic donors.

A

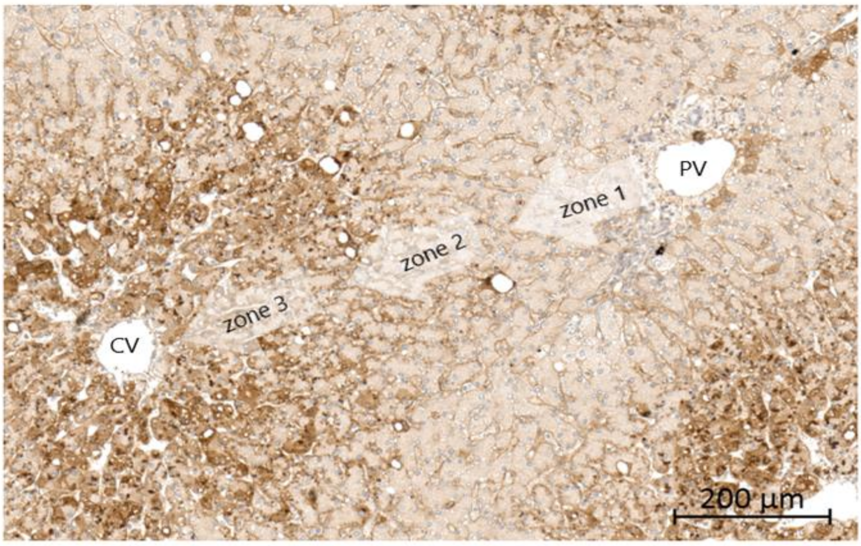

B

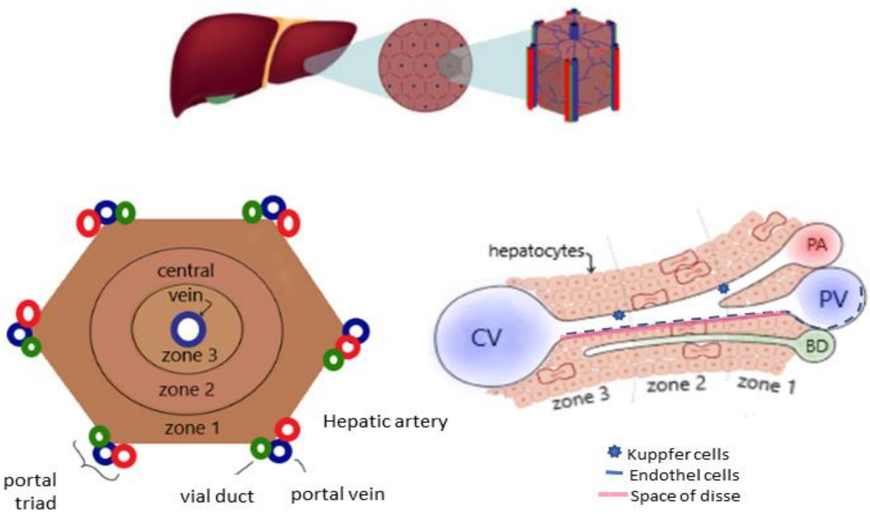

Figure 28. Endogenous FIX staining in human liver sections.
(**A**) Human liver sections were stained for FIX using DAB (dark brown) and nuclear counterstaining using hematoxylin (blue/grey). (**B**) Scheme of the hepatic structures. CV: central vein, PV: portal vein, PA: portal artery, BD: bile duct.

The samples were supplied by Amsbio (AMS Biotechnology (Europe) Limited, Oxfordshire, UK). The samples were purchased as paraffin-embedded normal human liver slices and were stained with DAB. Dark brown colored areas indicated FIX positive staining (Figure 28A).

Interestingly, similar to the observation in HB mice treated with exogenous rFIX, endogenous FIX in human liver was also not found uniformly distributed within all hepatic zones. Endogenous FIX was present mostly in areas surrounding the central vein (Figure 28A). A scheme illustrating the different zones can be found in Figure 28B. The significance of this observed difference in localization of FIX in different regions of the liver warrants further investigation. Within the liver, hepatocytes are involved in the synthesis of blood factors, such as FIX. In human liver FIX was found mostly intrahepatic, as expected. On the other hand, in sections stained with rFIX treated HB mice, FIX was found solely in extrahepatic areas (Figure 29).

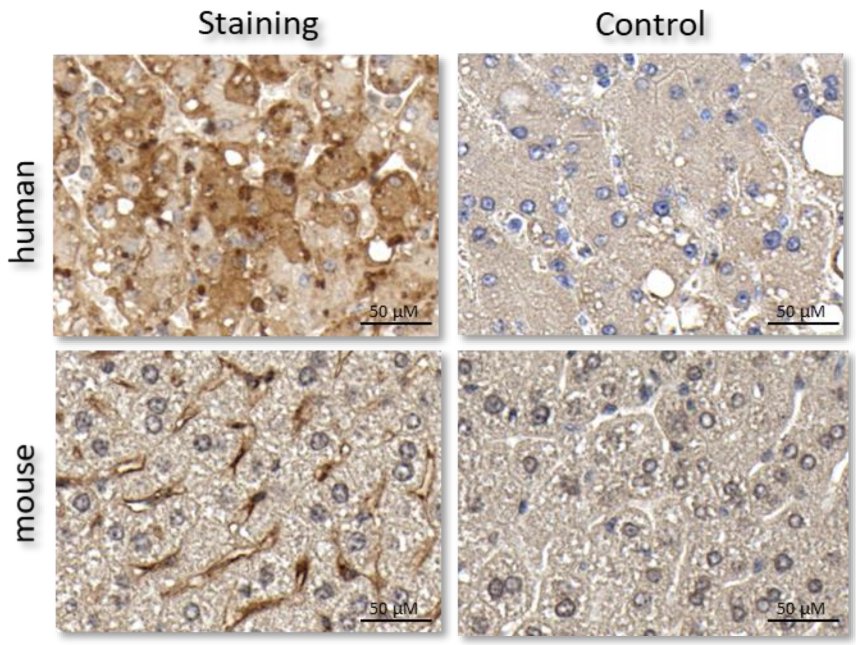

Figure 29. FIX staining in human and rFIX treated HB mouse liver tissues. Control refers to tissues treated with secondary antibody alone.

4.4 *In vivo* efficacy of non-fused rFIX in HB mice

The efficacy studies were focused on the non-fused rFIX proteins to enable better comparison to published literature data on the role of extravascular FIX (Cooley et al., 2016). The hemostatic efficacy of rFIX proteins in preventing bleeding was evaluated in HB mice. In addition, the role of rFIX in the process of thrombus formation was studied in mesenteric artery thrombus model after intravenous administration. The animals were dosed based on FIX activity, measured by OSCA.

4.4.1 *In vivo* pharmacodynamic profile of non-fused rFIX proteins

4.4.1.1 Tail clip bleeding model in HB mice

4.4.1.1.1 After intravenous administration

Hemostatic efficacy of rFIX proteins was evaluated at 15 minutes, 24 hours, 72 hours, 168 hours and 336 hours after i.v. injection by monitoring the total blood loss and bleeding incidence as detailed in materials and methods (Section 3.7.2). The results of blood loss and bleeding incidence are shown in Figure 30A and Figure 30B, respectively.

For statistical analysis, the set of rFIX molecules ($rFIX_{WT}$, $rFIX_{K5A}$ and $rFIX_{K5R}$) were compared at every timepoint individually and p values are summarized in Figure 30C. Treatment of HB mice with rFIX significantly protected the animals from total blood loss (vehicle:~ 10 µL/g of BW; rFIX treated: ~1 µL/g of BW, Figure 30A) until 24 hours post treatment. As depicted in Figure 30A, the total blood loss is comparable between rFIX treated groups until 168 hours. However, at 336 hours post-administration only the animals treated with $rFIX_{K5R}$ had nearly 50% decrease in blood loss compared to vehicle group though not statistically significant (vehicle: ~ 18 µL/g of BW; $rFIX_{K5R}$: ~9 µL/g of BW).

A significant effect in protection from bleeding incidence was observed for all the rFIX molecules at 15 minutes post treatment. However, at later timepoints the efficacy of individual rFIX proteins decreased over time at different rates. More specifically, the statistically significant effect on reducing bleeding incidence was lost at 24 hours post treatment for $rFIX_{K5A}$, at 72 hours for $rFIX_{WT}$ and at 168 hours for $rFIX_{K5R}$ (Figure 30C).

It is worth noting that both parameters, blood loss and bleeding incidence, need to be contextualized because these parameters reflect different aspects of hemostatis. For example, the bleeding incidence (Figure 30B) or bleeding time which indicates the time when mice stop bleeding reflects full occlusion of the vessel. On the other hand, non-occlusive thrombus could potentially reduce blood loss (Figure 30A) but animals may continue to bleed through out the observation time.

A

B

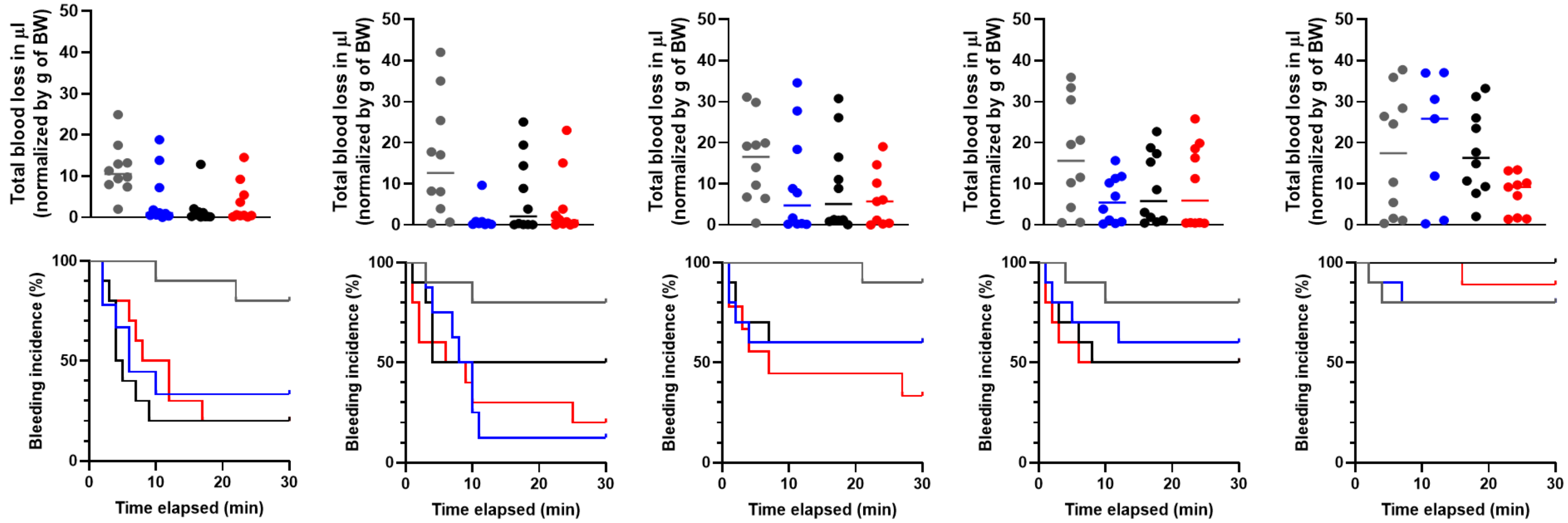

C

	Blood loss Dunnett´ test (ad. P value)	BI Log-rank test (P value)
$rFIX_{WT}$	**0.0182**	**0.0191**
$rFIX_{K5A}$	**0.0011**	**0.0017**
$rFIX_{K5R}$	**0.0064**	**0.0037**

	Blood loss Dunnett´ test (ad. P value)	BI Log-rank test (P value)
$rFIX_{WT}$	**<0.0001**	**0.0056**
$rFIX_{K5A}$	**0.0024**	0.1591
$rFIX_{K5R}$	**0.0003**	**0.0062**

	Blood loss Dunnett´ test (ad. P value)	BI Log-rank test (P value)
$rFIX_{WT}$	0.4929	0.106
$rFIX_{K5A}$	0.4662	0.1066
$rFIX_{K5R}$	0.1549	**0.008**

	Blood loss Dunnett´ test (ad. P value)	BI Log-rank test (P value)
$rFIX_{WT}$	0.0588	0.3228
$rFIX_{K5A}$	0.2081	0.1302
$rFIX_{K5R}$	0.2464	0.1192

	Blood loss Dunnett´ test (ad. P value)	BI Log-rank test (P value)
$rFIX_{WT}$	0.6242	0.9975
$rFIX_{K5A}$	0.9996	0.1464
$rFIX_{K5R}$	0.236	0.5609

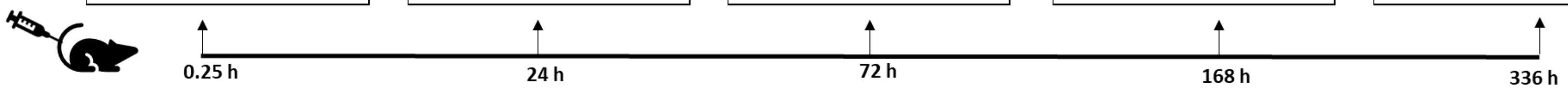

Figure 30. Tail clip bleeding model after intravenous administration.
Comparison of the hemostatic efficacy at different timepoints (0.25 – 336 hours post administration) after intravenous administration of hemophilia B mice with rFIX proteins (FIX:C 50 IU/kg) in a tail clip bleeding model. FIX_{WT} is depicted in blue, $rFIX_{K5A}$ in black, $rFIX_{K5R}$ in red and animals injected with saline were referred to as vehicle group (grey). The group size was n=8-10 animals and for statistical analysis the treatment groups were compared to the vehicle group. (**A**) The blood loss normalized to the body weight (gram) is depicted in a scatter plot. Each point represents the median. (**B**) The efficacy of rFIX to stop bleeding over 30 minutes is plotted using a Kaplan-Meier curve. (**C**) The (adjusted) P values were summarized in the tables below the respective graphs at each timepoint and were highlighted in bold if significant ($p < 0.05$). Statistics were performed using a 1-way ANOVA-test followed by a Dunnett´s post hoc test for the blood loss parameter. BI is the abbreviation for bleeding incidence and the statistical analysis was performed using a Log-rank (Mantel-Cox).

The FIX antigen (solid lines) vs. the activity (dashed lines) levels correlate with each other (Figure 31, Spearman r = 0.91; 95% confidence interval = 0.87 to 0.93; p value (two-tailed) = <0.0001; n of pairs = 140). rFIX antigen and activity was detectable in the plasma in the 15 minutes group and no detectable rFIX protein was present in the circulation after 24 hours (Figure 31). Hence, hemostatic efficacy observed at 24 hours and beyond is in part attributed potentially to extravascular FIX. The 2-fold difference between the FIX:Ag and FIX:C values in mIU/mL can be explained by the differences in the assays. The calibration curve of one stage clot assay (OSCA; FIX:C) is based on standard human plasma (SHP) and in ELISA the injection solution is used as a standard. Additionally, a matrix effect (normal ranges of other plasma proteins and activation od plasma proteins involved in the intrinsic pathway of the coagulation cascade) using OSCA can´t be ruled out due to the conditions under which mouse plasma samples were collected (after transection of a main peripheral artery and veins leading to major bleeding and consumption of coagulation factors).

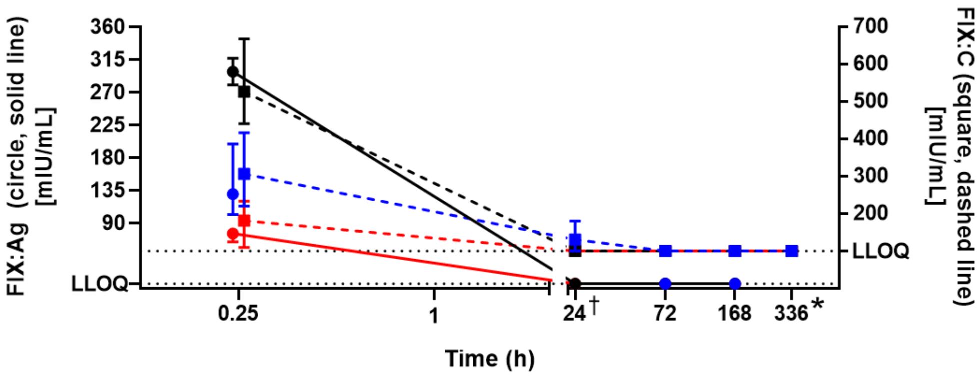

Figure 31. Exposure of rFIX in plasma of HB mice after tail clip model (intravenous administration).
HB mice were administered intravenously with $rFIX_{WT}$ (blue), $rFIX_{K5A}$ (black), and $rFIX_{K5R}$ (red). At the end of each experiment blood was collected from the injured animals for measurements of antigen levels (FIX:Ag, circle symbols and solid lines), and activity levels (FIX:C, square symbols and dashed lines). The antigen levels in the $rFIX_{WT}$ group at 24 hours is not available (†) because no blood samples were collected. Each symbol represents the median ± 95% CI of 8-10 animals. The LLOQ of FIX:Ag (6.25 mIU/mL) and of the FIX:C (100 mIU/mL) is indicated with black dotted lines against left and right Y-axis, respectively. No FIX:Ag levels were detectable in plasma at 336 hours, LLOQ differed at this timepoint and for all three proteins was 25 mIU/mL (*). Values ≤ LLOQ were plotted as 100 mIU/mL for FIX:C or 6.25 mIU/mL for FIX:Ag.

In general, all proteins are comparable regarding their ability to reduce blood loss. Though statistically not significant, $rFIX_{K5R}$ showed the longest efficacy in reducing blood loss until 14 days compared to vehicle group, even when no rFIX was detected in the circulation. This result suggests the presence of non-circulating but accessible rFIX to the site of injury. Beyond blood loss, the bleeding incidence suggest that $rFIX_{K5A}$ conveys good protection but loses this ability very fast, demonstrating that $rFIX_{K5A}$ may not be easily accessible at the site of injury after 24 hours, therefore, limiting the growth of a stable clot that requires both, circulating FIX in the thrombotic area and easily accessible FIX at the site, to achieve full vessel occlusion.

4.4.1.1.2 After subcutaneous administration

Hemostatic efficacy of rFIX proteins was evaluated at 24 hours, 72 hours, and 168 hours after subcutaneous injection of rFIX proteins (FIX:C 50 IU/kg) in a tail clip model (Figure 32). The plasma exposure at the end of the experiment (Figure 34) showed no detectable rFIX antigen levels (FIX:Ag, < 12.5 mIU/mL) in the samples, and only low levels of rFIX activity were detectable at 24 hours after subcutaneous administration in the clotting activity assay (FIX:C). The FIX:C activity levels were close to LLOQ and only neglectable amounts, if any, of FIX were detectable in circulation at the end of the experimental procedure.

The consumption of coagulation factors to maintain hemostasis during the tail clip induced bleeding might potentially have an impact on the plasma exposure measured at the end of the experiment (Figure 34). On the other hand, when reduced blood is lost the impact is minimized and can reflect the actual FIX levels in plasma at the beginning of the experiment.

Interestingly, the subcutaneous administration of $rFIX_{WT}$ and $rFIX_{K5R}$ compromised the efficacy of these two rFIX proteins as there was no significant difference in blood loss or bleeding incidence between vehicle and $rFIX_{WT}$ or $rFIX_{K5R}$ treated groups (Figure 32). Despite dosing at the same clotting activity, only $rFIX_{K5A}$ showed statistical significance in blood loss at 24 hours (Figure 32A and Figure 32C). The efficacy of rFIX$_{K5A}$ also diminished over time with no significant effect in blood loss after 72 hours (Figure 32A and Figure 32C).

A

B

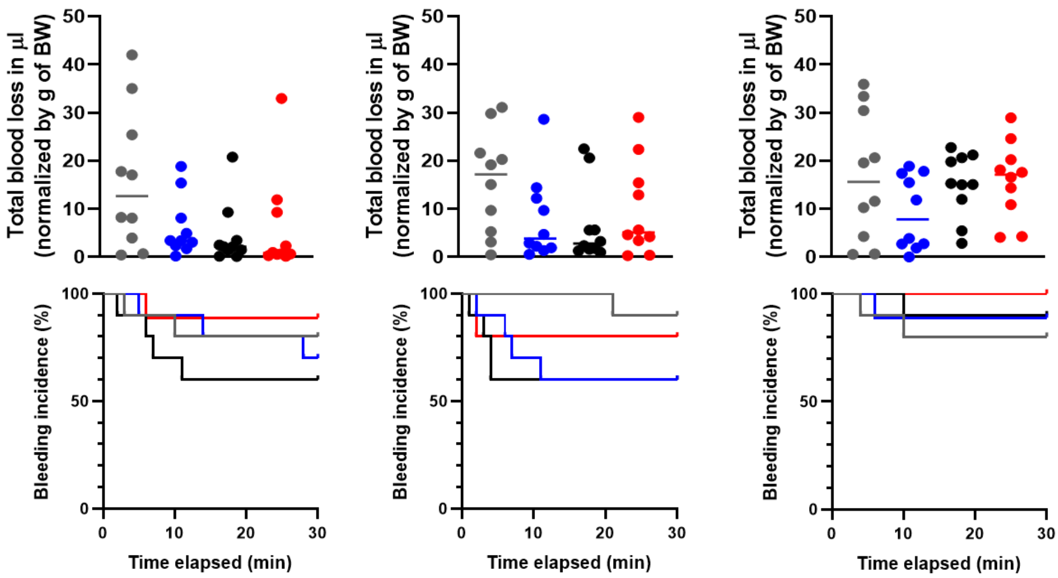

C

	Blood loss Dunnett´ test (ad. P value)	BI Log-rank test (P value)
rFIX$_{WT}$	0.0885	0.6909
rFIX$_{K5A}$	**0.0359**	0.346
rFIX$_{K5R}$	0.0819	0.6076

	Blood loss Dunnett´ test (ad. P value)	BI Log-rank test (P value)
rFIX$_{WT}$	0.4079	0.1045
rFIX$_{K5A}$	0.2403	0.1074
rFIX$_{K5R}$	0.7395	0.5128

	Blood loss Dunnett´ test (ad. P value)	BI Log-rank test (P value)
rFIX$_{WT}$	0.1926	0.6076
rFIX$_{K5A}$	0.9545	0.5151
rFIX$_{K5R}$	0.9957	0.1464

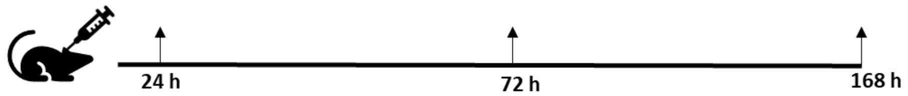

Figure 32. Tail clip bleeding model after subcutaneous administration.
Comparison of the hemostatic efficacy in a tail clip bleeding model after subcutaneous administration of rFIX (FIX:C 50 IU/kg). rFIX$_{WT}$ is depicted in blue, rFIX$_{K5A}$ in black, rFIX$_{K5R}$ in red and animals injected with saline were referred to as control vehicle group (grey). The group size was of n=9-10 animals and for statistical analysis the treatment groups were compared to the vehicle group. (**A**) The blood loss normalized to the body weight (gram) is depicted in a scatter plot. Each bar represents the median. (**B**) The bleeding incidence, determined by the time to stop bleeding over 30 minutes observation period is plotted using a Kaplan-Meier curve and statistical analysis was performed using a Log-rank (Mantel-Cox) test. (**C**) The (adjusted) P values were summarized in the tables below the respective graphs at each timepoint and were highlighted in bold if significant ($p < 0.05$). For blood loss, statistical analysis were performed using a 1-way ANOVA-test followed by a Dunnett´s post hoc test. BI is the abbreviation for bleeding incidence and the statistical analysis for BI was performed using a Log-rank (Mantel-Cox) test. *Vehicle at timepoints 24 hour and 168 hours were extracted from historical data (under similar conditions).*

Though not statistically significant, the maximum reduction in bleeding incidence following subcutaneous administration was observed for $rFIX_{WT}$ and $rFIX_{K5A}$ proteins at 72 hours (Vehicle: 90%, $rFIX_{WT}$: 60%, $rFIX_{K5A}$: 60%, $rFIX_{K5R}$: 80%, Figure 32B and Figure 32C). Overall, only $rFIX_{K5A}$ demonstrated a statistically significant efficacy after subcutaneous administration and the $rFIX_{WT}$ and $rFIX_{K5R}$ outcome, despite hemostatic protection, was slightly inferior compared to $tFIX_{K5A}$.

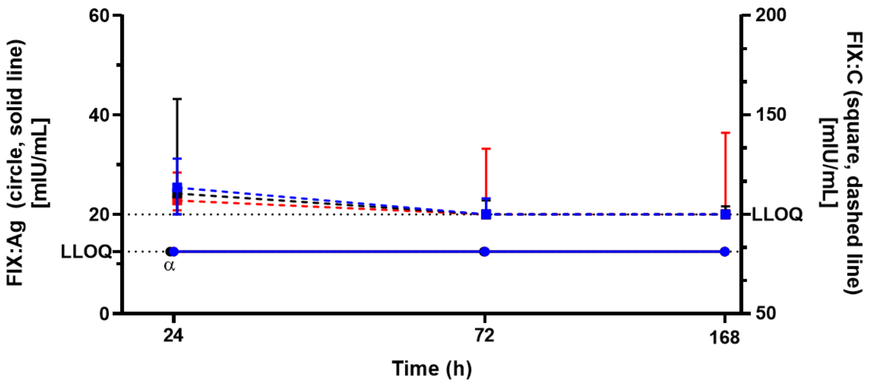

Figure 33. Exposure of rFIX in plasma of HB mice after tail clip (subcutaneous administration). HB mice were administered subcutaneously with $rFIX_{WT}$ (blue), $rFIX_{K5A}$ (black), and $rFIX_{K5R}$ (red). At the end of each experiment blood was collected from the injured animals for measurements of antigen levels (FIX:Ag, circle symbols and solid lines), and activity levels (FIX:C, square symbols and dashed lines). Each symbol represents the median ± 95% CI of 8-10 animals. The LLOQ of FIX:Ag (12.5 mIU/mL) and of the FIX:C (100 mIU/mL) is indicated with black dotted lines against left and right Y-axis, respectively. No FIX:Ag levels were detectable in plasma except at 24 hours by one out of 10 animals in the $rFIX_{K5A}$ group (α). Values ≤ LLOQ were plotted as 100 mIU/mL for FIX:C or 12.5 mIU/mL for FIX:Ag.

At the end of the experiment, blood samples collected from each animal were tested for antigen FIX:Ag and clotting activity FIX:C levels as depicted in Figure 33. No FIX:Ag levels were detectable at any timepoints, while the FIX:C levels at 24 hours were marginally above the detection limit.

4.4.1.2 Mesenteric thrombosis model

The clot formation was investigated *in vivo* in a thrombosis model using $FeCl_3$ as a chemical stimulus to induce thrombus and platelet aggregation and was visualized in real-time under brightfield intravital microscopy. The time to occlusion (TTO) of the artery, the time of appearance of first thrombi (TTAOFT) and thrombus area were observed.

4.4.1.2.1 Establishment of the experimental set-up

Published literature has shown that $FeCl_3$ injury induced a clot formation in C57BL/6J mouse artery but FXI ko mice were protected from arterial thrombosis in this model (Renné et al., 2005). Therefore, both strains were included as positive and negative controls, respectively.

C57BL/6J wildtype mice have normal blood clotting capacity. As expected, C57BL/6J mice formed an occlusive thrombus ~ 10 minutes after injury induction and FXI ko mice, a strain with impaired hemostasis, exhibited non-occlusive thrombus formation (Figure 34A). $FeCl_3$ induced thrombus was never studied in HB mice, and we found that HB mice showed a clear anti-thrombotic phenotype (Figure 34B).

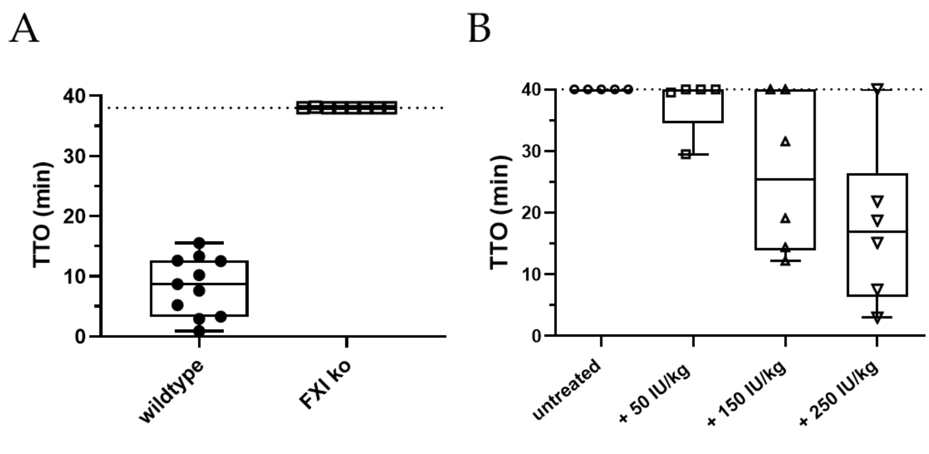

Figure 34. Establishment of the $FeCl_3$-induced mouse mesenteric arteriole model in HB mice. Small mesenteric arterioles were injured by topical application of $FeCl_3$ and occlusive thrombus formation was monitored using intravital microscopy. Each symbol represents one animal and time to occlusion (TTO) is plotted as a box and whisker plot (in minutes) where the box spans the 25th and 75th percentile, the marks the median time, and the whiskers mark the min. and max. data points (n=6-10 animals per group). The dotted line at 38 minutes represents the maximal observation time. (**A**) Pro-thrombotic phenotype of C57BL/6J wildtype strain (positive control, occlusion after ca. 10 minutes) and anti-thrombotic phenotype of FXI ko strain (negative control, no occlusion). (**B**) Anti-thrombotic phenotype of untreated HB mice (no occlusion) and a dose-dependent response of intravenous administration of rFIX approximately 20 minutes prior to injury with $FeCl_3$.

While the initial stimulatory response induced by $FeCl_3$ promotes platelets activation and transient aggregation of platelets in C57BL/6J wildtype mice, in contrast, HB mice lack the ability to form a proper stable thrombus. In a dose-response experiment, 50IU/kg, 100IU/kg and 250Iu/kg of $rFIX_{WT}$ were tested. In general, these data showed that rFIX treatment maintains hemostasis in HB mice after $FeCl_3$ injury.

Since maximum efficacy was observed with a dose of 250 IU/kg, this dose was selected to conduct further experiments (34B). The following parameters, detailed in the next section were taken into consideration for further analysis: the time to appearance of first thrombi (TTAOFT), reported as the time elapsed until appearance of first thrombi and the time to occlusion (TTO), referred to the time elapsed until the thrombus reached a size that blocked the blood flow (occlusion) of the vessel. Representative images of one experiment are depicted in Figure 35.

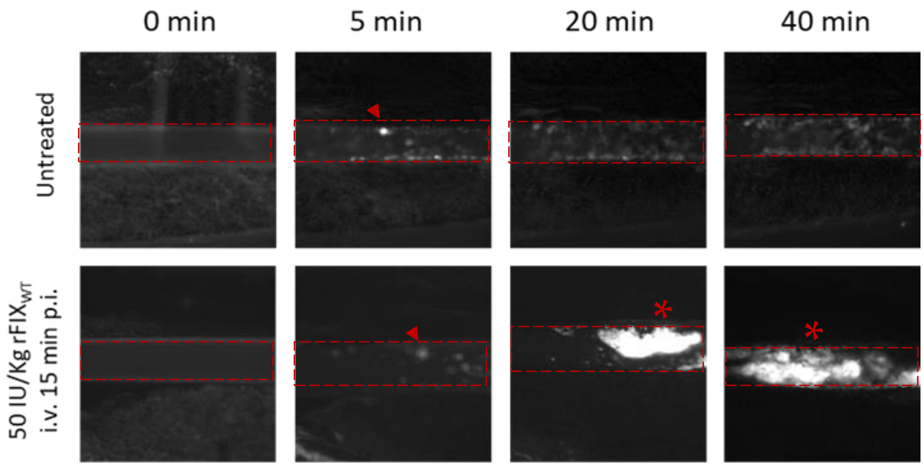

Figure 35. Representative images after $FeCl_3$ induced injury of mesenteric arteriole in HB mice. Untreated HB mice were injected with saline and the treatment group was treated with 50 IU/Kg $rFIX_{WT}$ intravenously (i.v.) around 15 minutes prior to $FeCl_3$ injury. The vessels are indicated with red dashed lines and in the injured regions the aggregation of platelets was visible as disseminated platelet clusters throughout the vessel. A clump diameter of > 10 µm (▲) was defined as the appearance of first thrombi. The growth of the thrombi over time was observed in the HB mouse treated previously with $rFIX_{WT}$ (*).

4.4.1.2.2 Pharmacodynamic assessment in HB mice

In a blinded study, the efficacy of intravenous administration of $rFIX_{WT}$, $rFIX_{K5A}$, and $rFIX_{K5R}$ were tested in the mesentric artery thrombosis model and compared to the vehicle group (treated with PBS). The time to appearance of first thrombi (TTAOFT) did not differ between groups (36A), but the time to occlusion was significantly lower in $rFIX_{WT}$ treated group compared to $rFIX_{K5A}$ and vehicle treated groups (Figure 36B).

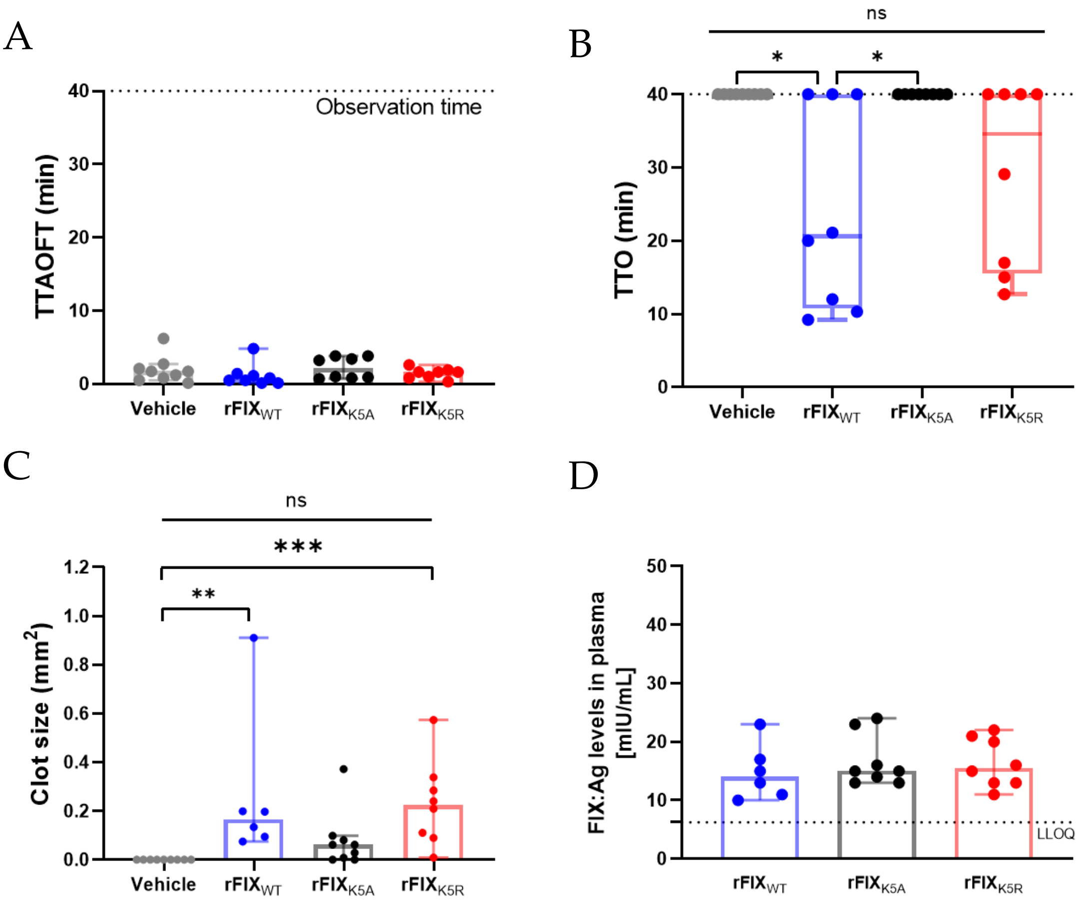

Figure 36. Efficacy of rFIX proteins in the mesenteric artery thrombosis model.
Animals (n=8 per group) were injected intravenously with $rFIX_{WT}$ (blue), $rFIX_{K5A}$ (black), $rFIX_{K5R}$ (red), or with saline (grey) 24 prior to $FeCl_3$ induced injury of the mesenteric vessel over 40 minutes. The saline group is referred to as vehicle. (**A**) The time to appearance of first thrombi (TTAOFT >10µm) is plotted as a scatter dot plot in minutes, each data point represents one animal (bars indicate the median ± 95 CI). (**B**) The time to occlusion of the artery (TTO in minutes) was recorded to assess the ability of rFIX to form occlusive thrombus. Each symbol represents one animal and TTO is plotted as a box and whisker plot (in minutes) where the box spans the 25th and 75th percentile, the marks indicate the median time, and the whiskers mark the min. and max. data points. The dotted line at 40 minutes represents the maximum observation time. (**C**) The quantification of the

maximum thrombus area of the injured vessels is depicted as clot size (CS) normalized to the vessel area in mm^2. It is plotted as a scatter dot plot and each data point represents one animal (bars indicate the median ± 95 CI). (**D**) FIX:Ag levels measured at the end of the experiment using ELISA. The concentration (mIU/mL) was plotted as a scatter dot plot and each data point represents plasma level from one animal (bars indicate the median ± 95 CI of 6-8 animals). The statistical significance (adjusted P value) was determined by Kruskal-Wallis test followed by Dunn´s post hoc test and was reported as not significant (ns), $p < 0.05$ (*), $p < 0.01$ (**), and $p < 0.001$ (***).

Although not statistically significant, there was a trend towards lower time to occlusion in $rFIX_{K5R}$ treated group compared to vehicle and $rFIX_{K5A}$ treated groups. The thrombus incidence, which refers to the full occlusion of the vessel within the observed time was around 38% (3 out of 8 animals) and 50% (4 out of 4 animals) in the $rFIX_{WT}$ and $rFIX_{K5R}$ groups, respectively (36B).

In contrast, $rFIX_{K5A}$ was comparable to vehicle group and was unable to form occlusive thrombus (36B). The $rFIX_{K5A}$ group showed reduction in clot size, while in the $rFIX_{WT}$ and $rFIX_{K5R}$ group the thrombus grew to occlusive dimensions (36C). Thrombus in the $rFIX_{K5A}$ group were stable but did not reach the occlusive dimensions. Blood samples collected at the end of the experiment were processed to isolate plasma to determine circulating levels of rFIX. As shown in Figure 36D, all rFIX treated groups had detectable levels of rFIX in the plasma. These results clearly show that despite detectable levels of plasmatic FIX, $rFIX_{K5A}$ was less effective in inducing thrombus possibly due to its weaker binding to extracellular matrix.

5 DISCUSSION

Maintenance of an appropriate level of FIX activity is crucial for prevention of bleeding in HB patients. If left untreated, lack of FIX activity can cause severe damage to the patient and can even lead to death. Over the last decades, several important milestones in research and advancement in treatment have been reached in the field of blood coagulation. Important findings like the role of vitamin K in induction of clotting and the discovery of several clotting factors have contributed to a better understanding of hemostasis. A turning point in the clinical treatment of hemophilia was the generation of recombinant extended half-life (EHL) products for prophylactic treatment with reduced frequency of dosing. From then on, disruptive and innovative approaches are being explored continuously to further improve the quality of life of hemophilic patients.

In the HB field, disruptive technologies like non-factor replacement therapies are being used, mostly in cases where patients develop anti-drug antibodies, and the replacement therapy becomes ineffective. Within the non-replacement therapies, the anti-thrombin III (ATIII) is a common target. The inhibition of this serine protease can restore hemostatic balance in hemophilic A or B patients independently of the missing coagulation factor (Pasi et al., 2021),(Phimister and Ragni, 2015). Another innovative approach, gene therapy, is already being employed in clinical trials with a significant reduction of annualized bleeding rates over the course of 5 years following treatment with adeno-associated virus gene therapy expressing a highly active variant of FIX (Samelson-Jones et al., 2021). The principle of this approach is the correction of the genetic abnormality and restoration of normal FIX clotting levels. One of the major clinical challenges in the gene therapy approach, which uses adeno associated virus (AAV) as a vector to deliver the FIX transgene, is the presence of cross-reactive antibodies against AAV in the HB population. Patients with these anti-AAV antibodies are ineligible for gene therapy. Furthermore, the eligibility criteria to receive gene therapy foresee that only adult HB patients with a healthy liver can receive the treatment, which excludes children from the trials at this time. Despite the encouraging safety data till current date, long-term follow-up data (> 10 years) demonstrating safety and efficacy will only be available in the future (Monahan, 2015).

To date the standard of care in HB is replacement therapy via intravenous infusion, which is supported by real world evidence regarding safety and efficacy but poses several clinical challenges including frequent injection and difficult venous access, particularly in infants. There are efforts put into the development of subcutaneous forms of administration for the delivery of exogeneous FIX into the patient´s circulation. Subcutaneous administration could be the preferred route of administration for convenience but has been limited historically by low bioavailability and tolerability (Brooks et al., 2013). This delivery route is governed by complex inter-related physiology and transport pathways governing the interstitial matrix, vascular system and lymphatic channels, which contribute to transport and biodistribution in the subcutaneous space. The bioavailability and the immune-inflammatory response toward subcutaneous administered proteins can be modulated not only by a proper drug formulation but also by modifications at molecular level, if for example the engineered protein is less immunogenic or less prone to interact with components of the subcutaneous space. Such a modification could potentially facilitate delivery into the blood stream as demonstrated by a full length rFIX with 3 amino acid substitutions that confers the product to have increased specific activity, enhanced FVIIIa binding, and reduced inhibition by antithrombin (AT III) that was assessed in a phase 2b clinical trial (You et al., 2021). These single point modifications improved subcutaneous bioavailability and could be highly beneficial for prophylactic therapy.

The concept of preventing, rather than treating, bleeds in HB patients has made of the engineered recombinant FIX (rFIX) proteins, a widely used product. Still, rFIX proteins are rather new and though deep knowledge has been gained there are still unanswered questions and unknowns regarding the dynamics and exact mode of action. Until now, plasma activity levels of factor IX (FIX) have been considered as being representative of the hemostatic competency of the patient. It is the only clinically measurable parameter to determine if a patient needs treatment – that is FIX activity levels more than 50% would provide robust hemostatic support and at levels progressively lower than this, an inadequate hemostatic response is more likely. However, recent studies on the hemostatic benefit of FIX have called this assumption into question (Cooley et al., 2016; Iorio et al., 2017). Since the FIX protein is relativelysmall (56 kDa), it can reside in both the intravascular and extravascular regions more easily (free diffusion between extravascular tissue and blood circulation) while proteins with larger molecular weight are most likely dependent on active transport mechanisms and are translocated more slowly to extravascular tissue. This might lead to the formation of a reservoir of FIX in the extravascular region, which conveys hemostatic protection. Extravascular space, as described in the introduction, refers to components outside the blood flow, including endothelial cells that are in contact with the lumen, and all other vascular components as depicted in Figure 37. The hemostatic role of exogeneous rFIX in the extravascular space was linked to the apparent reversible binding of rFIX to collagen type IV (Cooley et al., 2019).

In this work, the potential of extravascular rFIX to support hemostasis in the absence of measurable plasma FIX activity was addressed using a single point mutation that is described in the literature to have higher or lower affinity to components of the extracellular space. The mutation at position 5 from a lysine to an alanine (K5A) or an arginine (K5R) were thoroughly characterized *in vitro* and in vivo.

Published literature evidence has shown that the extravascular area can contain up to three times as much FIX as the circulating FIX, which is reversibly bound to the vascular endothelium and the subendothelial extracellular matrix (Feng et al., 2013).

The calcium-dependent high affinity binding between FIX and endothelial cells (EC) was first described in 1983 (Stern et al., 1985, 1983).

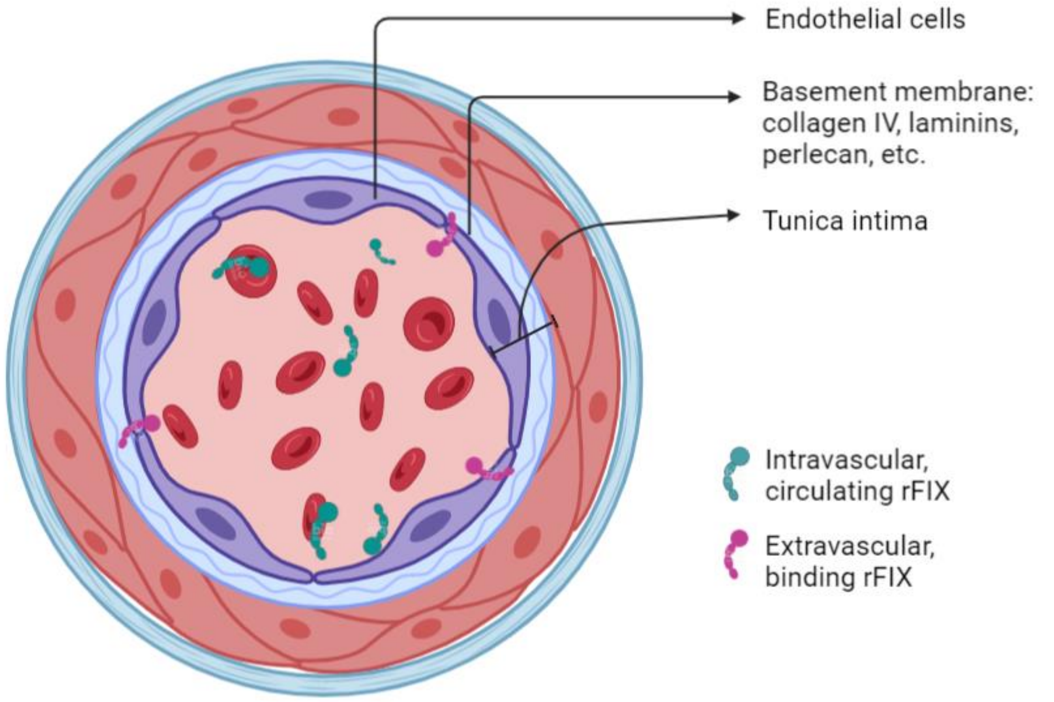

Figure 37. Intravascular vs. intravascular rFIX depicted in a vessel.
The vessels are made up of 3 layers. The external layer, tunica adventia. The layer containing smooth muscle cells, the tunica media. And the layer that is in direct contact with the lumen, the tunica intima. The tunica intima comprises of endothelial cells, basement membrane, and an internal elastic membrane. Image created using BioRender.

The clinical relevance of this binding was associated with the rapid loss of infused FIX from the circulation (Stern et al., 1983). Later on, experiments with chimeric FIX proteins that substituted the FIX-Gla domain by the coagulation FVII-Gla domain and point mutations in the Gla domain of FIX showed that the first 11 amino acids within the Gla domain (specific for FIX) are responsible for binding to EC (Cheung et al., 1992). Further analysis identified position 5 in the Gla domain as the binding site of FIX to ECs and leads to markedly reduced binding to ECs if lysine at position 5 is mutated to alanine (K5A), whereas the exchange to arginine (K5R) results in increased binding to ECs (Cheung et al., 1992). Identification of the extracellular binding partner of FIX on EC was postulated to be the extracellular matrix molecule collagen type IV (Cheung et al., 1996b). This interaction and its direct binding were confirmed in electron microscopy by Wolberg and colleagues (Wolberg et al., 1997b). The physiological outcome of this interaction between FIX and collagen type IV remained unclear. Therefore, the K5A and K5R single point substitution in the Gla domain of rFIX molecules were investigated for the first time *in vivo* in HB mice (Gui et al., 2002). The K5A variant showed increased bioavailability than K5R and wildtype rFIX in plasma immediately after intravenous injection, as evaluated in a 2-compartment model (Gui et al., 2002). During elimination phase, however, the K5A variant showed a faster overall clearance (Gui et al., 2002). One limitation of the mentioned publication was the lack of efficacy studies since the focus was on the pharmacokinetic characterization and the distribution of FIX in HB mice but in a subsequent publication a knock-in mouse carrying the K5A point mutation in the Gla domain of mouse FIX was generated. Studies performed in these mice showed a mild bleeding tendency suggesting the importance of extravascular FIX in hemostasis (Gui et al., 2009b).

The principal aim of this work was to elucidate the physiological relevance of extravascular rFIX and its distribution in an animal model of HB. Therefore, rFIX proteins with the point mutations K5A and K5R were generated in stable CHO cell lines. $rFIX_{K5A}$ is described as having lower binding affinity to ECs and $rFIX_{K5R}$ is described as having higher binding affinity to ECs compared to $rFIX_{WT}$ proteins. These proteins were characterized *in vitro* and *in vivo*. The single amino acid substituted mutants (K5A and K5R) were generated as non-fused rFIX ($rFIX_{K5A}$ and $rFIX_{K5R}$) and albumin fused ($rFIX_{K5A}$-FP and $rFIX_{K5R}$-FP) proteins. The respective wildtype proteins served as controls ($rFIX_{WT}$ and $rFIX_{WT}$-FP).

5.1 *In vitro* characterization of single point mutation at position 5 in albumin fused and non-fused rFIX

A thorough characterization was performed *in vitro* confirming the integrity and proper functionality of all the mutant and control wildtype proteins. Compared to the $rFIX_{WT}$ and $rFIX_{WT}$-FP molecules, no difference was detected in the activation of these mutant rFIX proteins by activated FXI (FXIa) in three different assays: a clot-based assay, aPTT (Figure 13), a SDS PAGE gel (Figure 14 and Figure 15), and a FIXa chromogenic assay (Figure 16 and Figure 17). This suggests that change of lysine to arginine or alanine at position 5 does not affect binding of rFIX to FXIa, neither does it affect the proteolytic conversion of FIX to the fully activated two-chain serine protease, namely FIXa. Additionally, the activity of FIX was evaluated using an assay that stimulates the assembly of the intrinsic Xase complex and the resultant generation of FXa as depicted in Figure 18. Modified FXa generation assay with serial dilutions of either FIX or the cofactor FVIII showed similar curve progression in all the proteins (Figure 19). The proteolytic activity of FIXa towards FX is known to increase ≥100,000-fold upon FVIIIa cofactor binding (Dieijen et al., 1981). In our hands, the calculated enzymatic parameters showed that $rFIX_{K5R}$ was more efficient in activating FX compared to $rFIX_{WT}$ and $rFIX_{K5A}$, when FVIII is the limiting factor in the reaction (> 1.2 nM of difference in Km) contrary to the albumin fused $rFIX_{K5R}$-FP, which displayed similar Km compared to $rFIX_{K5A}$-FP (Table 6). While the difference in Km was seen in the FXa chromogenic assay for $rFIX_{K5R}$, *in vitro* efficacy experiments showed comparable reduction of aPTT in human FIX deficient plasma in a clotting assay (OSCA) as previously mentioned (Figure 13). Here, all proteins decreased the aPTT from FIX-deficient human plasma similarly (from ca. 81 ± 4 seconds to 37 ± 1 seconds) suggesting that all six rFIX molecules are able to restore clot formation *in vitro* reaffirming their functional congruence.

The difference in Km of $rFIX_{K5R}$ compared to $rFIX_{WT}$ and $rFIX_{K5A}$, on the other hand, was observed only when rFVIII, but not when rFIX, was the limiting factor in the reaction. In general, the apparent faster activation of FX should be detectable when either FIX or FVIII are titrated; this is because the activation of FX occurs when the tenase (FIXa-FVIIIa-FX) complex assembles on platelets, respectively a phospholipids membrane. Therefore, the outcome of this assay was inconclusive in terms of the ability of $rFIX_{K5R}$ to activate FX faster and other techniques like Surface Plasmon Resoanance (SPR) could be more appropriate to evaluate the interaction of individual proteins during the formation of the tenase complex to determine the binding affinity between the proteins. The general setup of the assay was valid on a technical level and the outcomes regarding curve progression and the difference of V_{max} between the non-fused and albumin fused rFIX. The albumin fused rFIX entails an additional third cleavage (albumin) site that can slow down its full activation. V_{max} was reached faster by the non-fused proteins compared to albumin fused proteins.

Being mindful of the overall data, this effect seen in $rFIX_{K5R}$ is most likely explained by inherent variations within the assays (Marlar et al., 2020). The intrinsic tenase of FIXa and FVIIIa assemble on negatively charged phospholipid surface. In vivo, this surface is mainly provided by activated platelets. *In vitro*, the source of phospholipids can differ. They can be either obtained synthetically, as in the case of the chromogenic assay or from animals or from plants, as in the aPTT reagent. It is worth noting that these interactions are highly complex and multiple factors, and not only the binding affinity, can play a role on the activation of FX, as it was demonstrated in a similar chromogenic assay that revealed how a single point mutation (R338L, Padua) in the active site of the FIXa molecule enhances FXa generation due to an improved allosteric activation rather than an increased affinity of FVIIIa for FIXa (Samelson-Jones et al., 2019).

As mentioned previously, further studies to assess the binding of $rFIX_{K5R}$ to activated platelets and resting platelets could help to understand the real impact this single point mutation at position 5 has with respect of binding to activated or inactivated cell membranes.

Based on the current data, it was concluded that the single point mutation at position 5 has no major effect on the binding to the phospholipids contained in OSCA. These results are in-line with the literature, where the binding of $rFIX_{K5A}$ to phospholipids and platelets was investigated by Gui et al. and no differences were observed between wildtype and K5A variant (Gui et al., 2009b). In general, the *in vitro* data confirmed the integrity and functionality of the generated proteins.

5.2 PK profile and tissue levels of fused and non-fused $rFIX_{K5A}$ and $rFIX_{K5R}$ in HB mice

One aspect of this work was dedicated to the intravenous and subcutaneous pharmacokinetic (PK) characterization of the non-fused and albumin fused rFIX variants (K5R and K5A). The extravascular distribution as well as the elimination of the rFIX proteins from the plasma was assessed in HB mice.

5.2.1 PK of non-fused rFIX proteins

The PK results of the non-fused rFIX proteins (standard half-life proteins) suggest differences in 1) the *in vivo* recovery and the AUC in plasma, 2) clearance from plasma, and 3) volume of distribution between $rFIX_{K5A}$ and $rFIX_{K5R}$.

1) After intravenous administration, the plasma recovery (C_{max}_pred) of $rFIX_{K5A}$ immediately (~5 min) after bolus injection was higher compared to $rFIX_{K5R}$ and the reference wildtype molecule $rFIX_{WT}$ (Figure 20; Table 7). Similarly, the overall plasma exposure (AUC_$_{0\text{-last}}$ and AUC_$_{inf}$) was higher in the $rFIX_{K5A}$ group compared to $rFIX_{WT}$ and $rFIX_{K5R}$ group. Consistently, when $rFIX_{K5A}$ was administered subcutaneously it reached the highest plasmatic

concentrations and $rFIX_{K5R}$ had the lowest concentration in plasma as shown in Figure 21.

2) The $rFIX_{K5A}$ protein, after intravenous administration, has a slower elimination from plasma (clearance) over time compared to $rFIX_{K5R}$ and $rFIX_{WT}$ (Figure 20; Table 7). The effect on the clearance can be explained by the decreased binding affinity of $rFIX_{K5A}$ to the extravascular space. If $rFIX_{K5A}$ is found solely or mainly in the circulation, it would get gradually eliminated from plasma. Over time, the proteins that bind to extravascular space get released continuously into the circulation, from where they are eliminated. On the contrary, proteins that have higher binding affinity in the extravascular space (like $rFIX_{K5R}$) are not permanently circulating and could be protected from the normal degradation process that plasma proteins undergo. But since the fast initial clearance (rapid distribution to the extravascular space) results in a fast removal of rFIX from plasma, the total clearance from plasma is higher for $rFIX_{K5R}$. At early timepoints in the initial phase, the $rFIX_{WT}$ and $rFIX_{K5R}$ are removed rapidly from plasma potentially due to their interaction with accessible extravascular binding partners (insert in Figure 20). It was interesting to see that the progress of the curve in the $rFIX_{K5A}$ group, at initial timepoints, is more linear compared to $rFIX_{WT}$ and $rFIX_{K5R}$ (insert in the Figure 20) suggesting that the initial clearance (distribution) of $rFIX_{K5A}$ is less dependent on binding to the extravascular space and stays more in plasma compared to $rFIX_{WT}$ and $rFIX_{K5R}$. A difference between $rFIX_{WT}$ and $rFIX_{K5R}$ is not seen easily with the available timepoints but expectation would be that $rFIX_{K5R}$ (with increase binding affinity) should be cleared faster at early timepoints, meaning the bend of the curve is more pronounced with $rFIX_{K5R}$. Analysis of more timepoints between 5 minutes and 6 hours may help to observe potential differences between the $rFIX_{WT}$ and the $rFIX_{K5R}$ variants. In the subcutaneous arm, $rFIX_{K5A}$ seems to be cleared

faster compared to $rFIX_{WT}$ despite having a higher plasma exposure than $rFIX_{WT}$ (Figure 21).

3) The retention of rFIX proteins after intravenous administration was analyzed in the liver tissues sampled during the experiment at terminal timepoints. In a semi-quantitative histological analysis, all three rFIX proteins were detectable in the liver tissues at 15 minutes. $rFIX_{K5R}$ was detectable longer in liver until 24 hours compared to $rFIX_{K5A}$ and $rFIX_{WT}$ (Figure 22A). Differences between $rFIX_{K5A}$ and $rFIX_{WT}$ were not detectable at the analyzed timepoints. Analysis at an earlier timepoint e.g., at 8 hours or 16 hours would have been highly informative to potentially see the differences in tissue retention between $rFIX_{K5A}$ and $rFIX_{WT}$.

In summary, $rFIX_{K5A}$ with poor binding to the extravascular space, is found initially more in plasma but disappears faster from the body and later only $rFIX_{K5R}$ with a strong affinity to extravascular space is found in the tissue.

5.2.1.1 Potential therapeutic value

Despite the increased plasmatic concentrations in the intravenous arm, the half-life was reduced in the $rFIX_{K5A}$ group (Table 7). These results fit to the hypothesis that $rFIX_{K5A}$ molecules are more likely to circulate in plasma and not reside in the tissue most likely due to limited interactions with components of the extravascular space. This property of $rFIX_{K5A}$ could be beneficial in a subcutaneous setting as demonstrated in the subcutaneous PK profile in Figure 21. Here, increased concentrations reached in plasma (higher exposure) after subcutaneous administration suggested that $rFIX_{K5A}$ could offer the potential for therapeutic development of a subcutaneous form of administration of rFIX. The proposed mode of action is based on an improved bioavailability due to weaker interactions ($rFIX_{K5A}$) with components of the extracellular matrix that are abundant in the subcutaneous space, facilitating release into the circulation.

One limitation of the $rFIX_{K5A}$ was the faster elimination and decreased half-life. This kind of limitation could be easily counteracted by a combination of half-life extended modifications. A prolongation of the half-life can for example be achieved by fusion with proteins that already have a significantly longer half-life by nature [112]. Therefore, the PK profile of albumin fused rFIX proteins ($rFIX_{WT}$-FP, $rFIX_{K5A}$-FP, and $rFIX_{K5R}$-FP) was assessed and is tested in the next section 5.2.2.

5.2.2 PK of albumin fused rFIX proteins (rFIX-FP)

An obvious effect of albumin fused rFIX proteins on PK was observed: in the terminal phase of the intravenous arm, rFIX levels were quantifiable for up to 168 hours while non-fused rFIX were detected reliably only up to 48 hours. The last measurable concentration of $rFIX_{WT}$-FP was described to be detectable up to 240 hours (Pestel et al., 2021), while in our work the sampling scheme was limited to 168 hours. Taking into consideration the different setups used for PK assessment of albumin fused and non-fused rFIX proteins, it can be stated that the terminal half-life of all albumin fused rFIX-FP proteins, independently of the single point mutation at position 5, were extended in both the intravenous and the subcutaneous arm as expected.

A distinct (intravenous) PK profile was observed between the albumin fused proteins, where $rFIX_{K5R}$-FP and $rFIX_{WT}$-FP to a smaller degree, exhibited an initial rapid distribution phase, while $rFIX_{K5A}$-FP showed a monophasic plasma clearance behavior (Figure 24). Between these three proteins, the volume of distribution (Vss) was highest for $rFIX_{K5R}$-FP suggesting a higher uptake in the extravascular space for $rFIX_{K5R}$-FP (Table 8) as confirmed with immunofluorescence in Figure 26.

Interestingly, the previously described short half-life of $rFIX_{K5A}$ compared to the other non-fused proteins was corrected in the albumin fused setting. Here, the non-fused $rFIX_{K5A}$ had a ~3-fold shorter half-life compared to the non-fused $rFIX_{WT}$, while the albumin fused $rFIX_{K5A}$-FP is 2-fold higher compared to $rFIX_{WT}$-FP.

In the subcutaneous arm, in line with the data from non-fused proteins, FIX_{K5A}-FP showed an increased C_{max} and bioavailability compared to $rFIX_{K5R}$-FP and $rFIX_{WT}$-FP in Table 9; and $rFIX_{K5R}$-FP had a decreased bioavailability compared to $rFIX_{K5A}$-FP and $rFIX_{WT}$-FP (Figure 25; Table 9). The PK parameters of the subcutaneous route of administration of the albumin fused rFIX proteins showed that the K5A mutation led to a slight improvement in the bioavailability, while the comparison to K5R is less meaningful when the results are analyzed in the context of the extrapolated portion of AUC (Table 9), which is more comparable for $rFIX_{WT}$-FP (~1%) and $rFIX_{K5A}$-FP (~5%), but is much higher for $rFIX_{K5R}$-FP (~20%) compared to $rFIX_{WT}$-FP. In comparison with published studies, the calculated half-lives of non-fused rFIX mutants (K5A and K5R) as well as $rFIX_{WT}$ proteins can vary greatly (Gui et al., 2002). This depends not only on the specific properties of the recombinant protein (like the cultivation system) but also on the technical aspects of the PK study, like the timepoints of blood sampling selected to model PK profile. For example, in a study published by Gui et al. the wildtype rFIX and the plasma-derived FIX had a 7-hour half-life when the first sample was taken at 2 minutes, but when only timepoints after 30 minutes are considered, the half-life was estimated to be 18 hours (Gui et al., 2002). To our surprise, in this paper changes in the blood sampling times at initial phase led to different half-life estimates, which is unexpected since half-life is mostly dependent on the terminal phase. The selection of the appropriate model system for the calculation of these parameters also plays a decisive role. In general, the 2-compartment model, which incorporates the distribution between the two compartments of plasma and extravascular space, is characterized by a rapid sequestration of the infused rFIX protein into the extravascular space followed by a slower elimination of the rFIX from the plasma. The pharmacokinetic parameters presented in this work are based on non-compartmental model and while a look into the two-compartmental model would be highly informative, the lack of sufficient data points (measurable FIX levels) is a limiting factor in the results presented here. Nevertheless, the non-compartmental model is a robust and standard model.

Finally, the histological analysis of samples prepared and imaged in parallel under identical conditions indicates that the K5R mutation in the albumin fused proteins leads to a longer retention in the liver tissue compared to $rFIX_{WT}$-FP and $rFIX_{K5A}$-FP, similar to the observations made with the non-fused proteins. Blood samples collected 72 hours post-treatment had detectable Ag levels of $rFIX_{WT}$-FP, $rFIX_{K5A}$-FP, and $rFIX_{K5R}$-FP and the harvested livers of those animals revealed a significantly lower MFI in the $rFIX_{K5A}$-FP group. The detectable $rFIX_{K5A}$-FP protein in plasma was comparable to $rFIX_{WT}$-FP (~67 mIU/mL) and was higher than Ag plasma levels of $rFIX_{K5R}$-FP (~93 mIU/mL), as shown in Figure 26. Despite similar Ag levels at 72 hours, $rFIX_{K5A}$-FP exhibited significantly lower MFI in the livers compared to $rFIX_{WT}$-FP. No difference was observed between $rFIX_{WT}$-FP and $rFIX_{K5R}$-FP, most likely due to the saturation of these molecules in the liver at 72 hours. While at 144 hours post-treatment (Figure 26) the differences between $rFIX_{WT}$-FP and $rFIX_{K5R}$-FP became clear, $rFIX_{K5R}$-FP exhibited a higher MFI in the liver tissue, though not statistically significant.

5.2.3 Additional histological analysis of harvested liver tissues

Immunohistochemistry colocalization staining of rFIX and collagen type IV in the liver of HB mice treated with rFIX exhibited a high degree of spatial overlap because of similar distribution of FIX and collagen type IV, a ubiquitously expressed extracellular matrix protein. Interestingly, some areas surrounding hepatic vascular structures were restricted to collagen type IV but no FIX signal was shown at the same location, as highlighted by the white arrow in Figure 27.

No direct binding of rFIX proteins to collagen type IV could be detected in surface plasma resonance (data not shown here, Knoll Machado et al., manuscript accepted at Thrombosis and Hemostasis), which is in conflict to previously published results from Cheung et al. in 1996 based on radiolabeled competition assay with cultured endothelial cell matrix (Cheung et al., 1996b). Although no binding of rFIX proteins to collagen type IV could be detected, a clear binding of the positive control, fibronectin, was observed (data not shown here, Knoll Machado et al., manuscript submitted to Thrombosis and Hemostasis). Collagen type IV is a member of a 28-member protein family (Ricard-Blum, 2011). As a distinctive feature, collagen type IV is found exclusively in basement membranes. Despite several attempts to reproduce published data findings, using different methods we were unable to demonstrate direct binding of rFIX to collagen IV. Therefore, the binding partner or binding partners of FIX remains an open question that needs to be addressed to improve the understanding of the biology of FIX and how this can impact different forms of therapy. Unfortunately, the screening of direct binding and interaction partners of rFIX is beyond the scope of this work but it strongly supports the presence of at least one, if not more, binding partners. Overall, the histological analysis revealed insights into the distribution of FIX in the liver. Liver is not only the organ specialized for FIX synthesis under physiological conditions, but also, the preferred site of storage for exogeneous FIX with smaller amount localized in kidney, spleen, muscle and lung (Fuchs et al., 1984; Herzog et al., 2014; Stern et al., 1987b). During the histological analysis performed for this work, it was observed that exogeneous human rFIX given to HB mice accumulate in certain areas in the liver. The anatomical structure of the liver can be divided in zones. The zones of the liver lobules are characterized by distinguished biochemical pathways, nutrient gradients, and endothelial properties. Zone 1 is defined as the region closest to the "portal triad," consisting of the portal vein, the hepatic artery, and the bile duct (Figure 28B). The innermost zone (or zone 3) is located near the central vein and is referred to as the pericentral region. Different anabolic and catabolic pathways are differentially active in different zones. Liver sinusoidal endothelial cells fenestrae, for instance, are highly variable: size decreases closer to the central vein, but the number of fenestrae increases, which influences the transport of drugs (Chauhan et al., 2012). The FIX positive regions were detected mostly in Zone 3, the area surrounding the central vein (Figure 28), while the area around the peri-portal region was often free of FIX. Interestingly, the DAB staining of the human liver exhibited a similar pattern of distribution. The FIX positive areas were detected, as expected, intracellularly in the hepatocytes of human liver (Figure 28A). The hepatocytes surrounding the central vein had clear intracellular signal but as FIX nears the peri-portal region, it was restricted to the plasma membrane. Nevertheless, further analysis is needed to define the exact FIX positive structures detected in human liver. In general, FIX stains some but not all regions containing collagen type IV as shown in Figure 27A. Additionally, the FIX staining of endogenous human FIX in human liver presents similarities to the FIX staining in exogenous human FIX in murine tissue (Figure 29). The pattern of rFIX distribution observed in liver seems to be similar to that of sinusoidal endothelial cells (Walter et al., 2014) . This is not surprising, because endothelial cells are described in the literature as potential binding partner of rFIX but in our hands the exact receptor or component binding to rFIX is still unknown (Cheung et al., 1996b). Since the postulated binding partner, collagen IV, did not bind to rFIX in our hands (data not shown here, Knoll Machado, et al., submitted to Thrombosis and Hemostasis), further experiments, not only microscopic but also mass spectrometric and co-immunoprecipitation, are needed to screen for potential binding partners of rFIX.

5.3 Efficacy of rFIX mutants in HB mice

An important aspect of this work was the evaluation of the efficacy of the mutant rFIX proteins, K5A and K5R, to address the following questions:

1) Investigate and compare the efficacy of the K5A and K5R and 2) whether this single point mutation could add value in a therapeutic approach. Therefore, in this setting only non-fused proteins were tested in vivo. This was due to the fact that the published data around the K5 variants are restricted to the non-fused proteins, and they are better suited for investigating the effect of these mutations in the FIX

molecule and any further modification of the molecule can impact FIX beyond the substitution at position 5.

Efficacy was tested in the tail clip bleeding hemostasis and mesenteric artery thrombosis model. In the tail clip bleeding model, the tail of anesthetized mice was transected to assess hemostasis. After transection the bleeding time and blood loss are recorded/collected during 30 minutes. Despite the tight connection between hemostasis and thrombosis, their pathways differ from one another. A wide range of thrombosis models are available, and each resemble different pathophysiological conditions. The $FeCl_3$ induced thrombosis model relies on a chemical stimulus to induce a thrombus. This trigger is not biologically relevant, but it is a well-characterized and controlled stimulus that leads to activation and disruption of endothelial cells.

Experiments were conducted in HB mice, which exhibit a relevant bleeding tendency. HB mice were tested in a $FeCl_3$ model in the carotid artery, and it was described already that these animals are protected against occlusive thrombus formation (Kastetter et al., 2018). The primary readout of this model is time to occlusion. The time to occlusion is defined as the time until blood flow ceases for a certain amount of time or it drops to a certain percentage of the baseline. Similar to the published experiments in the carotid artery, HB mice showed a clear anti-thrombotic phenotype in the mesenteric arterioles. The mesenteric arterioles are relatively small (second-order arteries < ~150 µm) compared to carotid artery (~500 µm). The size of the vessel varies depending on the order of the branch, but they are generally very small and experience high shear-force from quicker blood flow related to the small diameter.

5.3.1 Efficacy of intravenous rFIX replacement therapy

5.3.1.1 Tail clip bleeding model

Effectiveness of prophylactic treatment after intravenous administration was assessed in a tail clip model, as shown in Figure 30. HB mice treated intravenously with $rFIX_{K5A}$ and $rFIX_{K5R}$ had reduced bleeding in an acute treatment setting, 15 minutes prior to the tail clip challenge. The same was observed for the wildtype reference molecule, $rFIX_{WT}$. At this timepoint, all proteins were highly efficacious. The tail clip challenge was conducted at 24 hours post-administration when the circulating FIX levels were expected to be very low, if any. The $rFIX_{K5R}$ and $rFIX_{WT}$ proteins were efficacious in reducing bleeding incidence and blood loss compared to vehicle. In contrast, $rFIX_{K5A}$ reduced blood loss but the bleeding incidence was not significantly different compared to vehicle. At the end of the experiment (Figure 31), residual level of $rFIX_{WT}$ was detected and levels of $rFIX_{K5A}$ and $rFIX_{K5R}$ were not measurable (< 0.006 IU/mL). Further, experiments were performed to evaluate the hemostatic efficacy of rFIX proteins after longer administration time. The results indicate that $rFIX_{K5R}$ had the longest efficacy based on the bleeding incidence (statistically significant compared to vehicle even at 72 hours, Figure 30A). On the contrary, the blood loss results showed no difference between the treatment groups, including $rFIX_{K5R}$, and the vehicle beyond 24 hours (Figure 30B).

Despite rFIX proteins show a tendency of reduction in the blood loss parameter even at day 7 (168 hours post administration), this effect is not statistically significant. This effect may be obscured by the high variability of the model. On the other hand, this effect could be potentially explained by biological relevant binding of rFIX molecules outside the plasma but readily available to the site of injury. The differences observed between blood loss and bleeding incidence are not surprising because of the nature of their respective outputs. The bleeding incidence is an arbitrary measure that depends on how the "stop of bleeding" is defined in the experimental set up and the observations are made by the naked eye. Therefore, bleeding incidence can be considered a hard endpoint that takes into account the presence or the lack of stable blood clots that can successfully stop bleeding in a rather extreme setting of tail clip (amputation of the principal arteries and venules, mid-ventral artery and two major lateral veins). Under these conditions, obvious effects are more likely to be detected and the discrimination of subtle effects may be better reflected in the blood loss parameter. Blood loss is an endpoint that also considers clots that reduce blood loss, but which may not necessarily lead to total occlusion of the vessel. Despite not statistically significant, our results showed that the blood loss was reduced even 14 days after a single dose of $rFIX_{K5R}$ (Figure 30A). This prolonged efficacy could be explained by the presence of $rFIX_{K5R}$ in the extravascular space. While on the contrary, the $rFIX_{WT}$ and $rFIX_{K5A}$ variants (with decreased extravascular binding affinity) are released into the circulation, whereof they are degraded by the normal intracellular (lysosomal) degradation.

In general, as shown in Figure 31 after 24 hours only residual or no rFIX plasma levels were measured at the end of the bleeding experiment. Because of the blood loss and consumption of coagulation factors at the end of the experiment, the PK profile data (section 4.3.1.1) gives a better estimate of the actual exposure of rFIX in plasma at the time when the tail was amputated. The dose used in the tail clip bleeding model is at least ~5-fold lower (50 IU/kg) compared to the dose used for PK assessment (25 nmol/kg that translates to 243 - 394 IU/kg depending on the specific activities). Therefore, based on the PK profile, no or only residual antigen (FIX:Ag) levels are expected to be present at 24 hours (half-lives of 4-14 hours, Table 7). Even though we cannot rule out that there might be residual amounts of rFIX in plasma that cannot be detected by our assay due to its intrinsic sensitivity, it is highly implausible that at later timepoints the residual amounts of rFIX present in plasma alone can display the hemostatic response observed in the experiments. The support from the extravascular but readily available rFIX is a plausible explanation for the overall prolonged efficacy of rFIX compared to the plasma levels of rFIX.

The long-lasting effects have been previously described in the literature for $rFIX_{WT}$ in a saphenous vein model (Cooley et al., 2016). In this model, non-fused, standard half-life $rFIX_{WT}$ retained bleeding efficacy 7 days after treatment despite no detectable FIX levels in plasma, similar to our results in blood loss reduction.

5.3.1.2 Mesenteric artery thrombosis model

This model provided insights on the mechanism underlying the rapid loss of efficacy of $rFIX_{K5A}$. The establishment of the model was conducted in HB mice. The hemostatic normal mice C57BL6/J were used as a positive control, while the FXI ko mice were included as a negative control. It is known that the FXI ko mice are protected from thrombosis in this model (Renné et al., 2005). In this model the thrombus formation is monitored over time under the microscope and an image is acquired every second. The time to occlusion (TTO) or the size of the thrombus can be analyzed from the time-lapse videos generated over the monitoring time. As mentioned earlier, the anti-thrombotic phenotype of the HB mice was described in the carotid artery thrombosis model, but it was assessed for the first time in the mesenteric artery thrombosis model in this work. As expected, the anti-thrombotic phenotype was confirmed in FXI ko mice (negative control), in which no vessel occluded during the observation time (Figure 34A). All C57BL6/J mice exhibited full occlusion of the injured vessels ~10 minutes after injury induction (Figure 34A). Under the same experimental conditions, HB mice (FIX ko mice, Figure 34B) failed to form an occlusive thrombus, similar to the FXI ko mice. Finally, the ability to form a thrombus was restored in a dose dependent manner when $rFIX_{WT}$ was dosed in an acute setting (ca. 20 minutes prior to the injury induction, Figure 35B). The shortest TTO was achieved with the highest tested dose of 250 IU/kg and this concentration was used for further experiments.

The efficacy of $rFIX_{WT}$, $rFIX_{K5A}$ and $rFIX_{K5R}$ was further investigated in the mesenteric thrombosis model at 24 hours post-administration. Interestingly, in this model the $rFIX_{K5A}$ group behaved similar to vehicle in terms of the inability to form occlusive thrombus until the end of the observation at 40 minutes. In the $rFIX_{WT}$ and $rFIX_{K5R}$ treated groups the TTO was decreased to 35 and 25 minutes, respectively and at least 50% of the vessels formed an occlusive thrombus. On the contrary, 0% of the vessels in $rFIX_{K5A}$ group formed an occlusive thrombus (Figure 36B). A secondary readout described further characteristics of the thrombus; the size of the clot was measured and normalized to the area of the vessel. These results indicate that $rFIX_{K5A}$ formed at least 2-fold smaller thrombus compared to the other rFIX-treated groups (the mean clot size is ranked as follows: 225 μm^2 $rFIX_{K5R}$ > 166 μm^2 $rFIX_{WT}$ > 62 μm^2 $rFIX_{K5A}$; (Figure 36C) while vehicle group failed to form a thrombus (> 10 µm of diameter) under identical conditions. Finally, at the end of the experiment blood was sampled from animals, when possible. It is important to highlight that these measurements can only be contemplated as a rough indicator of rFIX levels in plasma. The standardization of blood sampling in young animals was technically challenging and is, therefore, not robust. At the end of the experiment, before the animals are sacrificed, the circulatory depression due to the anesthesia in addition to the small size of the animals made the terminal blood sampling challenging. This should be taken into consideration when interpreting the data (Figure 36D). Under these conditions, the antigen levels of rFIX (~1.5% of the norm; Figure 36D) were comparable between all three groups. Because residual amounts of rFIX were present in the circulation 24 hours post administration, the extravascular load of FIX might depend on the extracellular matrix binding property rFIX variants and is estimated as follows: $rFIX_{K5R}$>$rFIX_{WT}$>$rFIX_{K5A}$. These results are explained best by the differences in the extravascular retention properties of the mutant proteins leading to a premature loss of efficacy in the $rFIX_{K5A}$ group. In general, the data generated in the tail clip model correlated with the findings in the mesenteric thrombosis model in the sense that K5A mutation led to the shortest duration of efficacy in both the models. It is worth to point out that highest efficacy (statistically significant) in the tail clip bleeding model after intravenous administration (Figure 30) was observed in all groups ($rFIX_{WT}$, $rFIX_{K5A}$, and $rFIX_{K5R}$), independently of their individual binding properties to the extravascular space, at 15 minutes post-administration when FIX plasma levels are very high and comparable. This suggests that plasmatic and circulating rFIX plays the major role for hemostasis. Overall, the efficacy results after intravenous administration showed prolonged hemostatic efficacy of $rFIX_{K5R}$ and this can be explained by the assumption $rFIX_{K5R}$ binds more tightly to the extravascular space, which is in-line with observations on the intravenous PK profile and longer detection of measurable $rFIX_{K5R}$ in the liver.

5.3.2 Efficacy of subcutaneous rFIX replacement therapy

As mentioned previously $rFIX_{K5A}$ protein exhibit impaired ability to bind to components of the extravascular space. This property confines the $rFIX_{K5A}$ molecules, at least to some extent, to the blood circulation. It is exactly this property that could have a positive outcome in a subcutaneous application.

In a subcutaneous setting, only the group treated with $rFIX_{K5A}$ reached a statistically significant hemostatic effect in blood loss at 24 hours (Figure 32A) and reduced the bleeding incidence to 60% compared to the other proteins and vehicle (100-80%) as shown in Figure 32B. Though not statistically significant $rFIX_{WT}$ and $rFIX_{K5R}$ also retained hemostatic properties (blood loss) up to 72 hours. No rFIX antigen was detectable in the plasma but very low activity levels were observed (Figure 33). Despite expected low exposure levels of rFIX, the $rFIX_{K5A}$ had a significant effect in reducing blood loss and maked the K5A mutation a potential target to improve the release of rFIX into the circulation following subcutaneous administration. Based on the PK parameters after intravenous administration, the half-life of $rFIX_{K5A}$ is expected to be lower (Gui et al., 2002) compared to $rFIX_{WT}$ but this could be corrected by half-life extension strategies like the fusion with albumin.

5.4 Final conclusions and outlook

The relevance of the extravascular space for hemostatic efficacy of rFIX is a challenging topic especially because there are no relevant biomarkers to determine the effect in the clinical setting. This work supports the presence of FIX in the extravascular space and demonstrates how a mutation at position 5 can impact PK profile. The exact molecular mechanism needs to be elucidated as the binding of rFIX to Collagen IV, shown in previous publications, could not be demonstrated in our work.

While plasma levels of FIX are still the major biomarker in HB, the presence of FIX beyond the circulation may help to understand the clinical observations that some patients benefit and may respond better to one or the other therapy (Cooley et al., 2019). At the end, it can be speculated that that an equilibrium between extravascular and intravascular FIX is the normal physiological state in hemostatic healthy individuals. Most likely, not only one but several binding sites may be found in the FIX molecule e.g., additional loss of binding to components of the extravascular space was achieved by an additional exchange of valine to lysine at position 10 (Cheung et al., 1992). Any modifications of the rFIX protein, for example fusion to albumin, may sterically hinder the capacity of the protein to bind its endogenous binding partner. It can be concluded that albumin fusion proteins have different binding partners which results in differential distribution in the extravascular space.

The clinical relevance of the extravascular storage of FIX was characterized in preclinical models and for clinical practice these results strongly support that the FIX plasma levels remain a major biomarker to determine therapeutic efficacy. The results add to the investigations on extravascular FIX and how the exposure should be considered as a main parameter because high levels of FIX in plasma reliably and safely prevent bleedings but FIX distribution to the extravascular compartment should not be underestimated in the clinical setting. Keeping high levels of rFIX in the plasma conveys the best and most reliable hemostatic protection independently of the FIX extravascular load but as clotting activities drop in the circulation, the lack or presence of the extravascular rFIX might potentially influence the clinical outcome. From a drug development perspective, both K5A and K5R substitution could have potential uses in different therapeutic approaches. For instance, the subcutaneous delivery where the release of rFIX into the circulation is the main goal, could benefit from the K5A mutation as an increase in the bioavailability would be expected. For an intravenous form of administration, the prolongation of the efficacy of non-fused rFIX proteins by introducing K5R, should be further investigated in extended half-life products, where the half-life is already prolonged, and it is not clear whether the K5R mutation would add on top of that.

Despite the evidence presented in this work using preclinical models, it is worth noting that the relevance of extravascular FIX in the clinical setting remains unclear. It can be speculated (based on published data and the data generated in this work) that FIX distribution in the extravascular space may differ from patient-to-patient depending on the endogenous levels of FIX. A patient that is not able to express FIX proteins, and where the potential extravascular receptors are free (not occupied), would have a different clinical outcome compared to patients expressing FIX proteins with an intact Gla domain that can bind extravascular receptors but is not functional because the injected FIX (exogeneous) will compete with the endogenous dysfunctional FIX. This hypothesis has not been explored in a clinical setting because of the challenges associated with the detection of extravascular FIX. To date, plasma levels of FIX activity remain the major factor to determine frequency of dosing in HB individuals. Hence, additional studies are required to identify the relevance of extravascular FIX in a clinical setting and further investigations are required to identify binding partner(s) of zymogen FIX in the extravascular compartment.

6 SUMMARY

Hemophilia B (HB) is an inherited bleeding disorder caused by deficiency of FIX. The severity is classified based on the FIX activity level in the plasma. The trough levels of FIX activity in the circulation above 5% is considered the relevant parameter to maintain hemostasis. Even though rFIX products with extended half-life have proven to be highly efficient in reducing annual bleeding rates in HB patients, there is an emerging concept that in addition to circulating FIX, extravascular (EV) FIX that is not circulating in plasma and is therefore not measurable, contributes to hemostasis. A single point mutation near the N-terminus of rFIX has been described as a determinant for the binding of FIX to extravascular space comprising endothelial cells and components of extracellular matrix. In this thesis the biological significance of rFIX in the extravascular space (EVS) was investigated using recombinant FIX proteins with a substitution at position 5, known to either enhance ($rFIX_{K5R}$) or reduce ($rFIX_{K5A}$) binding to EVS, more specifically collagen IV. Albumin fusion extends the half-life of rFIX and is a standard of care for prophylactic therapy. To understand the impact of albumin fusion in EV distribution and hemostatic efficacy of rFIX, albumin fused and non-fused rFIX protein K5 variants were generated and thoroughly characterized in vitro and in vivo. A functional characterization of the rFIX variants was conducted in a FIX one stage clotting assay and in a modified FIX chromogenic activity assay, mimicking the tenase complex *in vitro*. The pharmacokinetic (PK) profile was evaluated in HB (FIX ko) mice after intravenous and subcutaneous administration. Plasma levels of the rFIX proteins and the immunohistochemical evaluation of the liver samples confirmed published data that rFIX carrying a K5A and K5R mutation have an impact on PK behavior and tissue sequestration. The albumin fused and non-fused $rFIX_{K5R}$ was found in lower levels in the plasma when administered via both intravenous and subcutaneous routes and $rFIX_{K5R}$ was found to be retained in the tissue. Nevertheless, collagen IV alone seems not to be the binding partner in

the extravascular compartment as revealed in the surface plasma resonance experiments. The efficacy studies revealed that the ability of FIX to bind to components of the EVS has an impact on the hemostatic response in HB mouse models. Using two different in vivo models of hemostasis and thrombosis, we demonstrate that mutated rFIX protein with enhanced binding to components of the EVS ($rFIX_{K5R}$) confers prolonged hemostatic efficacy while the duration of efficacy of $rFIX_{K5A}$ was relevantly shorter after intravenous administration of the recombinant proteins. These results can be explained by an additional local accessible $rFIX_{K5R}$ at the site of injury, even at later timepoints. We showed that, after subcutaneous administration, only the group injected with $rFIX_{K5A}$ significantly reduced the blood loss in tail clip bleeding model. The decreased binding of $rFIX_{K5A}$ to EVS and the observed greater plasma exposure after subcutaneous administration potentially contributed to the hemostatic efficacy. These results further support that (1) maintaining a steady trough level of FIX is crucial for efficacy and (2) the modulation of the FIX binding property to extravascular can be an important therapeutic strategy for subcutaneous delivery.

7 ZUSAMMENFASSUNG

Hämophilie B (HB) ist eine vererbte Blutungsstörung, die durch einen Mangel an dem Gerinnungsfaktor IX (FIX) verursacht wird. Der Schweregrad wird auf der Grundlage der FIX-Aktivität im Plasma klassifiziert. Als relevanter Parameter für die Aufrechterhaltung der Hämostase gilt ein Talspiegel der FIX-Aktivität im Blutkreislauf von über 5 %. Obwohl sich rekombinante FIX (rFIX)-Produkte mit verlängerter Halbwertszeit bei der Verringerung der jährlichen Blutungsraten bei HB-Patienten als äußerst effizient erwiesen haben, gibt es ein neues Konzept, wonach zusätzlich zum zirkulierenden FIX auch extravaskuläres (EV) FIX, das nicht im Plasma zirkuliert und daher nicht messbar ist, zur Hämostase beiträgt. Eine einzelne Punktmutation in der Nähe des N-Terminus von rFIX wurde als bestimmend für die Bindung von FIX an den extravaskulären Raum beschrieben, der Endothelzellen und Komponenten der extrazellulären Matrix umfasst. In dieser Arbeit wurde die biologische Bedeutung von rFIX im extravaskulären Raum (EVR) unter Verwendung rFIX-Proteine mit einer Substitution an Position 5 untersucht, von der bekannt ist, dass sie die Bindung an EVR, insbesondere Kollagen IV, entweder verstärkt ($rFIX_{K5R}$) oder reduziert ($rFIX_{K5A}$). Eine Albuminfusion verlängert die Halbwertszeit von rFIX und ist ein Standard für die prophylaktische Therapie. Um die Auswirkungen der Albuminfusion auf die EV-Verteilung und die hämostatische Wirksamkeit von rFIX zu verstehen, wurden mit Albumin fusionierte und nicht fusionierte rFIX-Protein-K5-Varianten erzeugt und *in vitro* und *in vivo* untersucht. Eine funktionelle Charakterisierung der rFIX-Varianten wurde in einem einstufigen FIX-Gerinnungstest und in einem modifizierten chromogenen FIX-Aktivitätstest durchgeführt, der den Tenase-Komplex *in vitro* nachahmt. Das pharmakokinetische (PK) Profil wurde in HB (FIX ko) Mäusen nach intravenöser und subkutaner Verabreichung untersucht. Die Plasmaspiegel der rFIX-Proteine und die immunhistochemische Auswertung der Leberproben bestätigten veröffentlichte Daten, wonach rFIX, welches eine K5A- oder eine K5R-

Mutation trägt, einen Einfluss auf das PK-Verhalten und die Sequestrierung im Gewebe hat. Das mit Albumin fusionierte und nicht fusionierte $rFIX_{K5R}$ wurde sowohl bei intravenöser als auch bei subkutaner Verabreichung in niedrigeren Konzentrationen im Plasma gefunden, und es wurde festgestellt, dass $rFIX_{K5R}$ im Gewebe zurückgehalten wird. Dennoch scheint Kollagen IV allein nicht der Bindungspartner im extravaskulären Kompartiment zu sein, wie die Experimente zur Oberflächenplasmaresonanz zeigten. Die Wirksamkeitsstudien deuteten darauf hin, dass die Fähigkeit von FIX, an Komponenten des EVR zu binden, einen Einfluss auf die hämostatische Reaktion in HB-Mausmodellen hat. Anhand von zwei verschiedenen *in vivo*-Modellen der Hämostase und Thrombose konnten wir zeigen, dass ein mutiertes rFIX-Protein mit verstärkter Bindung an Komponenten des EVR ($rFIX_{K5R}$) eine verlängerte hämostatische Wirksamkeit verleiht, während die Dauer der Wirksamkeit von $rFIX_{K5A}$ nach intravenöser Verabreichung der rekombinanten Proteine deutlich kürzer war. Diese Ergebnisse lassen sich durch ein zusätzliches lokal zugängliches $rFIX_{K5R}$ am Ort der Verletzung erklären, auch zu späteren Zeitpunkten. Wir konnten nachweisen, dass nach subkutaner Verabreichung nur die Gruppe der $rFIX_{K5A}$ injiziert wurde den Blutverlust im Modell der Schwanzklammerblutung signifikant reduzierte. Die geringere Bindung von $rFIX_{K5A}$ an EVR und die beobachtete größere Plasmaexposition nach subkutaner Verabreichung trugen möglicherweise zur hämostatischen Wirksamkeit bei. Diese Ergebnisse belegen, dass (1) die Aufrechterhaltung eines konstanten Talspiegels von FIX für die Wirksamkeit entscheidend ist und (2) die Modulation der FIX-Bindungseigenschaften an extravaskulärem Gewebe eine wichtige therapeutische Strategie für die subkutane Verabreichung sein kann.

8 REFERENCES

Ahmad, S.S., Rawala-Sheikh, R., Walsh, P.N., 1989. Comparative interactions of factor IX and factor IXa with human platelets. J Biol Chem 264, 3244–3251. https://doi.org/10.1016/s0021-9258(18)94058-5

André, P., Delaney, S.M., LaRocca, T., Vincent, D., DeGuzman, F., Jurek, M., Koller, B., Phillips, D.R., Conley, P.B., 2003. P2Y12 regulates platelet adhesion/activation, thrombus growth, and thrombus stability in injured arteries. J Clin Invest 112, 398–406. https://doi.org/10.1172/jci17864

Anson, D.S., Choo, K.H., Rees, D.J., Giannelli, F., Gould, K., Huddleston, J.A., Brownlee, G.G., 1984. The gene structure of human anti-haemophilic factor IX. Embo J 3, 1053–1060. https://doi.org/10.1002/j.1460-2075.1984.tb01926.x

Bajzar, L., Manuel, R., Nesheim, M.E., 1995. Purification and Characterization of TAFI, a Thrombin-activable Fibrinolysis Inhibitor ∗. J Biol Chem 270, 14477–14484. https://doi.org/10.1074/jbc.270.24.14477

Becker, R.C., 2005. Cell-Based Models of Coagulation: A Paradigm in Evolution. J Thromb Thrombolys 20, 65–68. https://doi.org/10.1007/s11239-005-3118-3

Boland, E., Liu, Y., Walter, C., Herbert, D., Weaker, F., Odom, M., Jagadeeswaran, P., 1995. Age-specific regulation of clotting factor IX gene expression in normal and transgenic mice. Blood 86, 2198–2205. https://doi.org/10.1182/blood.v86.6.2198.bloodjournal8662198

Brady, J.N., Notley, C., Cameron, C., Lillicrap, D., 1998. Androgen effects on factor IX expression: in-vitro and in-vivo studies in mice. Brit J Haematol 101, 273–279. https://doi.org/10.1046/j.1365-2141.1998.00694.x

Brooks, A.R., Sim, D., Gritzan, U., Patel, C., Blasko, E., Feldman, R.I., Tang, L., Ho, E., Zhao, X. -Y., Apeler, H., Murphy, J.E., 2013. Glycoengineered factor IX variants with improved pharmacokinetics and subcutaneous efficacy. J Thromb Haemost 11, 1699–1706. https://doi.org/10.1111/jth.12300

Broos, K., Feys, H.B., Meyer, S.F.D., Vanhoorelbeke, K., Deckmyn, H., 2011. Platelets at work in primary hemostasis. Blood Rev 25, 155–167. https://doi.org/10.1016/j.blre.2011.03.002

Bryan, L., Clynes, M., Meleady, P., 2021. The emerging role of cellular post-translational modifications in modulating growth and productivity of recombinant Chinese hamster ovary cells. Biotechnol Adv 49, 107757. https://doi.org/10.1016/j.biotechadv.2021.107757

Buckner, T.W., Jr, R.S., Witkop, M., Guelcher, C., Cutter, S., Iyer, N.N., Cooper, D.L., 2019. Correlations between patient-reported outcomes and self-reported characteristics in adults with hemophilia B and caregivers of children with hemophilia B: analysis of the B-HERO-S study. Patient Relat Outcome Meas 10, 299–314. https://doi.org/10.2147/prom.s219166

Camerino, G., Grzeschik, K.H., Jaye, M., Salle, H.D.L., Tolstoshev, P., Lecocq, J.P., Heilig, R., Mandel, J.L., 1984. Regional localization on the human X chromosome and polymorphism of the coagulation factor IX gene (hemophilia B locus). Proc National Acad Sci 81, 498–502. https://doi.org/10.1073/pnas.81.2.498

Cawthern, K.M., Veer, C. van ’t, Lock, J.B., DiLorenzo, M.E., Branda, R.F., Mann, K.G., 1998. Blood coagulation in hemophilia A and hemophilia C. Blood 91, 4581–92.

Chauhan, V.P., Stylianopoulos, T., Martin, J.D., Popović, Z., Chen, O., Kamoun, W.S., Bawendi, M.G., Fukumura, D., Jain, R.K., 2012. Normalization of tumour blood vessels improves the delivery of nanomedicines in a size-dependent manner. Nat Nanotechnol 7, 383–388. https://doi.org/10.1038/nnano.2012.45

Cheung, W.F., Born, J. van den, Kühn, K., Kjellén, L., Hudson, B.G., Stafford, D.W., 1996a. Identification of the endothelial cell binding site for factor IX. Proc National Acad Sci 93, 11068–11073. https://doi.org/10.1073/pnas.93.20.11068

Cheung, W.F., Born, J. van den, Kühn, K., Kjellén, L., Hudson, B.G., Stafford, D.W., 1996b. Identification of the endothelial cell binding site for factor IX. Proc National Acad Sci 93, 11068–11073. https://doi.org/10.1073/pnas.93.20.11068

Cheung, W.F., Hamaguchi, N., Smith, K.J., Stafford, D.W., 1992. The binding of human factor IX to endothelial cells is mediated by residues 3-11. J Biol Chem 267, 20529–20531. https://doi.org/10.1016/s0021-9258(19)36713-4

Chu, K., Wu, S.M., Stanley, T., Stafford, D.W., High, K.A., 1996. A mutation in the propeptide of Factor IX leads to warfarin sensitivity by a novel mechanism. J Clin Invest 98, 1619–1625. https://doi.org/10.1172/jci118956

Collier, M.E.W., Akinmolayan, A., Goodall, A.H., 2017. Comparison of tissue factor expression and activity in foetal and adult endothelial cells. Blood Coagul Fibrin 28, 452–459. https://doi.org/10.1097/mbc.0000000000000621

Cooley, B., Broze, G.J., Mann, D.M., Lin, F.-C., Pedersen, L.G., Stafford, D.W., 2019. Dysfunctional endogenous FIX impairs prophylaxis in a mouse hemophilia B model. Blood 133, 2445–2451. https://doi.org/10.1182/blood.2018884015

Cooley, B., Funkhouser, W., Monroe, D., Ezzell, A., Mann, D.M., Lin, F.-C., Monahan, P.E., Stafford, D.W., 2016. Prophylactic efficacy of BeneFIX vs Alprolix in hemophilia B mice. Blood 128, 286–292. https://doi.org/10.1182/blood-2016-01-696104

Dieijen, G. van, Tans, G., Rosing, J., Hemker, H.C., 1981. The role of phospholipid and factor VIIIa in the activation of bovine factor X. J Biological Chem 256, 3433–42.

Dogné, J.-M., Hanson, J., Leval, X. de, Kolh, P., Tchana-Sato, V., Leval, L. de, Rolin, S., Ghuysen, A., Segers, P., Lambermont, B., Masereel, B., Pirotte, B., 2004. Pharmacological Characterization of N-tert-Butyl-N′-[2-(4′-methylphenylamino)-5-

nitrobenzenesulfonylurea (BM-573), a Novel Thromboxane A2 Receptor Antagonist and Thromboxane Synthase Inhibitor in a Rat Model of Arterial Thrombosis and Its Effects on Bleeding Time. J Pharmacol Exp Ther 309, 498–505. https://doi.org/10.1124/jpet.103.063610

Duffy, E.J., Parker, E.T., Mutucumarana, V.P., Johnson, A.E., Lollar, P., 1992. Binding of factor VIIIa and factor VIII to factor IXa on phospholipid vesicles. J Biol Chem 267, 17006–17011. https://doi.org/10.1016/s0021-9258(18)41885-6

Eckly, A., Hechler, B., Freund, M., Zerr, M., Cazenave, J. -P., Lanza, F., Mangin, P.H., GACHET, C., 2011. Mechanisms underlying FeCl3-induced arterial thrombosis. J Thromb Haemost 9, 779–789. https://doi.org/10.1111/j.1538-7836.2011.04218.x

Falati, S., Patil, S., Gross, P.L., Stapleton, M., Merrill-Skoloff, G., Barrett, N.E., Pixton, K.L., Weiler, H., Cooley, B., Newman, D.K., Newman, P.J., Furie, B.C., Furie, B., Gibbins, J.M., 2006. Platelet PECAM-1 inhibits thrombus formation in vivo. Blood 107, 535–541. https://doi.org/10.1182/blood-2005-04-1512

Feng, D., Stafford, K.A., Broze, G.J., Stafford, D.W., 2013. Evidence of clinically significant extravascular stores of factor IX. J Thromb Haemost 11, 2176–2178. https://doi.org/10.1111/jth.12421

Freedman, S.J., Blostein, M.D., Baleja, J.D., Jacobs, M., Furie, B.C., Furie, B., 1996. Identification of the Phospholipid Binding Site in the Vitamin K-dependent Blood Coagulation Protein Factor IX*. J Biol Chem 271, 16227–16236. https://doi.org/10.1074/jbc.271.27.16227

Fritsma, G.A., 2015. Platelet Structure and Function. Am Soc Clin Laboratory Sci 28, 125–131. https://doi.org/10.29074/ascls.28.2.125

Fuchs, H.E., Trapp, H.G., Griffith, M.J., Roberts, H.R., Pizzo, S.V., 1984. Regulation of factor IXa in vitro in human and mouse plasma and in vivo in the mouse. Role of the endothelium and the plasma proteinase inhibitors. J Clin Invest 73, 1696–1703. https://doi.org/10.1172/jci111377

Furie, B., Furie, B.C., 2007. In vivo thrombus formation. J Thromb Haemost 5, 12–17. https://doi.org/10.1111/j.1538-7836.2007.02482.x

Gailani, D., Jr., G.J.B., 1991. Factor XI Activation in a Revised Model of Blood Coagulation. Science 253, 909–912. https://doi.org/10.1126/science.1652157

Gailani, D., Renné, T., 2007. Intrinsic Pathway of Coagulation and Arterial Thrombosis. Arteriosclerosis Thrombosis Vasc Biology 27, 2507–2513. https://doi.org/10.1161/atvbaha.107.155952

Gilbert, G.E., Arena, A.A., 1996. Activation of the Factor VIIIa-Factor IXa Enzyme Complex of Blood Coagulation by Membranes Containing Phosphatidyl-L-serine (∗). J Biol Chem 271, 11120–11125. https://doi.org/10.1074/jbc.271.19.11120

Gillis, S., Furie, B.C., Furie, B., Patel, H., Huberty, M.C., Switzer, M., Foster, W.B., Scoble, H.A., Bond, M.D., 1997. γ-Carboxyglutamic acids 36 and 40 do not contribute to human factor IX function. Protein Sci 6, 185–196. https://doi.org/10.1002/pro.5560060121

Gomez, K., McVey, J.H., 2006. Tissue Factor Initiated Blood Coagulation. Front Biosci 11, 1349. https://doi.org/10.2741/1888

Greeene, T.K., Schiviz, A., Hoellriegl, W., Poncz, M., Muchitsch, E.-M., ISTH, 2010. Towards a standardization of the murine tail bleeding model. J Thromb Haemost 8, 2820–2822. https://doi.org/10.1111/j.1538-7836.2010.04084.x

Gui, T., Lin, H.-F., Jin, D.-Y., Hoffman, M., Straight, D.L., Roberts, H.R., Stafford, D.W., 2002. Circulating and binding characteristics of wild-type factor IX and certain Gla domain mutants in vivo. Blood 100, 153–158. https://doi.org/10.1182/blood.v100.1.153

Gui, T., REHEMAN, A., NI, H., GROSS, P.L., YIN, F., MONROE, D., MONAHAN, P.E., STAFFORD, D.W., 2009a. Abnormal hemostasis in a knock-in mouse carrying a variant of factor IX with impaired binding to collagen type IV. J Thromb Haemost 7, 1843–1851. https://doi.org/10.1111/j.1538-7836.2009.03545.x

Gui, T., REHEMAN, A., NI, H., GROSS, P.L., YIN, F., MONROE, D., MONAHAN, P.E., STAFFORD, D.W., 2009b. Abnormal hemostasis in a knock-in mouse carrying a variant of factor IX with impaired binding to collagen type IV. J Thromb Haemost 7, 1843–1851. https://doi.org/10.1111/j.1538-7836.2009.03545.x

Hanson, S.R., Griffin, J.H., Harker, L.A., Kelly, A.B., Esmon, C.T., Gruber, A., 1993. Antithrombotic effects of thrombin-induced activation of endogenous protein C in primates. J Clin Invest 92, 2003–2012. https://doi.org/10.1172/jci116795

Hansson, K., Stenflo, J., 2005. Post-translational modifications in proteins involved in blood coagulation. J Thromb Haemost 3, 2633–2648. https://doi.org/10.1111/j.1538-7836.2005.01478.x

Hechler, B., Freund, M., Alame, G., Leguay, C., Gaertner, S., Cazenave, J.-P., Petitou, M., Gachet, C., 2011a. The Antithrombotic Activity of EP224283, a Neutralizable Dual Factor Xa Inhibitor/Glycoprotein IIbIIIa Antagonist, Exceeds That of the Coadministered Parent Compounds. J Pharmacol Exp Ther 338, 412–420. https://doi.org/10.1124/jpet.111.181321

Hechler, B., Freund, M., Alame, G., Leguay, C., Gaertner, S., Cazenave, J.-P., Petitou, M., Gachet, C., 2011b. The Antithrombotic Activity of EP224283, a Neutralizable Dual Factor Xa Inhibitor/Glycoprotein IIbIIIa Antagonist, Exceeds That of the Coadministered Parent Compounds. J Pharmacol Exp Ther 338, 412–420. https://doi.org/10.1124/jpet.111.181321

Herrmann, S., Doerr, B., May, F., Kuehnemuth, B., Cherpokova, D., Herzog, E., Dickneite, G., Nolte, M.W., 2020. Tissue distribution of rIX-FP after intravenous application to rodents. J Thromb Haemost 18, 3194–3202. https://doi.org/10.1111/jth.15069

Herzog, E., Harris, S., Henson, C., McEwen, A., Schenk, S., Nolte, M.W., Pragst, I., Dickneite, G., Schulte, S., Zollner, S., 2014. Biodistribution of the recombinant fusion protein linking coagulation factor IX with albumin (rIX-FP) in rats. Thromb Res 133, 900–907. https://doi.org/10.1016/j.thromres.2014.02.010

Hoffbrand, A.V., Pettit, J.E., 1993. Clinical Hematology and Fundamentals of Hemostasis, Clinical & Laboratory Haematology. International Journal of Laboratory Hematology. https://doi.org/10.1111/j.1365-2257.1993.tb01089.x

Hoffman, M., 2008. Animal models of bleeding and tissue repair. Haemophilia 14, 62–67. https://doi.org/10.1111/j.1365-2516.2008.01729.x

Hoffman, M., 2003. Remodeling the Blood Coagulation Cascade. J Thromb Thrombolys 16, 17–20. https://doi.org/10.1023/b:thro.0000014588.95061.28

Iorio, A., Fischer, K., Blanchette, V., Rangarajan, S., Young, G., Morfini, M., IPSG), P. (PK) E.W.G. of the I.P.S.G. (the, 2017. Tailoring treatment of haemophilia B: accounting for the distribution and clearance of standard and extended half-life FIX concentrates. Thromb Haemostasis 117, 1023–1030. https://doi.org/10.1160/th16-12-0942

Jenne, C.N., Urrutia, R., Kubes, P., 2013. Platelets: bridging hemostasis, inflammation, and immunity. Int J Lab Hematol 35, 254–261. https://doi.org/10.1111/ijlh.12084

Jiménez-Yuste, V., Auerswald, G., Benson, G., Lambert, T., Morfini, M., Remor, E., Salek, S.Z., 2014. Achieving and maintaining an optimal trough level for prophylaxis in haemophilia: the past, the present and the future. Blood Transfus Trasfusione Del Sangue 12, 314–9. https://doi.org/10.2450/2014.0298-13

Kenneth K., Marshall A. Lichtman, Josef T. Prchal, Marcel M. Levi, Oliver W. Press, Linda J. Burns, Michael A. Caligiuri, 2016. Williams Hematology, 9th Edition. McGraw-Hill Education.

Kastetter, B., Matrai, A.B., Cooley, B.C., 2018. Optimizing outcome measurement with murine ferric chloride-induced thrombosis. Blood Coagul Fibrin 29, 636–643. https://doi.org/10.1097/mbc.0000000000000768

Lenting, P.J., Maat, H. ter, Clijsters, P.P.F.M., Donath, M.-J.S.H., Mourik, J.A. van, Mertens, K., 1995. Cleavage at Arginine 145 in Human Blood Coagulation Factor IX Converts the Zymogen into a Factor VIII Binding Enzyme (∗). J Biol Chem 270, 14884–14890. https://doi.org/10.1074/jbc.270.25.14884

Lin, H.-F., Maeda, N., Smithies, O., Straight, D.L., Stafford, D.W., 1997. A Coagulation Factor IX-Deficient Mouse Model for Human Hemophilia B. Blood 90, 3962–3966. https://doi.org/10.1182/blood.v90.10.3962

Lindquist, P.A., Fujikawa, K., Davie, E.W., 1978. Activation of bovine factor IX (Christmas factor) by factor XIa (activated plasma thromboplastin antecedent) and a protease from Russell's viper venom. J Biol Chem 253, 1902–1909. https://doi.org/10.1016/s0021-9258(19)62334-3

Macintyre, D.E., Pearson, J.D., Gordon, J.L., 1978. Localisation and stimulation of prostacyclin production in vascular cells. Nature 271, 549–551. https://doi.org/10.1038/271549a0

Marcus, A.J., Broekman, M.J., Drosopoulos, J.H., Islam, N., Alyonycheva, T.N., Safier, L.B., Hajjar, K.A., Posnett, D.N., Schoenborn, M.A., Schooley, K.A., Gayle, R.B., Maliszewski, C.R., 1997. The endothelial cell ecto-ADPase responsible for inhibition of platelet function is CD39. J Clin Invest 99, 1351–1360. https://doi.org/10.1172/jci119294

Marlar, R.A., Strandberg, K., Shima, M., Adcock, D.M., 2020. Clinical utility and impact of the use of the chromogenic vs one-stage factor activity assays in haemophilia A and B. Eur J Haematol 104, 3–14. https://doi.org/10.1111/ejh.13339

Monahan, P.E., 2015. Gene therapy in an era of emerging treatment options for hemophilia B. J Thromb Haemost 13, S151–S160. https://doi.org/10.1111/jth.12957

Monroe, D.M., Hoffman, M., Roberts, H.R., 2002. Platelets and Thrombin Generation. Arteriosclerosis Thrombosis Vasc Biology 22, 1381–1389. https://doi.org/10.1161/01.atv.0000031340.68494.34

Monroe, D.M., Roberts, H.R., Hoffman, M., 1994. Platelet procoagulant complex assembly in a tissue factor-initiated system. Brit J Haematol 88, 364–371. https://doi.org/10.1111/j.1365-2141.1994.tb05032.x

Motlagh, H., Pezeshkpoor, B., Dorgalaleh, A., 2018. Congenital Bleeding Disorders, Diagnosis and Management 139–160. https://doi.org/10.1007/978-3-319-76723-9_5

Neuenschwander, P.F., Morrissey, J.H., 1992. Deletion of the membrane anchoring region of tissue factor abolishes autoactivation of factor VII but not cofactor function. Analysis of a mutant with a selective deficiency in activity. J Biol Chem 267, 14477–14482. https://doi.org/10.1016/s0021-9258(19)49737-8

Ni, H., Denis, C.V., Subbarao, S., Degen, J.L., Sato, T.N., Hynes, R.O., Wagner, D.D., 2000. Persistence of platelet thrombus formation in arterioles of mice lacking both von Willebrand factor and fibrinogen. J Clin Invest 106, 385–392. https://doi.org/10.1172/jci9896

Okada, K., Nishioka, M., Kaji, H., 2020. Roles of fibrinolytic factors in the alterations in bone marrow hematopoietic stem/progenitor cells during bone repair. Inflamm Regen 40, 22. https://doi.org/10.1186/s41232-020-00128-5

Olson, S., Swanson, R., Raub-Segall, E., Bedsted, T., Sadri, M., Petitou, M., Hérault, J.-P., Herbert, J.-M., Björk, I., 2004. Accelerating ability of synthetic oligosaccharides on antithrombin inhibition of proteinases of the clotting and fibrinolytic systems Comparison with heparin and low-molecular-weight heparin. Thromb Haemostasis 92, 929–939. https://doi.org/10.1160/th04-06-0384

Østergaard, H., Bjelke, J.R., Hansen, L., Petersen, L.C., Pedersen, A.A., Elm, T., Møller, F., Hermit, M.B., Holm, P.K., Krogh, T.N., Petersen, J.M., Ezban, M., Sørensen, B.B., Andersen, M.D., Agersø, H., Ahmadian, H., Balling, K.W., Christiansen, M.L.S., Knobe, K., Nichols, T.C., Bjørn, S.E., Tranholm, M., 2011. Prolonged half-life and preserved enzymatic properties of factor IX selectively PEGylated on native N-glycans in the activation peptide. Blood 118, 2333–2341. https://doi.org/10.1182/blood-2011-02-336172

Park, J., Koh, J., 2018. Era of Bloodless Surgery: Spotlights on Hemostasic Materials and Techniques. Hanyang Medical Rev 38, 3–15. https://doi.org/10.7599/hmr.2018.38.1.3

Pasi, K.J., Lissitchkov, T., Mamonov, V., Mant, T., Timofeeva, M., Bagot, C., Chowdary, P., Georgiev, P., Gercheva-Kyuchukova, L., Madigan, K., Nguyen, H.V., Yu, Q., Mei, B., Benson, C.C., Ragni, M.V., 2021. Targeting of antithrombin in hemophilia A or B with investigational siRNA therapeutic fitusiran—Results of the phase 1 inhibitor cohort. J Thromb Haemost 19, 1436–1446. https://doi.org/10.1111/jth.15270

Patil, S.B., Jackman, L.E., Francis, S.E., Judge, H.M., Nylander, S., Storey, R.F., 2010. Ticagrelor Effectively and Reversibly Blocks Murine Platelet P2Y12-Mediated Thrombosis and Demonstrates a Requirement for Sustained P2Y12 Inhibition to Prevent Subsequent Neointima*. Arteriosclerosis Thrombosis Vasc Biology 30, 2385–2391. https://doi.org/10.1161/atvbaha.110.210732

Pestel, S., Peil, H., Machado, S.K., Claar, P., Raquet, E., Ponnuswamy, P., Mischnik, M., Ghobrial, O., Herzog, E., 2021. Pharmacokinetics and Pharmacodynamics of Recombinant FIX Variants in the FIX Knockout Mouse Tail Clip Bleeding Model. Blood 138, 3180–3180. https://doi.org/10.1182/blood-2021-147819

Phimister, E.G., Ragni, M.V., 2015. Targeting Antithrombin to Treat Hemophilia. New Engl J Medicine 373, 389–391. https://doi.org/10.1056/nejmcibr1505657

Puetz, J., Soucie, J.M., Kempton, C.L., Monahan, P.E., Investigators, H.T.C.N. (HTCN), 2014. Prevalent inhibitors in haemophilia B subjects enrolled in the Universal Data Collection database. Haemophilia 20, 25–31. https://doi.org/10.1111/hae.12229

Qasim, Z. and Hassan, 2014. Pattern of Bleeding in Haemophilia Patients. Journal of Islamabad Medical & Dental College (JIMDC).

Reijnen, M.J., Sladek, F.M., Bertina, R.M., Reitsma, P.H., 1992. Disruption of a binding site for hepatocyte nuclear factor 4 results in hemophilia B Leyden. Proc National Acad Sci 89, 6300–6303. https://doi.org/10.1073/pnas.89.14.6300

Renné, T., Pozgajová, M., Grüner, S., Schuh, K., Pauer, H.-U., Burfeind, P., Gailani, D., Nieswandt, B., 2005. Defective thrombus formation in mice lacking coagulation factor XII. J Exp Medicine 202, 271–281. https://doi.org/10.1084/jem.20050664

Ricard-Blum, S., 2011. The Collagen Family. Csh Perspect Biol 3, a004978. https://doi.org/10.1101/cshperspect.a004978

Riehl, T.E., HE, L., Zheng, L., Greco, S., Tollefsen, D.M., Stenson, W.F., 2011. COX-1+/−COX-2−/− genotype in mice is associated with shortened time to carotid artery occlusion through increased PAI-1. J Thromb Haemost 9, 350–360. https://doi.org/10.1111/j.1538-7836.2010.04156.x

Roberts1, H., Hoffman2, M., Monroe1, D., 2006. A Cell-Based Model of Thrombin Generation. Semin Thromb Hemost 32, 032–038. https://doi.org/10.1055/s-2006-939552

Römisch, J., Pock, K., 2012. Production of Plasma Proteins for Therapeutic Use 65–79. https://doi.org/10.1002/9781118356807.ch5

Ruggeri, Z.M., 2002. Platelets in atherothrombosis. Nat Med 8, 1227–1234. https://doi.org/10.1038/nm1102-1227

Saboor, M., Ayub, Q., Ilyas, S., Moinuddin, 2013. Platelet receptors; an instrumental of platelet physiology. Pak J Med Sci 29, 891–896. https://doi.org/10.12669/pjms.293.3497

Saldanha, L.J., Chan, A.K., Gross, P.L., 2011. Exploring the Impact of Clinical Anticoagulants on Venous Thrombosis Stability Using a Novel Intravital Murine Model. Blood 118, 1246–1246. https://doi.org/10.1182/blood.v118.21.1246.1246

Samelson-Jones, B.J., Finn, J.D., George, L.A., Camire, R.M., Arruda, V.R., 2019. Hyperactivity of factor IX Padua (R338L) depends on factor VIIIa cofactor activity. Jci Insight 4. https://doi.org/10.1172/jci.insight.128683

Samelson-Jones, B.J., Sullivan, S.K., Rasko, J.E.J., Giermasz, A., George, L.A., Ducore, J.M., Teitel, J.M., McGuinn, C.E., O'Brien, A., Winburn, I., Smith, L.M., Chhabra, A., Rupon, J., 2021. Follow-up of More Than 5 Years in a Cohort of Patients with Hemophilia B Treated with Fidanacogene Elaparvovec Adeno-Associated Virus Gene Therapy. Blood 138, 3975–3975. https://doi.org/10.1182/blood-2021-150541

Sandset, P.M., 1996. Tissue Factor Pathway Inhibitor (Tfpi) – An Update. Pathophysiol Haemo T 26, 154–165. https://doi.org/10.1159/000217293

Schuijt, T.J., Bakhtiari, K., Daffre, S., DePonte, K., Wielders, S.J.H., Marquart, J.A., Hovius, J.W., Poll, T. van der, Fikrig, E., Bunce, M.W., Camire, R.M., Nicolaes, G.A.F., Meijers, J.C.M., Veer, C. van 't, 2013. Factor Xa Activation of Factor V Is of Paramount Importance in Initiating the Coagulation System. Circulation 128, 254–266. https://doi.org/10.1161/circulationaha.113.003191

Sharda, A., Flaumenhaft, R., 2018. The life cycle of platelet granules. F1000research 7, 236. https://doi.org/10.12688/f1000research.13283.1

Smith, S.B., Gailani, D., 2014. Update on the physiology and pathology of factor IX activation by factor XIa. Expert Rev Hematol 1, 87–98. https://doi.org/10.1586/17474086.1.1.87

Srivastava, A., Brewer, A.K., Mauser-Bunschoten, E.P., Key, N.S., Kitchen, S., Llinas, A., Ludlam, C.A., Mahlangu, J.N., Mulder, K., Poon, M.C., Street, A., Hemophilia, 2013. Guidelines for the management of hemophilia. Haemophilia 19, e1–e47. https://doi.org/10.1111/j.1365-2516.2012.02909.x

Stafford, D.W., 2016. Extravascular FIX and coagulation. Thrombosis J 14, 35. https://doi.org/10.1186/s12959-016-0104-2

Stafford, D.W., 1992. The Binding of Human Factor IX to the Endothelial Cells Is Mediated by Residues 3-11.

Stern, D.M., Drillings, M., Nossel, H.L., Hurlet-Jensen, A., LaGamma, K.S., Owen, J., 1983. Binding of factors IX and IXa to cultured vascular endothelial cells. Proc National Acad Sci 80, 4119–4123. https://doi.org/10.1073/pnas.80.13.4119

Stern, D.M., Knitter, G., Kisiel, W., Nawroth, P.P., 1987a. In vivo evidence of intravascular binding sites for coagulation factor IX. Brit J Haematol 66, 227–232. https://doi.org/10.1111/j.1365-2141.1987.tb01303.x

Stern, D.M., Knitter, G., Kisiel, W., Nawroth, P.P., 1987b. In vivo evidence of intravascular binding sites for coagulation factor IX. Brit J Haematol 66, 227–232. https://doi.org/10.1111/j.1365-2141.1987.tb01303.x

Stern, D.M., Nawroth, P.P., Kisiel, W., Vehar, G., Esmon, C.T., 1985. The binding of factor IXa to cultured bovine aortic endothelial cells. Induction of a specific site in the presence of factors VIII and X. J Biological Chem 260, 6717–22.

Stoilova-McPhie, S., Villoutreix, B.O., Mertens, K., Kemball-Cook, G., Holzenburg, A., 2002. 3-Dimensional structure of membrane-bound coagulation factor VIII: modeling of the factor VIII heterodimer within a 3-dimensional density map derived by electron crystallography. Blood 99, 1215–1223. https://doi.org/10.1182/blood.v99.4.1215

Sweeney, J.D., Hoernig, L.A., 1993. Age-Dependent Effect on the Level of Factor IX. Am J Clin Pathol 99, 687–688. https://doi.org/10.1093/ajcp/99.6.687

Thomas, G.M., Panicot-Dubois, L., Lacroix, R., Dignat-George, F., Lombardo, D., Dubois, C., 2009. Cancer cell–derived microparticles bearing P-selectin glycoprotein ligand 1 accelerate thrombus formation in vivo. J Exp Medicine 206, 1913–1927. https://doi.org/10.1084/jem.20082297

Uprichard, J., Adamidou, D., Goddard, N.J., Mann, H.A., Yee, T.T., 2012. Factor IX replacement to cover total knee replacement surgery in haemophilia B: a single-centre experience, 2000–2010. Haemophilia 18, 46–49. https://doi.org/10.1111/j.1365-2516.2011.02552.x

Venkateswarlu, D., 2014. Structural insights into the interaction of blood coagulation co-factor VIIIa with factor IXa: A computational protein–protein docking and molecular dynamics refinement study. Biochem Bioph Res Co 452, 408–414. https://doi.org/10.1016/j.bbrc.2014.08.078

Versteeg, H.H., Heemskerk, J.W.M., Levi, M., Reitsma, P.H., 2013. New Fundamentals in Hemostasis. Physiol Rev 93, 327–358. https://doi.org/10.1152/physrev.00016.2011

Walter, T.J., Cast, A.E., Huppert, K.A., Huppert, S.S., 2014. Epithelial VEGF signaling is required in the mouse liver for proper sinusoid endothelial cell identity and hepatocyte zonation in vivo. Am J Physiol-gastr L 306, G849–G862. https://doi.org/10.1152/ajpgi.00426.2013

Wang, X., Smith, P.L., Hsu, M., Gailani, D., Schumacher, W.A., Ogletree, M.L., Seiffert, D.A., 2006. Effects of factor XI deficiency on ferric chloride-induced vena cava thrombosis in mice. J Thromb Haemost 4, 1982–1988. https://doi.org/10.1111/j.1538-7836.2006.02093.x

Wang, X., Xu, L., 2005. An optimized murine model of ferric chloride-induced arterial thrombosis for thrombosis research. Thromb Res 115, 95–100. https://doi.org/10.1016/j.thromres.2004.07.009

White, J.G., Clawson, C.C., 2009. Overview Article: Biostructure of Blood Platelets. Ultrastruct Pathol 1, 533–558. https://doi.org/10.3109/01913128009140561

Wolberg, A.S., Stafford, D.W., Erie, D.A., 1997a. Human Factor IX Binds to Specific Sites on the Collagenous Domain of Collagen IV*. J Biol Chem 272, 16717–16720. https://doi.org/10.1074/jbc.272.27.16717

Wolberg, A.S., Stafford, D.W., Erie, D.A., 1997b. Human Factor IX Binds to Specific Sites on the Collagenous Domain of Collagen IV*. J Biol Chem 272, 16717–16720. https://doi.org/10.1074/jbc.272.27.16717

Wood, J.P., Bunce, M.W., Maroney, S.A., Tracy, P.B., Camire, R.M., Mast, A.E., 2013. Tissue factor pathway inhibitor-alpha inhibits prothrombinase during the initiation of blood coagulation. Proc National Acad Sci 110, 17838–17843. https://doi.org/10.1073/pnas.1310444110

Wright, I.S., 1962. The Nomenclature of Blood Clotting Factors*. Thromb Haemostasis 07, 381–388. https://doi.org/10.1055/s-0038-1655480

Yau, J.W., Teoh, H., Verma, S., 2015. Endothelial cell control of thrombosis. Bmc Cardiovasc Disor 15, 130. https://doi.org/10.1186/s12872-015-0124-z

You, C.W., Hong, S., Kim, Suyeong, Shin, H., Kim, J.S., Han, J.W., Kim, Soo-Jeong, Kim, D.Y., Lee, M., Levy, H., 2021. Safety, pharmacokinetics, and pharmacodynamics of a next-generation subcutaneously administered coagulation factor IX variant, dalcinonacog alfa, in previously treated hemophilia B patients. J Thromb Haemost 19, 967–975. https://doi.org/10.1111/jth.15259

Zögg, T., Brandstetter, H., 2009. Activation mechanisms of coagulation factor IX. Biol Chem 390, 391–400. https://doi.org/10.1515/bc.2009.057

9.2 Own contribution

I planned, performed, and analyzed the described experiments and the respective data with the help of my supervisor Dr. Padmapriya Ponnuswamy, Dr. Sabine Pestel, and Dr. Philipp Claar.

The progress of the project was presented to Prof. Dr. Michael Bacher and every 6-12 months I gave a presentation at the Institute for Immunology seminar at Biomediziniche Forschungszentrum (BMFZ) of the Philipps Universität Marburg.

My PhD thesis focused on the characterization of single point mutations in the rFIX molecule. The generation of the constructs and cloning of the expression plasmids was performed by Herbert Dersch. The stable transfection in CHO cells was performed by Elke Block, Martina Ortkamp, and Natascha Koester. The large-scale production of the recombinant proteins was performed by Thomas Peppinghaus, Moritz Boland, and Thomas Rein.

The purification of the recombinant proteins was carried out by Waltraud Seyfert-Brandt and Sonja Beckmann-Scheld in the Lab of Holger Lind. The final stocks of the recombinant proteins were kindly provided by Dr. Philipp Claar in the Department of Recombinant Technology at CSL Behring Innovation GmbH.

I characterized the generated recombinant proteins in a series of coagulation and enzymatic assays. I performed the clot-based assays, and the activity levels were confirmed by two independent laboratories in the Department of Recombinant Technology and in the Department of Recombinant Product Development.

I performed the activation assays at the Department of Recombinant Product Development and enzymatic activity assays were conducted by myself, with technical assistance of Waltraud Seyfert-Brandt and scientific guidance of Dr. Philipp Claar. Animal experiments were planned together with Dr. Sabine Pestel and Dr. Padmapriya Ponnuswamy, and experimental help was provided by Hendrik Peil, Julia Riedesel, and Peter Niebl. As part of the project, I established a

$FeCl_3$ thrombosis model in-house. Therefore, I visited the lab of Prof. Nieswandt in the Center for Integrative and Translational Bioimaging of the Rudolf-Virchow Center. I discussed the scientific considerations around preparation, conduction, and analysis of the $FeCl_3$ thrombosis models with Sarah Beck, a Postdoc working in the lab of Prof. Nieswandt.

In-house, the establishment of the model was discussed regularly with Dr. Sabine Pestel and Dr. Padmapriya Ponnuswamy. The pharmacokinetic analysis was performed by Dr. Marcel Mischnick and together with Dr. Sabine Pestel and Dr. Padmapriya Ponnuswamy we discussed the scientific and biological reasoning and planed the next experimental steps. Finally, I performed the statistical analysis under guidance of Dr. Brandon Green.

The histological analysis was planned and executed by me with hands-on support of Tanja Viertelhausen and Tina Höhne. Dr. Benjamin Kuehnemuth helped me during troubleshooting. Dr. Benjamin Kuehnemuth advised and supported me on issues related to histology and technical questions. The immunofluorescence analysis was performed by me with technical and scientific input of Greg Bass from Bio21 Institute in Australia for the usage and setup of image processing programs like Fiji.

In an additional project, I planned and executed experiments on an ex-vivo skin model in collaboration with Bio21 Institute in Australia and under direct supervision of Dr. Padmapriya Ponnuswamy. The *ex vivo* skin model is human skin discarded from cosmetic surgery but a standardize technology keeps the donated human skin biopsies alive for up to seven days. With this model we intended to establish a model to assess absorption kinetics of drugs after subcutaneous kinetics. In this model, we injected albumin fused rFIX (rFIX-FP) at several concentrations and a commercially available IgG product for subcutaneous administration (Cuvitru) as a positive control. Over 7 days the culture medium was sampled daily and at day 7 the skin tissue was processed for histological analysis. Results showed that Cuvitru´s recovery in the medium was rather low, 26% only, compared to the Cuvitru bioavailability of at least 70% in the clinical setting (Clinical Review - CUVITRU- US Food and Drug Administration). rFIX-FP recovery in medium was ~2% only. After 7 days, FIX was detected in the tissue samples in a concentration dependent manner (as different concentrations were injected), mostly surrounding the fat cells. Relative to Cuvitru, rFIX-FP recovery was much low. In the end we concluded that this model would not be suitable to reliably quantify release of drugs after subcutaneous administration due to the inherent lack of interstitial pressure in this model. The results were presented and discussed regularly with the team members of the project at the Bio21 Institute in Australia.

During my PhD I participated in several meetings with a scientific focus: I attended the science day at CSL Behring Innovation GmbH, Research Europe Seminar, and an intensive course on hematology organized by the Society of Thrombosis and Haemostasis Research in Germany (Gesellschaft für Thrombose- und Hämostaseforschung). I attended a course concerning histological processing and staining. I presented my data in a forum aimed to discuss technical issues and the scientific reasoning of imaging data analysis as well as in a CSL seminar series "Research Seminar". The *in vivo* data was presented in internal meetings that include different in vivo pharmacology groups within CSL Limited to discuss scientific rational, model-specific advantages and limitations as well as the predictiveness and translatability of the animal models. I was involved in technical and scientific discussions about the purification and characterization of recombinant proteins, bioanalytics, and in vivo pharmacology.

9.3 Publication list

Peer review publications:

Knoll Machado S*., Peil H., Kraushaar T., Claar P., Mischnik M., Lind H., Herzog E., Bacher M., Wolfgang Nolte M., Bielohuby M., Pestel S. and Ponnuswamy P;* Modulation of Extravascular Binding of Recombinant Factor IX Impacts duration of Efficacy in Mouse Models, manuscript accepted, Thrombosis and Haemostasis.

Pestel, S., Peil, H., ***Knoll Machado, S.****, Claar, P., Raquet, E., Ponnuswamy, P., Mischnik M., Ghobrial O., and Herzog, E;* Pharmacokinetics and Pharmacodynamics of Recombinant FIX Variants in the FIX Knockout Mouse Tail Clip Bleeding Model. Blood (2021), 138(Supplement 1), doi:10.1182/blood-2021-147819

Patent:

Knoll Machado S., Ponnuswamy, P., Pestel S, and Claar P; European Patent Application 22200505.0 "Factor IX variant polypeptides for administration to soft tissue". Patent was filed at the European Patent Office on the 10th of October 2022

Posters:

Knoll Machado S.*, Kraushaar T., Röder J., Claar P., Hardy C., Nolte M.W., Pestel S., Bacher M., Ponnuswamy P;* In vitro characterization of K5A and K5R variants of Factor IX, Poster at 65th Meeting of the Society of Thrombosis and Haemostasis Research (GTH e. V.), February 23-26, 2021

Knoll Machado S.*, Peil H., Kraushaar T., Claar P., Mischnik M., Lind H., Herzog E., Bacher M., Wolfgang Nolte M., Bielohuby M., Pestel S. and Ponnuswamy P;* Modulation of Extravascular Binding of Recombinant Factor IX Impacts Hemostatic Efficacy in Mouse Models. Blood 2022; 140 (Supplement 1): 2701–2702. doi: https://doi.org/10.1182/blood-2022-168756

9.4 Acknowledgement

To start I would like to thank the Research Department at CSL Behring Innovation GmbH for giving me to opportunity to join the Pharmacology and Toxicology group and learn not only about interesinting scientific projects but also the culture and the structures of the company. I would like to express my profound gratitute to my advisor and supervisor Dr. Padmapriya Ponnnuswamy. Her patience, support, guidance, and training in all aspects of being a good research scientist are greatly appreciated and will not be forgotten. I also would like to thank Prof. Michael Bacher, my supervisor at the university, for supporting my external doctarate and providing valuable input. I want to thank the Recombinant Technology group for providing the recombinantly generated proteins. A special thanks to Holger Lind's lab that was responsible for the protein purification and Dr. Peter Schmidt for letting me use his illustration in Figure 2.

Being in CSL Behring Innovation GmbH I had the privilege of working with many excellent scientists and colleagues. I would like to thank Dr. Sabine Pestel for her valuable feedback and insights on pharmacokinetics and *in vivo* studies. I would also like to thank Dr. Philipp Claar for his support. His great expertice in the production of recombinant proteins and *in vitro* testing in the coagulation field was very helpful. I am grateful to Dr. Benjamin Kühnemuth for his advice and constructive criticism in scientific topics.

I really enjoyed working together with all my colleagues in the experimental unit. A big thanks goes to Hendrik Peil, Julia Riedesel, Waltraud Seyfert-Brandt, Katharina Iliev, Jennifer Marciniak, Antje Fischer, Tanja Viertelhausen and Peter Niebl for their great support in the lab and the nice work enviroment. To Sabine Schweißgut, who was a PhD student in the Development Department, I would like to thank her for all the interesting discussions about the clotting FIX post-translational modifications and for our brainstorming sessions related to the coagulation assays. I am grateful to Dr. Marcel Mischnik for the modelling work and Dr. Brandon Green for guiding and helping me with the statistical analysis.

Lastly, I would like to thank my family for their incredible support, encouragement and understanding. Most importantly, thank you to my father for never stopped believing in me even when I was doubtful. I want to dedicate this work to him, Kurt Erich Knoll Hoffmann, who passed away during the course of this research. Whithout him none of this would have been possible. Thank you to my fiancé Kevin for always supporting me. His advice and support were always there when I needed it most.

9.5 Verzeichnis der akademischen Lehrer

Dr. Andreas Kaufmann

Dr. Brandon Greene

Dr. Christian Wrocklage

Dr. Dominique Brandt

Dr. Dorothea Strauer

Dr. Markus Eickmann

Dr. Matthias Conrad

Dr. Michael Schween

Dr. Mikhail Matrosovich

Dr. Nina Timmesfeld

Dr. Philipp Reiß

Dr. Philipp Yu

Dr. Ralf Kinscherf

Dr. Ralf Wagner

Dr. Sabrina Höbenreich

Dr. Thomas Strecker

Dr. Ulrich Mühlenhoff

Dr. Wiebke Milani

PD Dr. Buchholz

PD Dr. Gert Zimmer

PD Dr. Ingrid Böhm

PD Dr. Olga Dolnik

PD Dr. Reiner Westermann

Prof. Dr. Alexander Brehm

Prof. Dr. Alexander Visekruna

Prof. Dr. Andrea Maisner

Prof. Dr. Bernd Schmeck

Prof. Dr. Dominik Oliver

Prof. Dr. Dr. Jürgen Daut

Prof. Dr. Eva Friebertshäuser

Prof. Dr. Friedemann Weber

Prof. Dr. Guntram Suske

Prof. Dr. Hans-Peter Elsässer

Prof. Dr. Heinz Jänsch

Prof. Dr. Johannes Oberwinkler

Prof. Dr. Jörg Großhans

Prof. Dr. Magdalena Huber

Prof. Dr. Markus Schnare

Prof. Dr. med. Roland Moll

Prof. Dr. Michael Bacher

Prof. Dr. Michael Lohoff

Prof. Dr. Ralf Jacob

Prof. Dr. Roland Lill

Prof. Dr. Rolf Müller

Prof. Dr. Stefan Bauer

Prof. Dr. Stephan Becker

Prof. Dr. Thorsten Stiewe

Prof. Dr. Timothy D. Plant

Prof. Dr. Ulrich Steinhoff